Wheel Profile Maintenance Guidelines

DETAILS

137 pages | 8.5 x 11 | PAPERBACK
ISBN 978-0-309-43264-1 | DOI 10.17226/22168

AUTHORS

Xinggao Shu

ACKNOWLEDGMENT

This work was sponsored by the Federal Transit Administration (FTA) in cooperation with the Transit Development Corporation. It was conducted through the Transit Cooperative Research Program (TCRP), which is administered by the Transportation Research Board (TRB) of the National Academies.

THE NATIONAL ACADEMIES

Advisers to the Nation on Science, Engineering, and Medicine

The **National Academy of Sciences** is a private, nonprofit, self-perpetuating society of distinguished scholars engaged in scientific and engineering research, dedicated to the furtherance of science and technology and to their use for the general welfare. Upon the authority of the charter granted to it by the Congress in 1863, the Academy has a mandate that requires it to advise the federal government on scientific and technical matters. Dr. Ralph J. Cicerone is president of the National Academy of Sciences.

The **National Academy of Engineering** was established in 1964, under the charter of the National Academy of Sciences, as a parallel organization of outstanding engineers. It is autonomous in its administration and in the selection of its members, sharing with the National Academy of Sciences the responsibility for advising the federal government. The National Academy of Engineering also sponsors engineering programs aimed at meeting national needs, encourages education and research, and recognizes the superior achievements of engineers. Dr. C. D. Mote, Jr., is president of the National Academy of Engineering.

The **Institute of Medicine** was established in 1970 by the National Academy of Sciences to secure the services of eminent members of appropriate professions in the examination of policy matters pertaining to the health of the public. The Institute acts under the responsibility given to the National Academy of Sciences by its congressional charter to be an adviser to the federal government and, upon its own initiative, to identify issues of medical care, research, and education. Dr. Victor J. Dzau is president of the Institute of Medicine.

The **National Research Council** was organized by the National Academy of Sciences in 1916 to associate the broad community of science and technology with the Academy's purposes of furthering knowledge and advising the federal government. Functioning in accordance with general policies determined by the Academy, the Council has become the principal operating agency of both the National Academy of Sciences and the National Academy of Engineering in providing services to the government, the public, and the scientific and engineering communities. The Council is administered jointly by both Academies and the Institute of Medicine. Dr. Ralph J. Cicerone and Dr. C. D. Mote, Jr., are chair and vice chair, respectively, of the National Research Council.

The **Transportation Research Board** is one of six major divisions of the National Research Council. The mission of the Transportation Research Board is to provide leadership in transportation innovation and progress through research and information exchange, conducted within a setting that is objective, interdisciplinary, and multimodal. The Board's varied activities annually engage about 7,000 engineers, scientists, and other transportation researchers and practitioners from the public and private sectors and academia, all of whom contribute their expertise in the public interest. The program is supported by state transportation departments, federal agencies including the component administrations of the U.S. Department of Transportation, and other organizations and individuals interested in the development of transportation. **www.TRB.org**

www.national-academies.org

Wheel Profile Maintenance Guidelines

PART 1

Survey of Current Wheel Profiles and Maintenance Practices

Table of Contents

TABLE OF CONTENTS i
LIST OF FIGURES ii
LIST OF TABLES iii
ACKNOWLEDGMENTS iv
SUMMARY 1
CHAPTER 1 Introduction 2
CHAPTER 2 Transit System Maintenance Survey 3
2.1 Wheel Flats 3
2.2 Wheel Wear 4
2.3 Wheel Diameter Differences in One Axle 7
2.4 Wheel Diameter Tolerance in One Truck 10
2.5 Wheel Diameter Tolerance in One Car 11
2.6 Wheel Flange Angle 11
2.7 Other Wheel Inspections 12
2.8 Wheel Truing 12
2.8.1 Truing Cycle and Wheel Life 12
2.8.2 Truing Surface Roughness 13
2.8.3 Truing Templates 15
CHAPTER 3 State-of-the-Art Wheel Profile Design and Maintenance Principles 18
3.1 Wheel Profile Design Methodology 18
3.2 Wheel Profile Design and Maintenance Criteria 20
3.3 Wheel/Rail Contact Conicity 20
3.4 Correlation between Wheel Wear and Equivalent Conicity 23
CHAPTER 4 Conclusions and Recommendations 25
REFERENCES 26

List of Figures

Figure 1. Flat Spots on Two Wheels....3
Figure 2. Worn, Unworn Wheels, and Unworn Rail....5
Figure 3. Freight Car Hollow Wheel Stability Test....7
Figure 4. Effect of Wheel Diameter Difference on Freight Car Stability (1 Tape equals 0.125 inch on the circumference)....8
Figure 5. Longitudinal Forces on the Right Wheel of the Leading Wheelset at 60 mph (96.6kmh)....9
Figure 6. Effect of Mismatching Wheel Circumference on the Leading and Trailing Axle with Empty Freight Car and Pitch and Bounce Input....10
Figure 7. Milling Type Wheel Truing Machine....13
Figure 8. Lathe Type Wheel Truing Machine....14
Figure 9. Rough Wheel Surface from Milling Type Truing Machine....15
Figure10. New Wheel Contact on Worn High Rail....16
Figure 11. Worn Wheel Contact on Worn High Rail....17
Figure 12. Wheel and Rail Contact Geometry....20
Figure 13. Contact of New AAR-1B Narrow Flange Wheel on New AREMA 136RE Rail, 10-inch Crown Radius, 1:40 Cant, at a Gage of 56.5 inches....22
Figure 14. Contact of Hollow Worn Wheel on Tangent Worn Track at a Gage of 56.5 inches....22
Figure 15. RRD Functions Measured in a Freight Railcar....24

List of Tables

Table 1. Lists of Rail Transit Agencies Surveyed 2
Table 2. Details of Worn Wheels in Configuration 1 (Freight Car Stability Test).....6
Table 3. Details of Worn Wheels in Configuration 2 (Freight Car Stability Test).....6
Table 4. Transit Agency Wheel Diameter Tolerances.....9
Table 5. Maximum Flange Angle of Transit Agency Designed Wheels.....11
Table 6. Transit Agency Wheel Truing Cycles and Wheel Life.....12

Acknowledgments

The authors appreciate the Transit Cooperative Research Program for providing the funding for this work. We also thank TCRP D-7 committee members for their comments and suggestions and TTCI employees Nicholas Wilson, Michael Brown, and Program Manager Dingqing Li for their advice and project management.

Summary

Transportation Technology Center, Inc., (TTCI), a wholly owned subsidiary of the Association of American Railroads (AAR), conducted a survey on wheel profile maintenance practices in rail transit agencies, for the Transportation Research Board's (TRB) Transit Cooperative Research Program (TCRP) as part of a project to develop wheel profile maintenance guidelines for transit operations.

The first task of this project reviewed current wheel profiles and maintenance practices (including representative light rail and heavy rail transit agencies) through system visits and literature review.

This report compiles the survey information from a questionnaire, site visits of transit agencies, information from previous TCRP projects, and state-of-the-art research results on wheel profile design and maintenance methodologies from a literature review.

The following conclusions and recommendations are made from the Task 1 study:

Wheel slide and wheel flats are mainly caused by braking and low adhesion conditions. New anti-slip technologies and devices are needed to reduce wheel flats.

Wheel diameter difference on one axle has a significant effect on car lateral stability performance. Allowable wheel diameter difference maintenance limit depends on the vehicle and truck design, especially the truck suspension, and the maintenance limits of other components.

Wheel diameter difference in one truck affects car vertical performance such as the wheel load equalization capability.

Most transit agencies surveyed do not have wheel tread wear limits. Wheel wear has significant effects on vehicle and track performance. Setting up wear limits on wheels is a complicated issue. It depends on vehicle and track design, maintenance standards of truck components, and operation environment.

New wheel design or truing templates should be optimized on the basis of existing rail wear conditions, vehicle design and maintenance standards, and special trackwork maintenance requirements.

Wheel truing template profiles need to be evaluated periodically to take into account existing rail wear conditions.

Rough surfaces on wheels from wheel truing can increase the risk of flange climb derailment. Smooth surfaces and lubrication could reduce the flange climb derailment risk.

The effect of the following maintenance limits on rail car performance will be further investigated in Task 2 of this project:

- Wheel diameter differences on one axle, one truck, and one car
- Wheel wear and patterns
- Multiple-axle wheel wear and patterns
- Car type and suspension parameters
- The nonlinear equivalent conicity function is a promising index to characterize variations of wheel/rail contact geometry caused by wheel wear or mismatching after truing. However, the correlation between the wheel wear or mismatched wheel diameter and the nonlinear equivalent conicity function has not been fully established.
- The application of equivalent conicity defined in International Union of Railways UIC 518 and UIC 519 standards to North American rail transit vehicle performance assessment needs to be further investigated.

Guidelines for wheel profile maintenance will be established in Task 2 of this project.

CHAPTER 1

Introduction

The Transportation Technology Center, Inc. (TTCI) has conducted a "Wheel Profile Maintenance Guidelines for Transit System" project for the Transit Cooperative Research Program (TCRP). The objectives of this study were to:

Investigate the effects of wheel profiles (include both new and worn profiles) on transit vehicle performance (safety and ride quality)

Develop wheel profile maintenance guidelines for transit operations (light rail and heavy rail systems)

Develop guideline implementation procedures for wheel profile maintenance demonstrated with examples

The tasks of this project include the following:

Task 1 – Survey current wheel profiles and maintenance practices

Task 2 – Develop wheel profiles maintenance guidelines

Task 3 – Demonstrate wheel maintenance guideline implementation procedures

In Task 1, TTCI conducted a survey on current wheel profiles and maintenance practices in transit agencies through a questionnaire survey, site visits, and a literature review. The survey focused on wheel-related issues, including wheel defects, wheel profile design drawings and truing templates, wheel truing cycles, maintenance limit such as wheel hollowing, flange thickness, wheel diameter tolerance, rail grinding cycles, rail grinding objectives, and wheel and rail lubrication practices.

This Task 1 report compiles the survey information from the recent questionnaire survey, site visits to rail transit agencies, survey information from a previous TCRP project (Wu et al. 2005), and state-of-the-art research results on wheel profile design and maintenance methodologies from the literature review. Table 1 lists the visited rail transit agencies, rail transit agencies responding to the questionnaire, and rail transit agencies visited in a previous TCRP project (Wu et al. 2005).

Table 1. Lists of Rail Transit Agencies Surveyed

Rail Transit Agencies Visited on Site with Wheel and Rail Profile Measurement	Denver Regional Transportation District (RTD), Port Authority Trans-Hudson Corporation (PATH)
Rail Transit Agencies Responding to the Questionnaire	Houston Metro, San Francisco Bay Area Rapid Transit District (BART), RTD, PATH
Rail Transit Agencies Surveyed in a Previous TCRP Project (Wu et al. 2005)	Massachusetts Bay Transportation Authority (MBTA) New Jersey Transit Corporation (NJTC) Washington Metropolitan Area Transit Authority (WMATA) Southeastern Pennsylvania Transit Authority (SEPTA) Chicago Transit Authority (CTA) Chicago Metra

CHAPTER 2

Transit System Maintenance Survey

Supporting the weight of a heavily loaded car, wheelsets withstand much abuse from extreme thermal (if tread braking is used) and mechanical stresses caused by such factors as brake shoe friction, pounding from rail joints and special trackwork, and wheel/rail forces.

Both the wheel flange and the tapered tread provide forces on the contact points between wheel and rail to steer the wheel through curves and tangent track. Wheel/rail forces act positively to steer the vehicle; however, they also lead to rolling contact stresses that work negatively to cause wear, cracks, spalls, and shell defects on both wheels and rails.

Wheel maintenance is critical for rail vehicle safety and ride quality. The following sections summarize wheel maintenance practices and standards used in different rail transit agencies. Brief descriptions of the theories related to wheel maintenance and standards are provided for a better understanding of the causes of the problems and the damages that might result.

2.1 Wheel Flats

Almost every transit system surveyed has experienced wheel sliding, and consequently, wheel flat problems, as Figure 1 shows. Wheel flats are one of the main reasons for wheel truing. Other wheel defects caused by wear, such as uneven wear and thin flange, etc., also have to be removed by wheel truing.

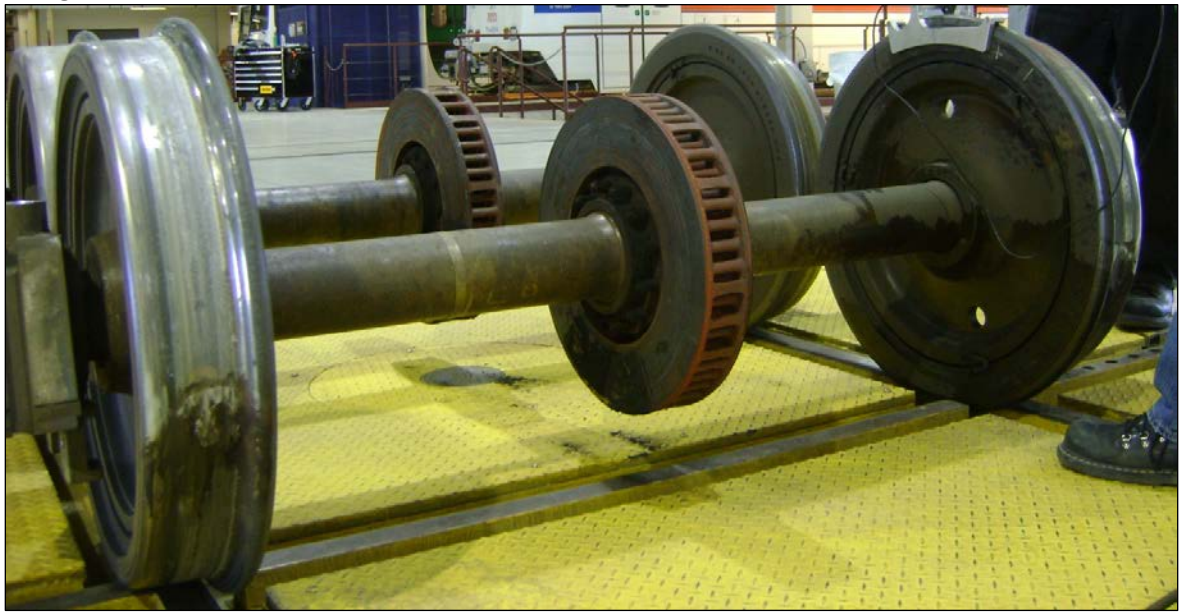

Figure 1. Flat Spots on Two Wheels

When a wheel slides, frictional energy flows into the wheel through the contact patch. As soon as the wheel stops sliding, the overheated steel in the contact patch is quenched by the large thermal mass of the wheel. The steel in the contact patch transforms into martensite, which is a very hard but brittle phase of steel. As a result of the skid, the wheel has a flat spot at the martensitic area, causing an impact at each revolution. Cracks can further develop in and propagate through the martensite. When cracks branch together below the surface, the martensite piece breaks off the tread, leaving a spall on the wheel surface.

Wheel slide is caused by velocity differences between wheel and rail; sliding can result from sticking brakes or because of heavy braking in low friction conditions. Wheel slide and flats are especially problematic during the fall season on some rail transit systems due to leaf residue contaminating the rails.

Investigations showed contaminants, such as rust (iron oxides), dirt (silica and aluminum), and road salts (potassium, calcium, sodium, chlorine, and sulphur), petroleum oil products, and vegetable oils from pine and cedar trees, can form pastes with small amounts of water or oil and significantly reduce adhesion (Kumar 1997).

Both traction and braking may lead to wheel slide. However, the existing literature and the TTCI survey interviews indicate that slides due to braking are more common. Magel and Kalousek (1998) report that skid flats for transit and passenger operations are due primarily to rapid and frequent brake applications under light axle loads, highly variable friction coefficients, and general over-capacity of the braking systems.

Wheel flats not only generate significant impact forces that can damage track and degrade ride quality, but also increase noise. Significant maintenance efforts and cost have been devoted to reduce wheel slide and wheel flats.

To control wheel slide and wheel flats, several techniques have been applied to mitigate the problems, including the following:

Pressurized spray rail cleaners
Hi-rail based wire brushes
Sander operations
Grit-filled gels (sandite)

Both NJT and SEPTA use high-pressure washers. According to a NJT press release, it invested $420,000 in an AquaTrack™ device, which sprays 17 gallons per minute at 20,000 psi spray and uses two 250-horsepower engines on a flatcar (New Jersey Transit 2003). The AquaTrack operates primarily on the Morris & Essex and Montclair-Boonton lines (commuter rail). SEPTA cleans the track on light rail, Norristown, and commuter rail lines during their 3-hour overnight work window with a 5,000-psi high-pressure washer. In addition to spray cleaning, SEPTA also operates a gel and grit delivery system and manually places compressed sand disks (“torpedoes”) on its system in periods of severe weather.

New Jersey Transit’s Newark City Subway had previously tried a modified rail grinder to wire brush its rails, but the results were not satisfactory. Kumar reports similar ineffectiveness (Kumar 1997). However, Chicago Metra regularly uses a Hi-Rail™ engine-powered brush on its Electric District and reports acceptable cleaning results. Chicago Metra also operates additional locomotives using sanders to clean the rails during severe weather conditions.

Automated slip-slide control devices have greatly improved braking performance. These devices modulate one or more control parameters such as service braking pressures, dynamic brakes, motor torques, and sanding to adjust the brake forces or adhesion conditions. After employing such devices, Nelson and Wilson report wheel flats can be reduced by roughly 50 percent (Nelson and Wilson 1997). However, wheel flats still occur with a slip-slide system, and the technology needs to be further improved to reduce wheel flats.

2.2 Wheel Wear

Wheel wear is another reason for wheel truing. Wheels wear into worn shapes in service, with most wear on the tread and flange, as Figure 2 shows.

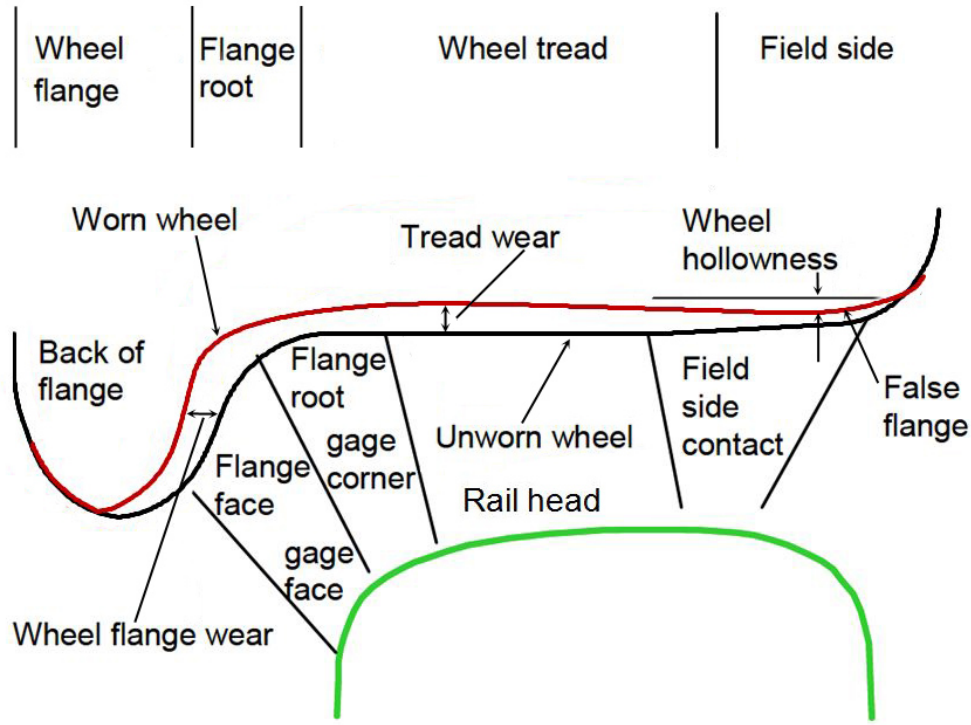

Figure 2. Worn, Unworn Wheels, and Unworn Rail

Wear on wheel treads and flanges is usually characterized by measuring tread hollowness and flange thickness. The worn wheel in Figure 2 is a hollow wheel with hollow depth labeled as "Wheel hollowness". For rail transit agencies running on track governed by FRA rules or adopting Association of American Railroads (AAR) interchange rules (AAR 2012), the tread hollow limit is 0.158 inch (4 millimeters (mm)), and the flange thickness limit is 0.938 inch (23.8mm). It should be noted that the 0.158 inch (4mm) hollow limit was adopted by AAR in 2004. The survey showed that most rail transit agencies have a flange thickness limit (0.938 inch (23.8mm) or 0.875 inch (22.2mm)), but do not have a wear limit on tread hollowness. One possible reason is that wheels in most rail transit systems do not wear as severely hollow as freight railroad wheels do before they are trued. However, hollow wear on wheels is unavoidable, and hollow wheels do cause problems in transit cars.

Observations showed that hollow wheels in rail transit cars lead to car lateral instability (hunting) and degraded ride quality (Smith and Kalousek 1991); however, no comprehensive study of the effects of hollow wheels or wheels with mismatched diameters on transit vehicle stability has been performed recently. Instability caused by hollow wheels is commonly observed in freight car operation. A freight car stability test was performed by TTCI in 2001 (Sawley et al. 2005). The "new" wheelsets used for the test had been recently turned (at less than 5,000 miles) with AAR-1B narrow flange profiles. The worn wheelsets selected were revenue service worn wheels with moderate hollow wear. Table 2 lists the details of the wear of these worn wheelsets as installed for the first series of worn-wheel tests. These tests were termed as Configuration 1. Table 2 shows that the wheelsets in Configuration 1 are diagonally worn within a truck; e.g., the L1 and R2 wheels are hollow, whereas the R1 and L2 wheels are not. To test whether the hollow wheel pattern in a truck influences the stability, tests were conducted using

Configuration 2. As Table 3 shows, the left and right side of the first and fourth axles were exchanged so each truck had hollow wheels only on one side.

Table 2. Details of Worn Wheels in Configuration 1 (Freight Car Stability Test)

Axle No.	Wheel ID	Hollow Wear	Flange Wear*
1	L1	0.075 inch (1.9mm)	1.047 inch (26.6mm)
	R1	0	1.339 inch (34.0mm)
2	L2	0	1.350 inch (34.3mm)
	R2	0.102 inch (2.6mm)	1.055 inch (26.8mm)
3	L3	0.051 inch (1.3mm)	1.201 inch (30.5mm)
	R3	0	1.284 inch (32.6mm)
4	L4	0	1.205 inch (30.6mm)
	R4	0.039 inch (1.0mm)	1.164 inch (29.6mm)

* Measured 0.625 inch (15.9mm) up from a point on the tread 3.0625 inch (77.8mm) from the back face of the wheel.

Table 3. Details of Worn Wheels in Configuration 2 (Freight Car Stability Test)

Axle No.	Wheel ID	Hollow wear	Flange wear*
1	L1	0	1.339 inch (34.0mm)
	R1	0.075 inch (1.9mm)	1.047 inch (26.6mm)
2	L2	0	1.350 inch (34.3mm)
	R2	0.102 inch (2.6mm)	1.055 inch (26.8mm)
3	L3	0.051 inch (1.3mm)	1.201 inch (30.5mm)
	R3	0	1.284 inch (32.6mm)
4	L4	0.039 inch (1.0mm)	1.164 inch (29.6mm)
	R4	0	1.205 inch (30.6mm)

* Measured 0.625 inch (15.9mm) up from a point on the tread 3.0625 inch (77.8mm) from the back face of the wheel.

Figure 3 is a plot of the maximum standard deviation of carbody lateral acceleration over 2,000 feet (609.6meters (m)) of track. It shows a critical speed of 55 miles per hour (mph) (88.5kilometers per hour (kmh)) for the new AAR-1B wheels and a critical speed of 50 mph (80kmh) for the hollow wheels. It also shows that the car with hollow wheels has higher lateral accelerations at speeds below the onset speed than is seen with new AAR1B wheels. It also shows that the hollow wheel distribution pattern (hollow wheel on one side of the truck or diagonally implemented in the truck) has little effect on stability.

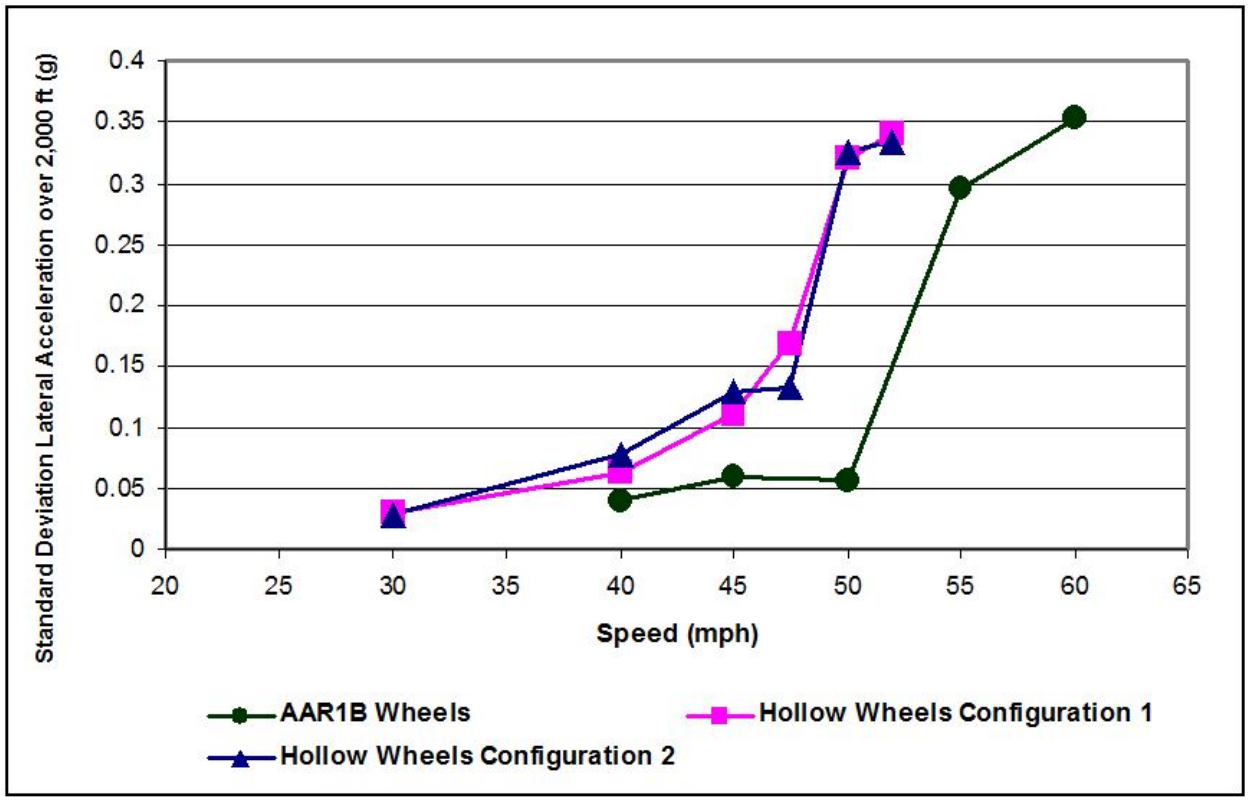

Figure 3. Freight Car Hollow Wheel Stability Test

Wheel wear on treads can lead to the formation of false flanges. There are two types of false flange: one kind is due to wheel hollowing so the false flange is on the field side of tread; the other kind is a raised ridge in the flange root. Field side false flanges with severe hollowness on tread not only generated high contract stresses on low rail in curve, but could also cause stock rail (in a switch) rollover derailment (Kerchof 2004, Wolf 2006).

Wheel wear on treads and flanges could also generate high impact on frogs. Hollow wheels (wheels with false flange) were present in the New York City Transit system (Cabrera and Gobbato 2000), which contributed to the fast wearing of the Frog noses and risers on standard frogs, and the associated vibration and noise. It was recommended in the report to investigate the most appropriate profile for re-trued wheels that will counteract the development of false flanges. It was also suggested to limit the false flange (hollowness) to a maximum of 0.125 inch (3.2mm), as part of the wheel maintenance criteria.

The Denver RTD light rail transit system uses a 0.05-inch (1.3mm) tread wear (hollowness) limit for wheel maintenance. The wheel profile was checked against the template profile every 40,000 miles, and the wheel is trued if the tread shows 0.05-inch (1.3mm) gap.

Setting up a wear limit for wheels is a complicated issue. It depends on vehicle and track design, maintenance standards, and operational environment. Wear limit also needs to be justified through economic analysis. Section 3 discusses the effects of wheel wear on contact geometry and vehicle performance.

2.3 Wheel Diameter Differences in One Axle

The two wheels on one axle can wear into asymmetric shapes, which results in a wheel diameter difference on one axle. Wheel diameter differences caused by wear or truing has significant effects on car performance.

No comprehensive study of the effects of wheel diameter differences on rail transit vehicle stability has been performed recently. In 2006, a freight car tolerance study (Tunna et al. 2006) was conducted to investigate the effect of the opposite wheels on the same axle with mismatching circumferences. As Figure 4 shows, the lateral accelerations of a car with one tape size mismatch in circumference increased gradually with speed above 40 mph (64.4kmh). In contrast, the car with matching wheel circumferences had a sudden increase in lateral accelerations at the critical speed. In the case of the one tape mismatch, the acceleration was above the AAR Chapter 11 limit of 0.13 g for speeds less than or equal to 70 mph (112.7kmh) — at the time of the study, the AAR lateral acceleration limit was 0.26g so at that time neither case exceeded the limit below 70 mph (112.7kmh).

Similar trends can be found in Figure 3, even though these two studies were conducted for different purposes. The same conclusion is that wheel diameter differences, caused by either asymmetric wear or by wheel truing, can lead to car instability.

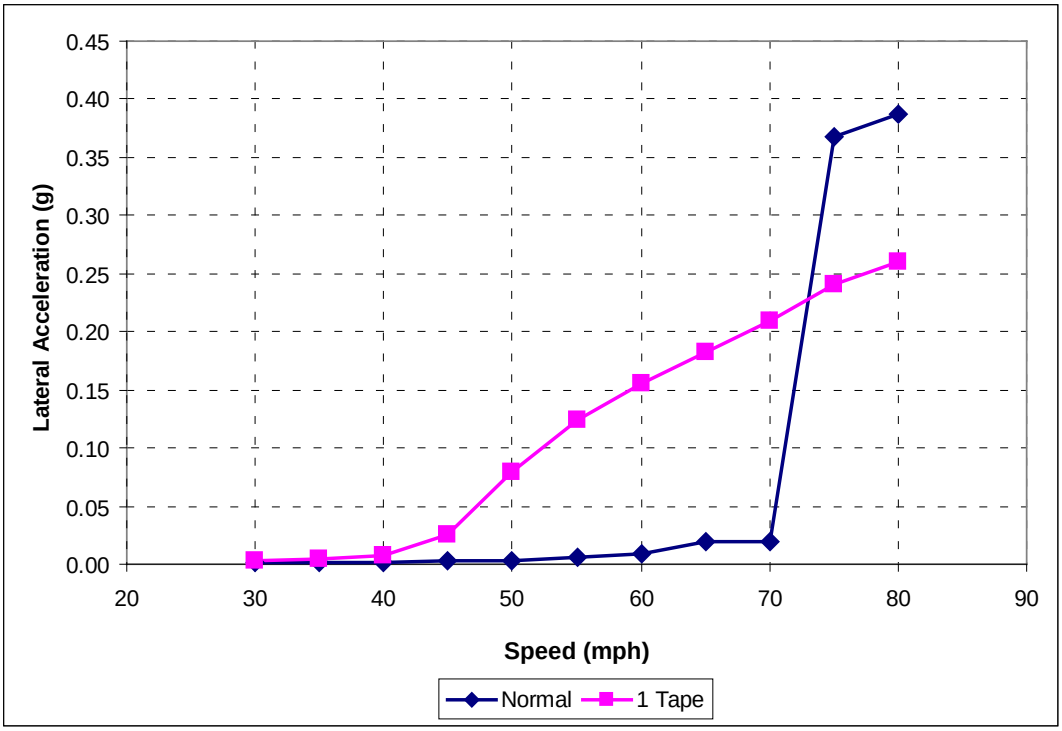

Figure 4. Effect of Wheel Diameter Difference on Freight Car Stability (1 Tape equals 0.125 inch on the circumference)

When a wheelset has wheels with mismatched circumferences, longitudinal wheel and rail creep forces are generated that steer the wheelset away from the centerline. The conicity of the wheels reduces the rolling radius difference (RRD) until an equilibrium rolling line is reached. The wheelset may have gained enough momentum to pass the equilibrium rolling line and develop longitudinal creep forces in the opposite direction. In this way, a cyclic pattern of wheelset displacement and forces can develop. This is shown for a wheelset with mismatching wheel circumferences in Figure 5. The cyclic pattern begins at the start of the run, before the lateral input to excite hunting, and continues throughout.

In contrast, for a wheelset with equal wheel circumferences, longitudinal forces are produced by the lateral track input, but these soon die away. The wavelength of the oscillations of the normal wheelset is approximately 50 feet (15.2m), which corresponds to the wheelset's kinematic wavelength. The wavelength of the oscillation of the wheelset with wheel circumferences that mismatch by one tape is approximately 17 feet (5.2m). Three cycles of oscillation appear to be in one kinematic wavelength.

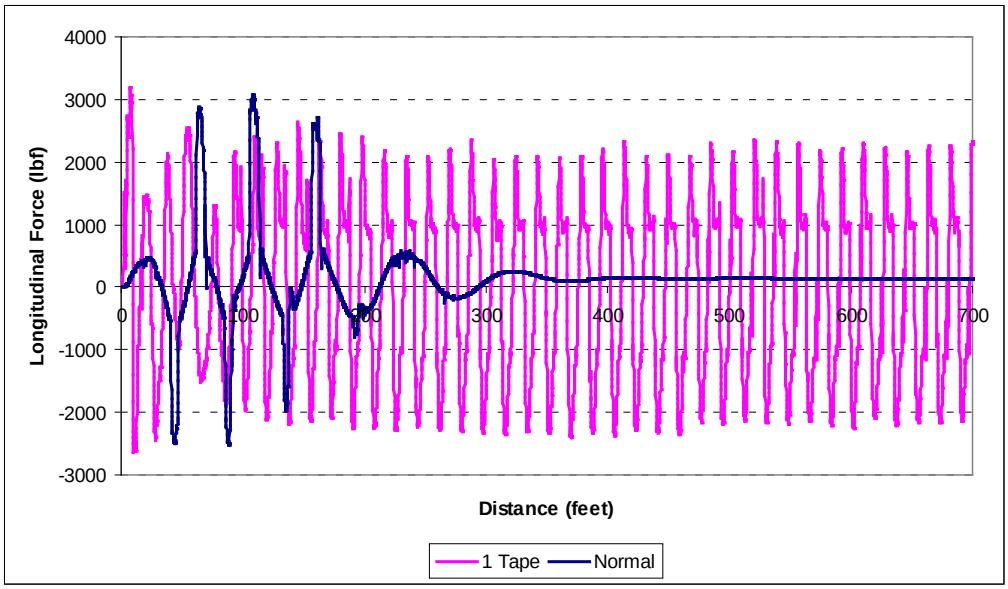

Figure 5. Longitudinal Forces on the Right Wheel of the Leading Wheelset at 60 mph (96.6kmh)

Clearly, both test and simulation show that car stability and ride quality are sensitive to wheel diameter differences in one axle. It is one of the key parameters for rail transit agencies to control in service and maintenance quality, as Table 4 shows.

Table 4. Transit Agency Wheel Diameter Tolerances

System	Diameter Tolerance after Wheel Re-profiling
Denver RTD	0.05 inch (1.27mm) within an axle 0.05 inch (1.27mm) for DS100 Truck, 0.25 inch for SD160 Truck 2.3 inches (58.4mm) truck-to-truck within the same car
PATH	0.125 inch (3.2mm) variation left-to-right within an axle 0.125 inch (3.2mm) axle-to-axle within a truck 0.25 inch (6.4mm) truck-to-truck within a car
BART	In service, 0.03 inch (0.8mm) within an axle; After cutting, 0.005 inch (0.13mm) 0.3125 inch (7.9mm) axle-to-axle within a truck 0.50 inch (12.7mm) truck-to-truck within a car
SEPTA	0.125 inch (3.2mm) within the same axle 0.25 inch (6.4mm) axle-to-axle in the same truck 0.50 inch (12.7mm) truck-to-truck in the same car
WMATA	0.0625 inch (1.6mm) within the axle 0.25 inch (6.4mm) axle-to-axle in the same truck 0.50 inch truck-to-truck in the same car
Chicago Metra Electric	0.125 inch (3.2mm) variation left-to-right within an axle 0.25 inch (6.4mm) axle-to-axle within a truck 0.25 inch (6.4mm) truck-to-truck within a car
CTA	0.047 inch (1.2mm) within an axle 1 inch (25.4mm) axle-to-axle in the same truck 1 inch (25.4mm) truck-to-truck within the same car

MiniProf™ (Greenwood Engineering A/S, Denmark) profilometers and software have been widely used for wheel and rail cross section profile measurement. The twin-head MiniProf can help to make accurate measurement of the two wheels on same radial position, but it cannot be used directly to measure wheel diameter. Recent developments in MiniProf extended its function to calculate wheel diameter, but additional input of inner diameter has to be measured with special MiniProf wheel instruments. Wheel tapes can also measure diameter, but the location of measurement is dependent on the flange wear. A portable wheel diameter measurement device is needed for rail transit agencies to accurately measure wheel diameters and variations caused by asymmetric wear or machining. The allowable wheel diameter difference maintenance limit depends on the vehicle and truck design, especially the truck suspension and other component maintenance limit. The effect of wheel diameter difference on vehicle performance will be investigated in Task 2 of this study.

2.4 Wheel Diameter Tolerance in One Truck

The wheel diameter difference in one truck does not affect car stability, but it may affect wheel load equalization. The freight car tolerance study (Tunna et al. 2006) showed that the vertical car performance affected by mismatching circumferences between the leading and trailing wheels were the empty cars with pitch and bounce track inputs. Figure 6 shows the minimum vertical load on the left wheel of the leading wheelset. The minimum vertical load is lower with the mismatching wheel circumferences, but it is still above the AAR Chapter 11 limit.

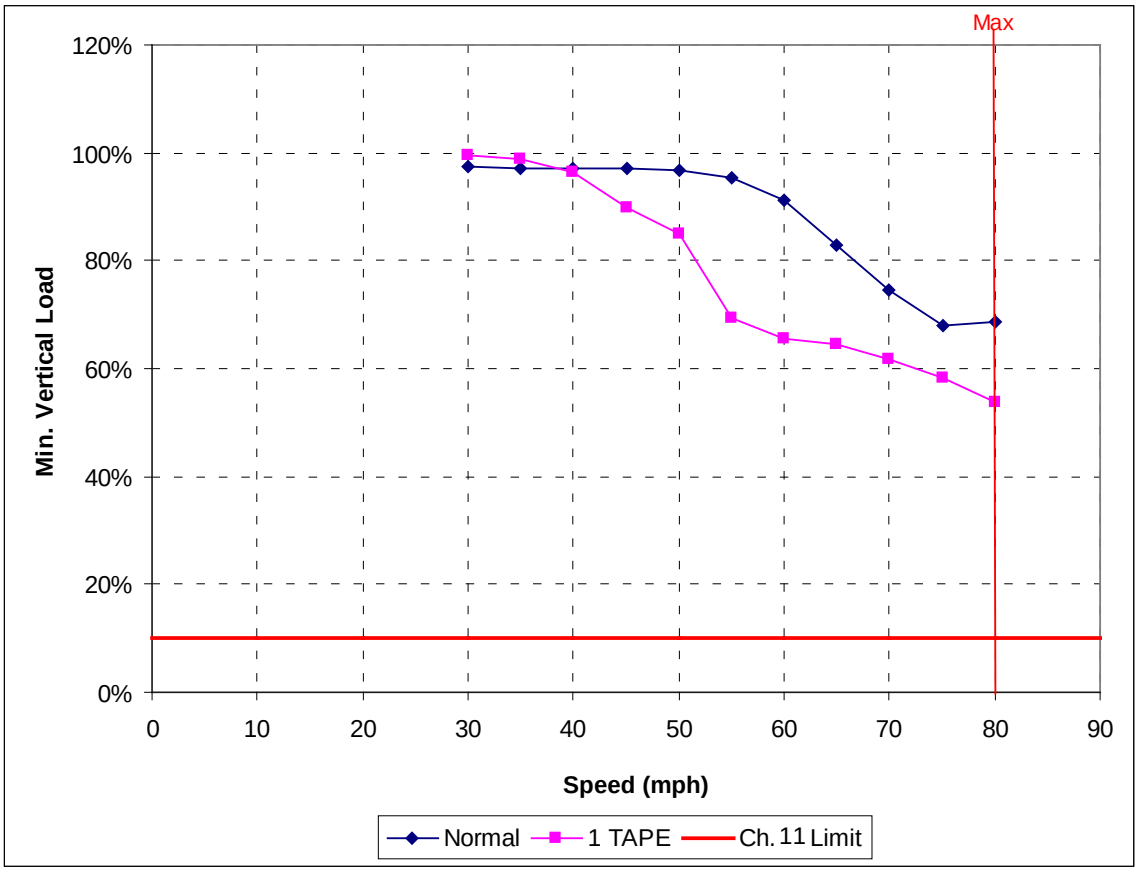

Figure 6. Effect of Mismatching Wheel Circumference on the Leading and Trailing Axle with Empty Freight Car and Pitch and Bounce Input

The effects of wheel diameter difference in one truck on transit vehicle dynamic performance, such as wheel load equalization, will be examined based on American Public Transportation Association (APTA) criteria (APTA 2007) in Task 2 of this project.

2.5 Wheel Diameter Tolerance in One Car

The wheel diameter difference from truck-to-truck in one car may cause unbalanced loading, leading to carbody vertical and pitch vibrations and deteriorated vertical ride quality. These effects were investigated in Part 2 Report of this study.

2.6 Wheel Flange Angle

The maximum flange angle of the designed wheel profiles applied in transit operation ranges between 63 and 75 degrees. Table 5 lists the wheel flange angles adopted by different rail transit agencies.

Table 5. Maximum Flange Angle of Transit Agency Designed Wheels

System	Light Railcars* (degrees)	Heavy Railcars** (degrees)	Commuter Railcar*** (degrees)
Denver RTD	66	NA	NA
PATH	NA	68	NA
BART	NA	68	NA
MBTA	72	NA	75
NJTC	75		72
SEPTA	60-65 (in specified tolerance)	63	72
WMATA		63	
Chicago Metra Electric			75
CTA		68	
Houston Metro	70		
DART	70		

*Light railcars: Two trucks or three trucks with articulation. Examples include MBTA (Boston, green line), Denver RTD, NJ Transit, Baltimore, Pittsburgh, Charlotte, MUNI (San Francisco), San Diego, San Jose (Valley), Portland, St. Louis, and SEPTA. These cars can be high floor, low floor, or a combination of both, and are formerly referred to as street cars or trolley cars.

**Heavy railcars: These types of cars have two trucks, examples include: NYC Transit, PATH, SEPTA (Philadelphia, subway), WMATA, MARTA, Baltimore, CTA, Los Angeles, MBTA (Boston) and BART.

***Commuter railcars: These types of cars have two trucks, examples include: Metro North, LIRR, METRA (Chicago), SEPTA (Philadelphia, commuter service), Caltrans (California), MARC (Baltimore), MBTA (Boston).

Increasing the design wheel flange angle to reduce the risk of flange climb derailment has been a common practice for rail transit agencies. Due to historic reasons, some older rail transit agencies have adopted the relatively low wheel flange angles in the range of 63 to 65 degrees. The low flange angles are prone to flange climb derailment and have less compatibility with different truck designs. Newer rail transit agencies generally start with a wheel profile having a flange angle of 72 to75 degrees, as recommended by APTA (APTA SS-M-015-06 2007).

A wheel profile with a higher flange angle can reduce the risk of flange climb derailment and can have much better compatibility with any new designs of vehicles and trucks that may be introduced in the future compared to wheels with lower flange angles. Also, with a higher lateral to vertical (L/V) ratio limit, high flange angles will tolerate greater levels of unexpected track irregularity.

Measurements showed the wheel flanges usually wear into a steeper flange angle in service, which decreases the flange climb derailment risk (Shu and Tunna 2007). However, wheels with high flange angles and nonconformal contact on rails can result in higher wear rates than wheels with shallow flange angles. Rail transit agencies suffering flange climb derailments may need to change to wheels with steeper flange angles to reduce derailments, but they may also have to contend with excessive wear through rail grinding and lubrication (Griffin 2006).

A detailed study on wheel flange climb derailment and criteria was published from a previous study for TCRP (Wu et al. 2005).

2.7 Other Wheel Inspections

Transit railcar maintenance also includes inspections of any cracks or fatigue shells on wheel flanges and treads. If a crack or shelling defect on the tread or flange surface is larger than 0.375-inch (9.5mm) diameter, the wheel is usually considered nonserviceable. If a crack or shelling defect on the tread or flange surface is smaller than 0.375-inch (9.5mm) diameter, the wheel is to be scheduled for truing. Other wheel inspections may include the following:

Wheel separation
Loose retaining ring if applicable
Rotation of wheel hub with respect to axle and/or wheel tire with respect to wheel center
Safety wired axle caps

2.8 Wheel Truing

2.8.1 Truing Cycle and Wheel Life

Wheel truing is performed to remove any defects on wheels such as flats, shellings, and spalls, or to restore the worn wheel shape to a designed shape (truing template). Wheels are usually trued several times until the wheel rim thickness reaches its limits. Table 6 lists the fixed truing cycles and wheel life periods in different rail transit agencies.

Table 6. Transit Agency Wheel Truing Cycles and Wheel Life

System	Truing Cycle	Wheel Life
Denver RTD	40,000 miles	400,000 miles (6~7 years)
Houston Metro	30,000 miles	Power Truck 350,000 miles Center Truck 250,000 miles
PATH	3 years	New fleet about 8 years with 40,000 miles/year
SEPTA (Streetcar lines)	150,000 miles	10 years
WMATA	1 year	400,000 miles or 4.5 years
NJT Commuter Rail	60,000 miles	250,000 miles
CTA	NA	5 years
BART	108,000 miles	324,000 miles

Most rail transit agencies trued wheels based on fixed cycle (certain number of mileage or service years) regardless of condition. Many rail transit agencies also trued wheels because of diameter mismatch, not just hollow or flange wear. Some rail transit agencies trued wheel either in a fixed cycle or based on the service conditions. For example, NJT wheel truing (light rail) is performed either at fixed intervals, i.e., every 30,000 to 40,000 miles depending on the truck design, or as periodic measurements indicate the need for corrective action (Lovejoy et al. 2012).

2.8.2 Truing Surface Roughness

Two types of wheel re-profiling machines are commonly used. Figure 7 shows the milling type that has a cutting head with many small cutters. The arrangement of the cutters forms the wheel profile. Figure 8 shows the lathe type truing machine. The single cutter cuts the wheel by following the shape of a template.

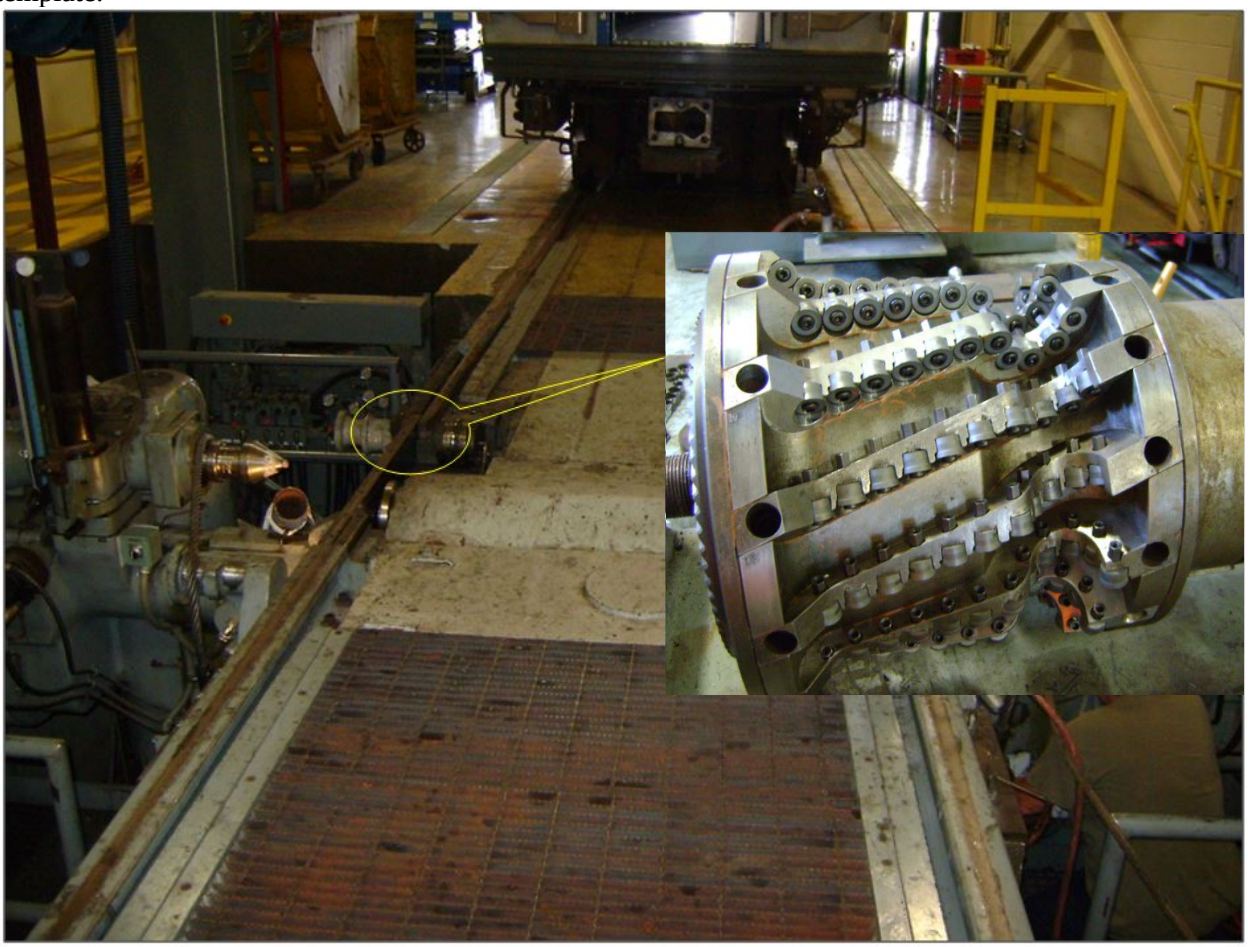

Figure 7. Milling Type Wheel Truing Machine

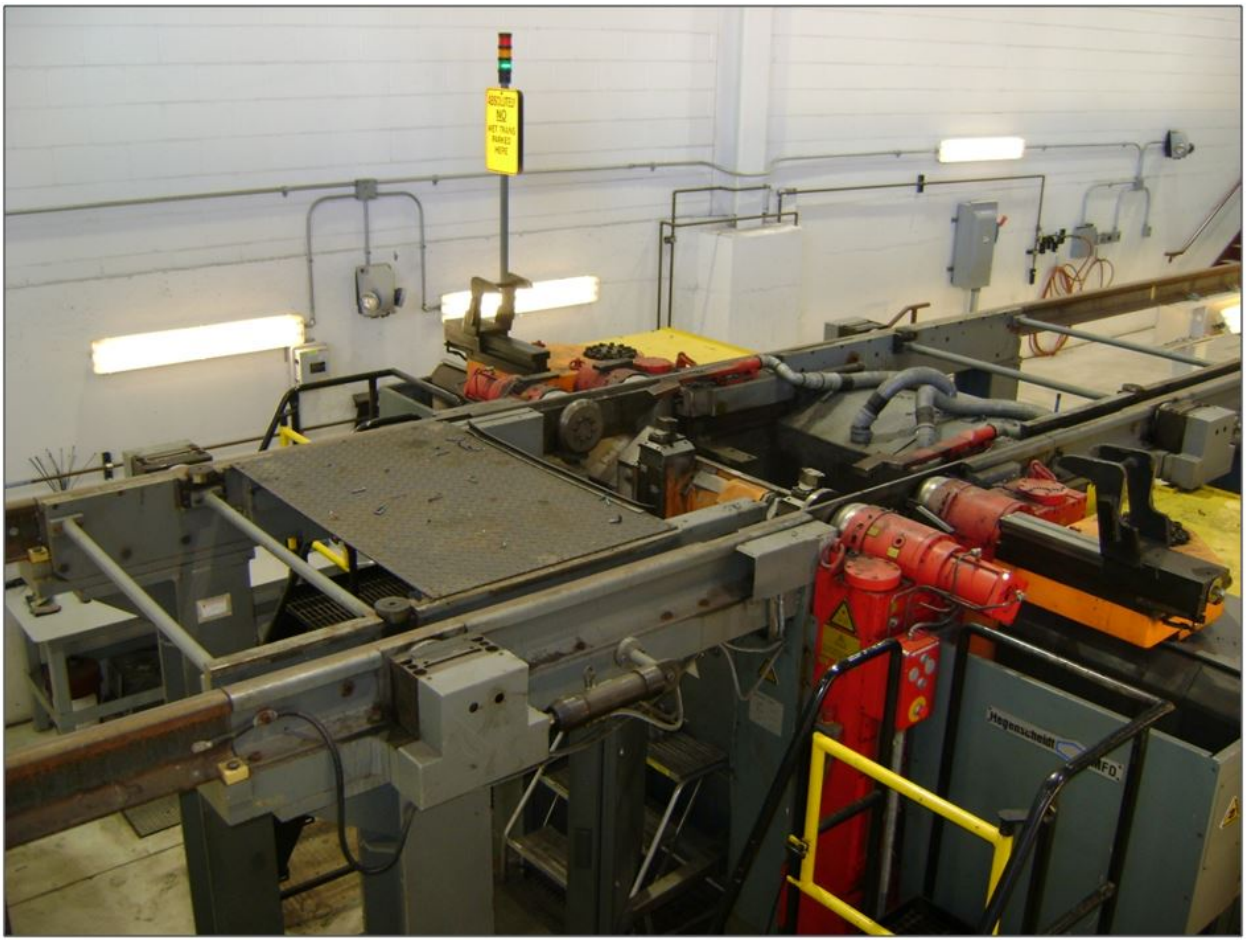

Figure 8. Lathe Type Wheel Truing Machine

Several rail transit agencies have reported flange climb derailments occurring at curves or switches in yards when the cars were just out of the wheel re-profiling machines. This type of derailment is often caused by the wheel surface roughness after wheel truing. Figure 9 shows the rough wheel surface just after truing with a milling type truing machine. The wheel surface trued by a lathe type truing machine is usually smoother than that trued by a milling type machine.

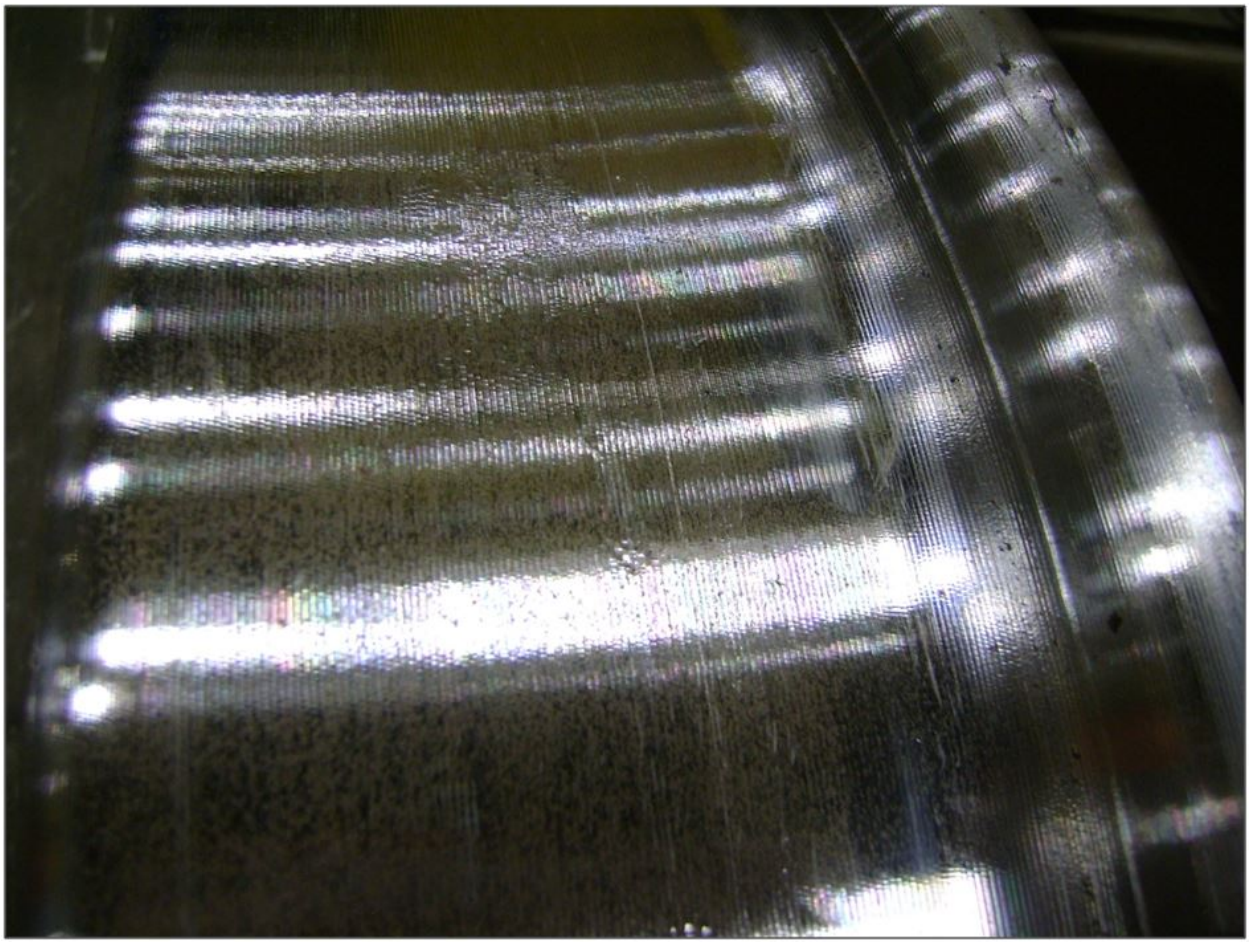

Figure 9. Rough Wheel Surface from Milling Type Truing Machine

The rough surface produced by wheel truing increases the effective coefficient of friction between wheel and rail, which significantly reduces the L/V ratio limit for flange climb. A low flange angle further increases the derailment risk.

Several remedies may improve the surface condition:

Frequently inspecting the cutting tools — especially for the milling type machine. Dulled tools can produce a very rough surface. Sometimes the grooves on the wheels were obvious.

Addressing the final surface turning. In this step, there is no significant material removal, but rather a light cut for smoothing the surface. WMATA has included this step in its wheel re-profiling procedures.

Further, lubrication after wheel truing can be an effective way to prevent flange climb derailment on newly trued wheels. WMATA now manually lubricates all wheels immediately after truing. CTA has installed wayside lubricators on the curves as well as guardrails in their yards to prevent derailment.

2.8.3 Truing Templates

Most rail transit agencies trued wheels to restore their shape to the original design shape. The original wheel design profiles usually came from car manufacturers. They may or may not be the optimal profiles for the vehicle and track in a transit, according to current understanding of rail and wheel contact mechanics. An optimal wheel profile has to be compatible with the rail profiles in various track configurations, including tangent, curves, and special trackwork, such as switches, frogs, and guards and restraining rails.

Once a new wheel profile has been accepted, any changes to the wheel profile (especially tread and flange width) must be evaluated by both vehicle and track designers. New wheels generally wear much faster during the wear-in period, and then reach a relatively stable shape compatible with rail shapes. The length of the wear-in period depends on the conformality of wheel and rail shapes. The design wheel profile is usually compatible with new rail profile, but less compatible with the worn rail shape. The worn wheel does not necessarily need to be restored to its design shape; instead, it should be trued to be compatible with the majority of the existing worn rails.

NJT has developed intermediate wheel profiles for their wheel truing template. The template is determined by software incorporated in the wheel truing machines. As many as 20 variants of corrective actions are recommended by the machine so as to minimize the removal of metal from the wheels. With this program in place, the NJT light rail system has increased resilient wheel life dramatically, typically achieving 200,000 to 250,000 miles of service before tire replacement is necessary (Lovejoy et al. 2012).

The survey of PATH found that the design wheel generates two-point contact on the worn rail, as Figure 10 shows. The two-point wheel/rail contact results in not only high contact stress and wear, but also poor steering performance. However, the worn wheel has a conformal contact on worn rail, as Figure 11 shows, which is in favor of good truck curving performance.

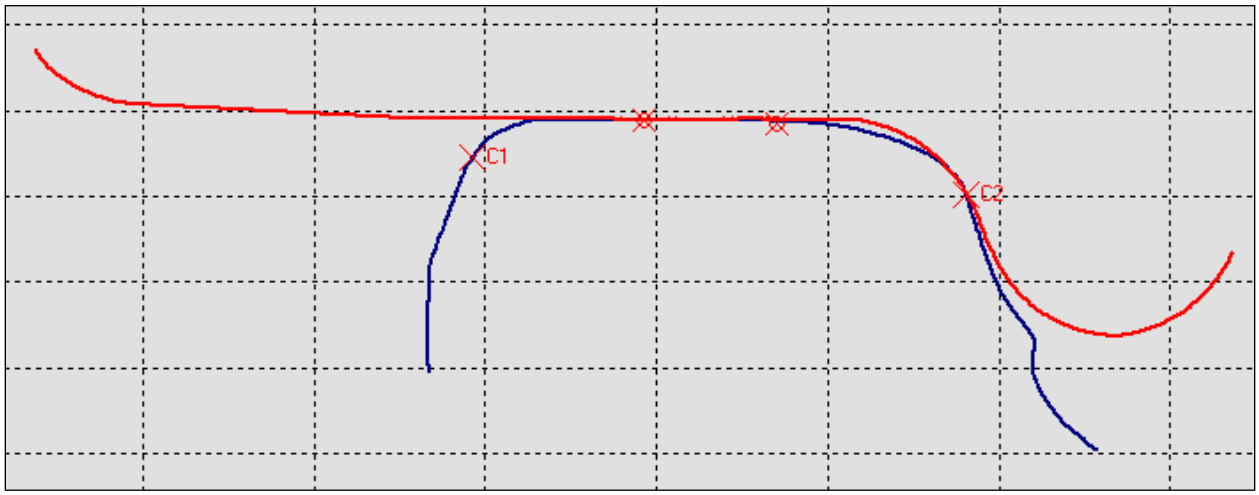

Figure 10. New Wheel Contact on Worn High Rail

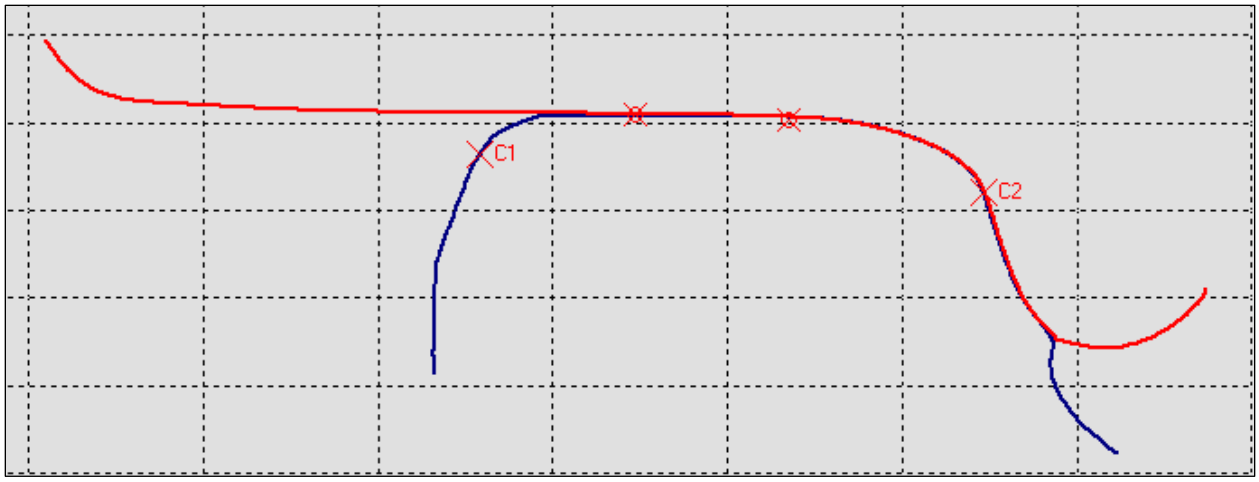

Figure 11. Worn Wheel Contact on Worn High Rail

The design wheel profile (truing template) used by PATH is not compatible with the majority of the existing rails, and thus it is not recommended for wheel truing. Detailed wheel/rail dynamic analysis will be conducted in Task 2 of this study to generate guidelines for wheel maintenance, including how to generate an optimized wheel profile for truing. A new wheel truing template for PATH will be proposed to demonstrate the procedures using these guidelines.

CHAPTER 3

State-of-the-Art Wheel Profile Design and Maintenance Principles

Wheel profiles have a significant effect on wheel/rail contact and overall vehicle and track dynamic performance. A design of a new wheel profile well suited for a specific vehicle, track, and service environment can improve vehicle and track dynamic performance and reduce wear and damage on wheel and rail. In spite of a large number of publications on this topic, wheel profile design still remains a challenge for truck design and maintenance.

3.1 Wheel Profile Design Methodology

Researchers have adopted various methods with different targets and strategies to develop a new theoretical wheel profile, and the following are examples of profile design based on:
Target RRD function (Smith and Kalousek 1991, Shevtsov et al. 2005)
Target contact angle (Shen et al. 2003)
Target conicity and wide contact range (Polach 2009)

Typically, a wheel profile was designed using a trial and error approach to reach design targets. Wheels cannot be designed without reference to rail profiles. Theoretical or measured rail and/or wheel profiles were usually selected as "seeds" or references during the design process.

Smith and Kalousek 1991 developed a numerical procedure for design of a wheel profile described by a series of arcs. Although the procedure was specifically developed for steered axle rail transit vehicles, some important aspects of it can be applied to conventional rail transit systems as well.

Shevtsov et al. 2005 proposed a procedure for design of a wheel profile that improves wheel and rail interaction by reducing wear while taking into account rolling contact fatigue. The procedure uses an optimality criteria based on a RRD function. The criteria accounts for stability of a wheelset, minimum wear and contact stresses of wheels and rails as well as safety requirements. Using the proposed procedure, Shevtsov et al. designed a new wheel profile and conducted simulations using ADAMS/Rail software.

Shen et al. 2003 proposed a wheel profile design method using a target wheel/rail contact angle function and rail profile information. A computer program was developed to produce an independent wheelset profile for a rail transit car.

Polach 2009 investigated the relationship between the equivalent conicity, contact angle, and location of the contact area in nominal position, the contact stress, and lateral contact spreading on worn rail profiles. New wheel profiles were created with a target conicity and at the same time wide contact spreading.

Persson and Iwnicki 2004 and Novales et al. 2006 used optimization procedures based on a genetic algorithm to design a wheel profile for railway vehicles. Two existing wheel profiles were chosen as "parents," and "genes" were formed to represent these profiles. These genes were mated to produce offspring genes and then reconstructed into profiles that had random combinations of the properties of the parents. Each of the offspring profiles were evaluated by running a computer simulation of the behavior

of a vehicle fitted with these wheel profiles and calculating a penalty index. An inverted penalty index was used as the fitness value in the genetic algorithm. The method was used to produce optimized wheel profiles for two variants of a typical vehicle, one with a relatively soft primary suspension and the other with a relatively stiff primary suspension.

The development of the standard AAR-1B wheel profile for North American railroads involves methodologies of traditional manually modifying wheel profiles, computer–aided analysis (NUCARS®* simulations), and revenue service tests (Leary et al. 1991). Until 1990, the AAR 1:20 wheel profile was the AAR standard for interchange service. Experience showed that a substantial amount of the tread and flange wear occurred before a steady state of wear was established by the wheel. Additionally, when the 1:20 wheel wore in to a new profile after 20,000 to 50,000 miles of service, problems with lateral stability and truck hunting were frequently encountered.

The awareness of the need for a new standard profile was heightened by the introduction of a "Heumann" profile wheel by the Canadian railroads. The Canadian National (CN) Heumann profile was created based on expansions of rail shapes. This profile was designed to provide single-point contact with the then prevailing AREMA 115-pound rail section. The reported reduction in wheel wear brought about by this wheel was quite significant.

As a result, the Research and Test Department of the AAR was requested by its Mechanical Division to develop an alternative wheel profile that would provide better performance than the 1:20 wheel profile.

The development of the now standard AAR-1B wheel profile advanced through four different research phases. The first phase was concerned with the general definition of the problem, accompanied by a statistical field survey of existing worn wheel and rail shapes. In the second phase, a method was derived that allowed the development of statistically and analytically based profiles. These profiles were established from known wheel and rail shapes and kept within generally accepted safety and performance criteria. In the third research phase, the candidate profiles developed in the first two steps were put through a series of acceptance tests, design adjustments were made to the flange throat, and a partial 1:20 profile was added to the tread. In the final phase, revenue service tests were carried out. The results of the wear tests indicated very favorable economics in terms of reduced wear and fuel consumption.

Over the last decade, heavy haul operation in North America railroads has been changing the vehicle and track service environment, and freight railroads are facing new challenges related with maintenance of wheel and rail interface (Tournay 2009).

In 2006, failures of primary suspension adapter pads and loaded car hunting were reported on a particular type of heavy axle load 286,000-pound grain railcars. Associated with these failures was some degradation of polymer elements in the constant contact side bearings used on these railcars. Initial observations revealed that the railcars were hunting under load at speeds approaching 50 mph (80 kmh). The root causes have been found to be system related: a combination of low truck warp restraint, high wheelset conicity and loaded body inertial and suspension characteristics. This leads to coupled resonance at speeds as low as 47 mph (75 kmh) between the kinematic motion of the wheelset and body yaw. An interim solution is the use of stiffer and more durable adapter pads; longer term solutions are a truck with higher warp stiffness combined with management of the wheel/rail interface to reduce conicities from the observed high values of 0.7.

A new standard freight car wheel profile is being evaluated at TTCI under the AAR Strategic Research Initiatives (SRI) Program to replace the AAR-1B profile for improving railcar stability and reducing wheel and rail rolling contact fatigue in freight rail operations (Wu 2007).

*NUCARS® is a registered trademark of Transportation Technology Center, Inc., Pueblo, Colorado

3.2 Wheel Profile Design and Maintenance Criteria

The objectives of optimum wheel and rail profiles are to provide:
Stable performance over the range of normal train speeds
Safety from derailment under adverse but realistic operating conditions
Maximized wheel and rail life

Wheel and rail profile design is a matter of optimizing several criteria. Some criteria must be satisfied, but some can be compromised to achieve an overall optimum solution. The following criteria are usually used to design a wheel profile:
Lateral Stability — should be achieved for normal operating speeds in the empty and loaded conditions; hunting performance depends on the nonlinear conicity function
Maximum Contact Angle — should be greater than 72 degrees to avoid flange climbing derailments; APTA recommends at least 72 degree (suggested tolerance +3° and -2°) angle for commuter cars (APTA SS-M-015-06 2007)
L/V Ratio — should be less than 0.8 to avoid flange climbing derailments
Wear Index — should be as low as possible to avoid wear on wheels and rail in curves
Contact Stress — should be as low as possible; high contact stress contributes to rolling contact fatigue and metal flow
Contact Position — should be widely spread to avoid concentrated wear; should not be too far toward the field side of the rail to avoid rail rollover moments
Rolling Resistance — should be as low as possible to reduce power consumption and draft forces

In theory, all these criteria apply to not only new wheel design, but also to wheel maintenance. However, wheels and rails gradually wear and change their profiles in service; therefore, their contact geometry properties can never keep constant. Three of these performance indices, car lateral stability, wheel/rail contact position, and stress, are significantly affected by wheel/rail wear. The effects of wear on these criteria are mostly negative, leading to car instability, deteriorated ride quality, and damage to wheels and rails.

3.3 Wheel/Rail Contact Conicity

Conical wheels have a conical taper on tread, as Figure12 shows. The taper is to promote self-centering in tangent track and generates some degree of steering in shallow curves.

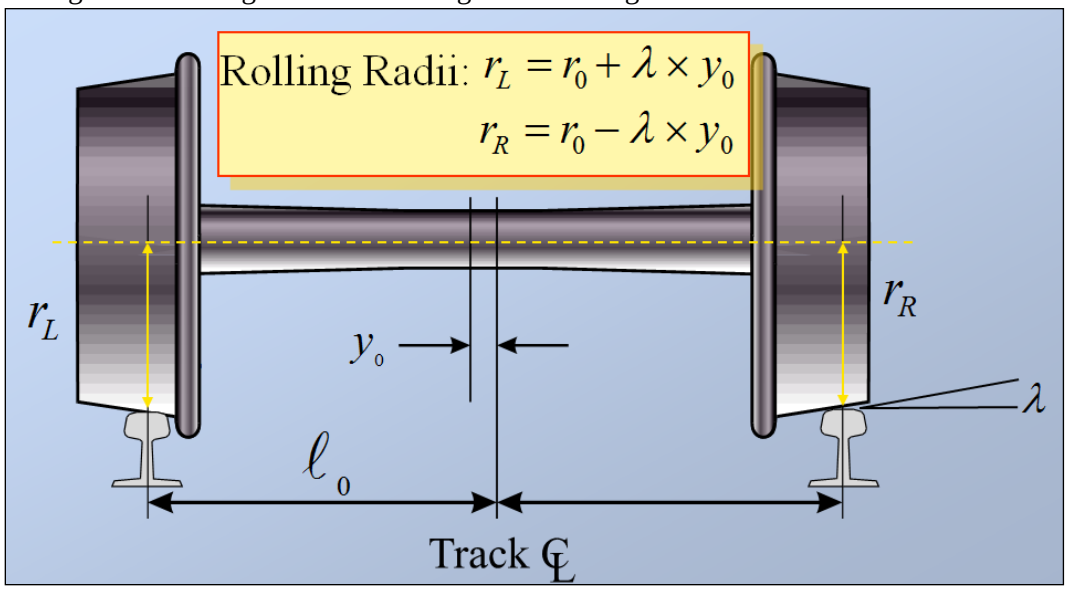

Figure 12. Wheel and Rail Contact Geometry

The kinematical properties of wheel and rail contact, such as rolling radius, contact angles, and wheelset roll angle vary as the wheelset moves laterally relative to the rails. The nature of the functional dependence between these geometrically constrained variables and the wheelset lateral position is defined by the wheel and rail profiles.

An important characteristic of the contact between wheels and rails is the rolling radius of a wheel at the contact point. This radius can be different for the right and the left wheel as a wheelset moves laterally. The RRD results in relative creep movement between wheel and rail on the contact points. The forces generated from the contact geometry constraints and wheel/rail friction can not only steer the wheelset to move along the track center, but also lead to hunting. The wheel/rail contact geometry has significant effects on vehicle dynamic performance including curving and hunting.

An important parameter to characterize the wheel/rail contact geometry is equivalent conicity (or effective conicity). In general, the effective conicity is defined by Equation 1 (IHHA 2001):

$$\lambda = \frac{RRD}{2y_0} \tag{1}$$

where y_0 is the wheelset lateral shift.

In 2007, APTA drafted a standard to define a stability taper for the measurement of wheel tread taper on wheels used in commuter rail service in relation to vehicle and truck stability (APTA SS-M-017-06 2007). The stability taper is similar to the traditional tread taper, but calculated with a contact location weighting function that uses a normal distribution centered on the mean value of wheelset lateral shift with a standard deviation.

Critical hunting speed is inversely proportional to square root of conicity; the higher the conicity the lower the critical speed. A high equivalent conicity can lead to wheelset and truck hunting, whereas a very low conicity can lead to combined oscillation of vehicle body and truck due to a resonance between the truck weaving movement and an eigenmode (natural frequency) of the vehicle body (Smith and Kalousek 1991, Polach 2009).

The equivalent conicity defined in Equation 1 is half of the slope of the linearized wheel RRD function in the range of wheel lateral shift before reaching flange contact. For a new wheel with constant taper on the tread, the RRD function is almost linear in the range of wheel/rail clearance, as Figure 13 shows. The equivalent conicity for a new tapered wheel and rail is proportional to the tread taper slope.

For a worn wheel, the RRD function is nonlinear, and the equivalent conicity defined in Equation 1 is negative, as Figure 14 shows. The negative equivalent conicity reveals the limit of the definition in Equation 1.

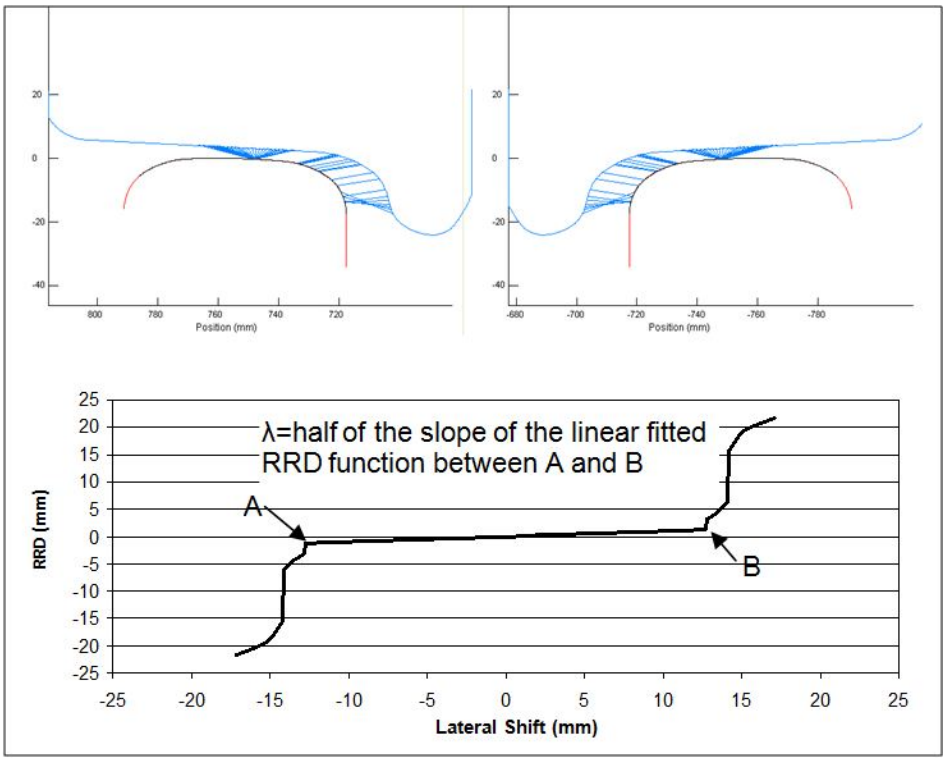

Figure 13. Contact of New AAR-1B Narrow Flange Wheel on New AREMA 136-RE Rail, 10-inch Crown Radius, 1:40 Cant, at a Gage of 56.5 inches

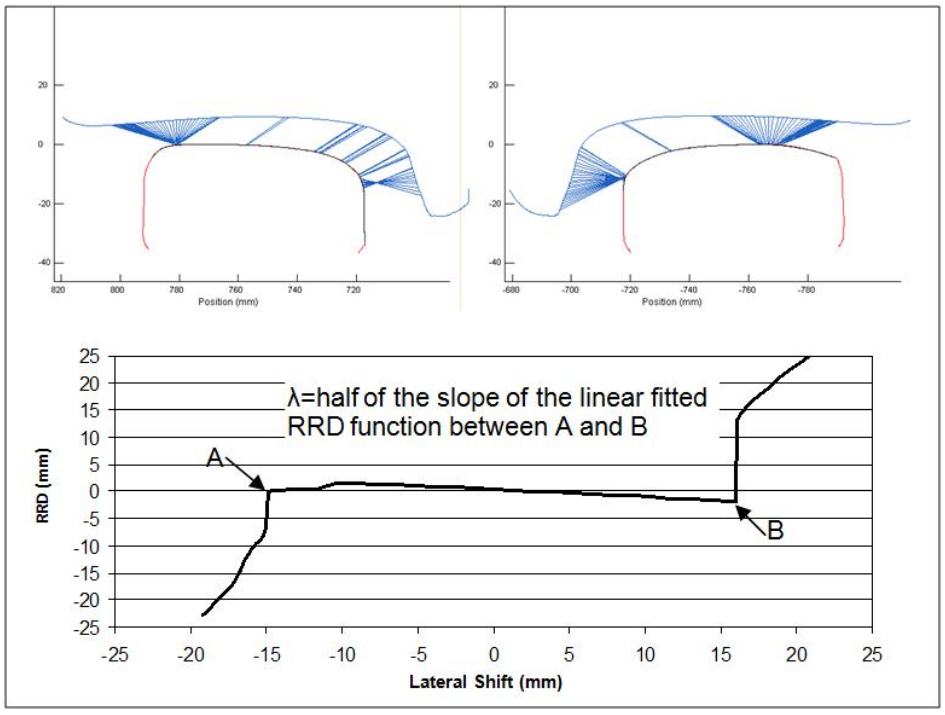

Figure 14. Contact of Hollow Worn Wheel on Tangent Worn Track at a Gage of 56.5 inches

There are several other definitions and methods for equivalent conicity calculation. Among them the following methods are frequently used to calculate the equivalent conicity:
Equivalent linearization by the application of Klingel formula defined in International Union of Railways UIC 519 standard 2004
Linear regression of the function of RRD defined in UIC 519 standard 2004
Harmonic quasi-linearization (Polach 2009)

These three methods produce a nonlinear equivalent conicity function over the range of wheelset lateral displacement that is different from the single value conicity defined in Equation 1.

Polach 2009 investigated the effects of nonlinearity of the equivalent conicity function on car instability performance and proposed two parameters to characterize the car hunting behavior: (1) the equivalent conicity at the specified wheelset lateral shift, and (2) its slope on the equivalent conicity function. His study concluded that:
A wheel/rail contact with low equivalent conicity and positive slope of the equivalent conicity function usually leads to a sudden occurrence of a limit cycle wheelset movement with large lateral shift amplitude at a critical speed. The critical speed is usually referred to as hunting speed.
A wheel/rail contact with high equivalent conicity and negative slope of the equivalent conicity function usually leads to a limit cycle wheelset movement with an amplitude slowly growing with increasing speed. The limit cycle usually occurs at speeds far below the traditional hunting speed.

UIC 518 standard 2005 recommends that wheel/rail contact equivalent conicity values for all axles in a car should be distributed so that the equivalent conicity value 0.2±0.05 occurs in a range of wheelset lateral displacement between ±2mm and ±4mm for the majority of assessed conditions. Because the wheel/rail clearance in Europe is usually less than that in North America, the application of UIC 518 and UIC 519 standards on rail transit vehicle performance assessment needs to be further investigated.

3.4 Correlation between Wheel Wear and Equivalent Conicity

Wheel profiles, regardless of tapered or cylindrical wheel, change from new shapes to worn shapes during service. Even a new wheel profile that is based on worn shapes often changes its tread shape due to tread wear. Wheel/rail wear results in wheel/rail contact geometry change and consequently changes car dynamic performances including curving, hunting, and ride quality.

Guidelines or standards for wheel wear limits or wheel diameter mismatching tolerance could be generated from the nonlinear equivalent conicity function to improve car dynamic performances and maintenance efficiency.

A nonlinear equivalent conicity function is a promising index to characterize variation of wheel/rail contact geometry caused by wheel wear or mismatching after truing. However, the correlation between the wheel wear or wheel diameter mismatching and the nonlinear equivalent conicity function is not fully understood. Further, wheel/rail contact equivalent conicity functions in one truck or in a railcar could be different from axle-to-axle, as Figure 15 shows. The effects of multiple-axle equivalent conicity functions and truck suspensions on railcar performances are unclear. This is an area that requires additional research.

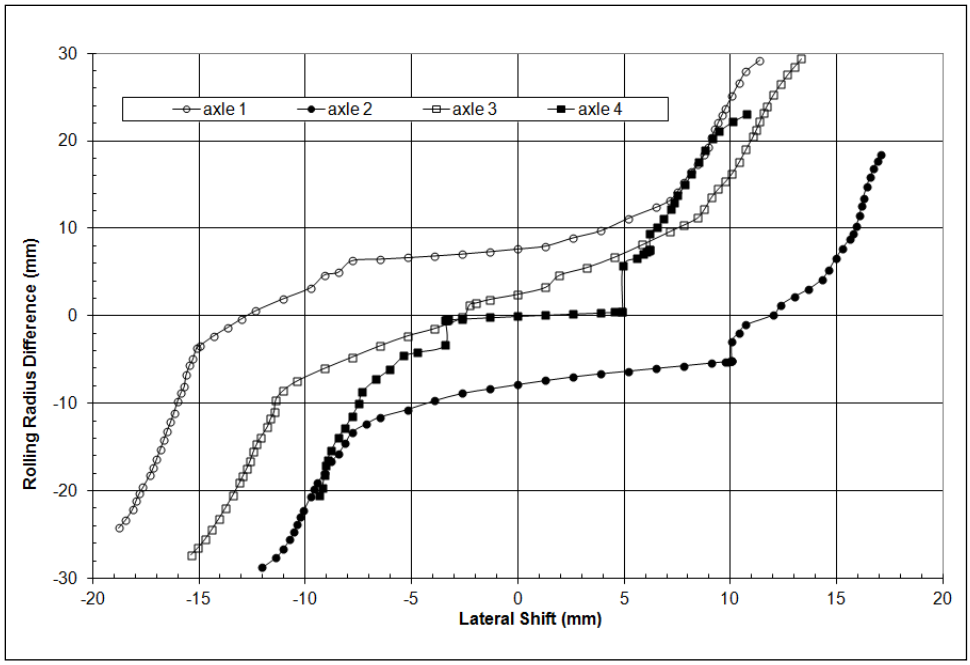

Figure 15. RRD Functions Measured in a Freight Railcar

CHAPTER 4

Conclusions and Recommendations

The following conclusions and recommendations are made from the survey of wheel profile maintenance practices in rail transit agencies and the literature review:

- Wheel slide and wheel flats are mainly caused by braking and low adhesion conditions. New anti-slip technologies and devices are needed to reduce wheel flats.
- Wheel diameter difference on one axle has a significant effect on car lateral stability performance. Allowable wheel diameter difference maintenance limit depends on vehicle and truck design, especially the truck suspension and the maintenance limits of other components.
- Wheel diameter difference in one truck affects car vertical performance such as the wheel load equalization capability.
- Most rail transit agencies surveyed do not have wheel tread wear limits. Wheel wear has significant effects on vehicle and track performance. Setting up wear limits on wheels is a complicated issue. It depends on vehicle and track design, the maintenance standards of truck components, and operational environment.
- A new wheel design or truing template should be optimized on the basis of existing rail wear conditions, vehicle design and maintenance standards, and special trackwork maintenance requirements.
- Wheel truing template profiles need to be evaluated periodically to take into account existing rail wear conditions.
- Rough surfaces on wheels from wheel truing can increase the risk of flange climb derailment. Smooth surfaces and lubrication could reduce the flange climb derailment risk.
- The effect of the following maintenance limits on railcar performance will be further investigated in Task 2 of this project:
  - Wheel diameter differences on one axle, one truck and one car
  - Wheel wear and patterns
  - Multiple-axle wheel wear and patterns
  - Car type and suspension parameters
  - The nonlinear equivalent conicity function is a promising index to characterize variation of wheel/rail contact geometry caused by wheel wear or mismatching after truing. However, the correlation between the wheel wear or mismatched wheel diameter and the nonlinear equivalent conicity function has not been fully established.
  - The application of equivalent conicity defined in UIC 518 and UIC 519 standards to North American rail transit car performance assessment needs to be further investigated.

Guidelines for wheel profile maintenance will be established through Task 2 of this project.

References

American Public Transit Association. APTA SS-M-014-06, Standard for Wheel Load Equalization of Passenger Railroad Rolling Stock, 2007.

American Public Transit Association. APTA SS-M-015-06, Standard for Wheel Flange Angle for Passenger Equipment, 2007.

American Public Transit Association. APTA SS-M-017-06, Standard for Definition and Measurement of Wheel Tread Taper, 2007

Association of American Railroads. *Field Manual of the AAR Interchange Rules*, Washington, D.C., 2012

Cabrera, A. and G. Gobbato. Redesign of Frog Geometry at New York City Transit to Reduce Vibration, Noise and Accelerated Wear, *Proceedings of AREMA Conference*, September 2000.

Griffin, T. *TCRP Report 114: Center Truck Performance on Low-Floor Light Rail Vehicles*. Transportation Research Board of the National Academies, Washington, D.C., 2006.

International Heavy Haul Association. Guidelines to Best Practices for Heavy Haul Railway Operations: Wheel and Rail Interface Issues. Virginia Beach, Virginia, May 2001.

Kerchof, B. Interaction of Tread-hollow Wheel and Worn Switch Point / Stock Rail, *Proceedings of AREMA Conference*, 2004.

Kumar, S. (Tranergy Corp.) *TCRP Research Results Digest 17: Improved Methods for Increasing Wheel/Rail Adhesion in the Presence of Natural Contaminants*. TRB, National Research Council, Washington, D.C., 1997.

Leary, J.F., S.N. Handal, and B. Rajkumar. Development of Freight Car Wheel Profiles – A Case Study. Vol. 144. *Wear*, 1991.

Magel, E. and J. Kalousek. Martensite and Contact Fatigue Initiated Wheel Defects, *Proceedings 12th International Wheelset Congress*, Qingdao, China, September 1998, pp. 110-111.

Nelson, J. and T. Wilson (Ihrig, & Associates, Inc.). *TCRP Report 23: Wheel/Rail Noise Control Manual*. TRB, National Research Council, Washington, D.C., 1997.

New Jersey Transit press release. NJ Transit Unveils Aqua Track to Prevent Wheel-Slip Conditions, http://www.njtransit.com/tm/tm_servlet.srv?hdnPageAction=PressReleaseTo&PRESS_RELEASE_ID=721, Accessed December 2003.

Novales, M., A. Orro, M.R. Bugarín. A New Approach for the Design of Wheel Profile Geometries. *Proceedings of 7th World Congress on Railway Research*, Montreal, Canada, 2006.

Parsons Brinckerhoff, Inc. *TCRP Report 155: Track Design Handbook for Light Rail Transit*, Second Edition, Transportation Research Board of the National Academies, Washington, D.C., 2012.

Persson, I. and S.D. Iwnicki, Optimisation of Railway Profiles using a Genetic Algorithm. *Vehicle System Dynamics*, Supplement to Vol. 41, 2004.

Polach, O. Wheel Profile Design for the Target Conicity and Wide Contact Spreading. *Proceedings of the 8th International Conference on Contact Mechanics and Wear of Wheel/Rail System*, Italy, 2009.

Sawley, K., C. Urban, and R. Walker. The Effect of Hollow-Worn Wheels on Vehicle Stability in Straight Track, *Wear*, Vol. 258, Issues 7–8, 2005.

Shen, G., J.B. Ayasse, H. Chollet, and I. Pratt. A Unique Design Method for Wheel Profiles by Considering the Contact Angle Function. *Proc. Instn. Mechanical Engineers*, Part F: *J. Rail and Rapid Transit*, Vol. 217, 2003.

Shevtsov., I.Y., V.L. Markine, C. Esveld. Design of Railway Wheel Profile Taking into Account Rolling Contact Fatigue and Wear, *Wear*, 2005.

Shu, X. and J. Tunna. Investigation into Flange Climbing Derailment and Distance Criterion with Wheel and Worn Rail Profiles. Research Report R-982, Association of American Railroads, Transportation Technology Center, Inc., Pueblo, CO, 2007.

Shu, X. and N. Wilson. *TCRP Report 71 : Track-Related Research, Volume 7 : Guidelines for Guard/Restraining Rail Installation*. Transportation Research Board of the National Academies, Washington, D.C., 2010.

Smith, R.E. and J. Kalousek. A Design Methodology for Wheel and Rail Profiles for Use on Steered Railway Vehicles, *Wear*, Vol. 144, 1991.

Tournay, H. Investigation of Vehicle/Track and Bogie Parameters Leading to Loaded Wagon Lateral Instability. *Proceeding of International Heavy Haul Association Conference*, Shanghai, China, 2009].

Tunna, J., X. Shu, and J. Dasher. Investigation into the Effects of Geometric Tolerances on Freight Car Dynamics, *Proceedings of ASME International Mechanical Engineering Congress*, November 2006.

UIC Leaflet 519, Method for Determining the Equivalent Conicity, 2004.

UIC Leaflet 518, Testing and Approval of Railway Vehicles from the Point of View of Their Dynamic Behavior – Safety – Track Fatigue – Ride Quality, 2005.

Wolf, G. Switch Point Derailments: Is It the Point or the Wheel, *Journal of Wheel/Rail Interaction*, 2006.

Wu, H., X. Shu, and N. Wilson. *TCRP Report 71 : Track-Related Research, Volume 5 : Flange Climb Derailment Criteria and Wheel/Rail Profile Management and Maintenance Guidelines for Transit Operations*. Transportation Research Board of the National Academies, Washington, D.C., 2005.

Wu, H. Control of Wheel/Rail Wear and Rolling Contact Fatigue. *Proceedings of International Heavy Haul Association Conference*, Kiruna, Sweden, 2007.

Wheel Profile Maintenance Guidelines

PART 2

Wheel Profiles Design and Maintenance Guidelines for Rail Transit Operation

Table of Contents

TABLE OF CONTENTS i
LIST OF FIGURES ii
LIST OF TABLES iv
SUMMARY 1
CHAPTER 1 Introduction 3
CHAPTER 2 Development of Wheel Profile Design and Maintenance Guidelines for Rail Transit Operations 4
2.1 Wheel Profile Design Considerations 4
2.2 Guidelines for Improving Curving Performance 5
2.3 Guidelines for Improving Hunting Performance 10
2.3.1 Hunting and Safety Criteria 10
2.3.2 Development of a W/R Contact Geometry Based Hunting Criterion 14
2.3.3 New Design Wheel Hunting Performance Evaluation 20
2.4 Guidelines for Contact Stress and Wear Performance 22
2.5 Guidelines for Compatibility with Special Trackwork 26
2.5.1 Turnouts 26
2.5.2 Switch Point Protectors 28
2.5.3 Spring Switches 30
2.6 Wheel Profile Maintenance Guidelines 31
2.6.1 Wheel Diameter Difference 31
2.6.2 Wheel Wear 36
CHAPTER 3 Conclusions and Recommendations 44
REFERENCES 46
APPENDIX Light Railcar Hunting Speed Contour Chart 47

List of Figures

Figure 1. Measured Wheel Profiles 6
Figure 2. Existing and New Design Wheel Profiles 6
Figure 3. L/V Ratio, Existing 63-degree Wheel on New Rail, No Track Perturbations 8
Figure 4. L/V Ratio, New Design 70-degree Wheel on New Rail, No Track Perturbations 8
Figure 5. L/V Ratio, Existing 63-degree Wheel on New No. 8 Turnout, Down-and-out Track Perturbations 9
Figure 6. L/V Ratio, New Design 70-degree Wheel on New No. 8 Turnout, Down-and-out Track Perturbations 9
Figure 7. A Constrained Single Axle with Conical Wheel 10
Figure 8. Effect of Conical Wheel Conicity on Hunting Speed 11
Figure 9. Relationship between Hunting Speed and Root Square of Conicity 11
Figure 10. Time History Comparisons of Conical Wheel Hunting (65 mph) and No Hunting (64 mph) 12
Figure 11. Limit Cycle Movements of Conical Wheel Hunting (65 mph) and No Hunting (64 mph) 13
Figure 12. Two-line Wheels Contact on AREMA 115RE Rails Used for Hunting Simulations 14
Figure 13. Subcritical and Supercritical Hunting Cases 15
Figure 14. Ride Quality of Subcritical and Supercritical Hunting 16
Figure 15. Truck Frame Accelerations at Different Speeds (45-degree flange angle wheel) 17
Figure 16. Truck Frame Accelerations at Different Speeds (63-degree flange angle wheel) 17
Figure 17. Truck Frame Accelerations at Different Speeds (70-degree flange angle wheel) 18
Figure 18. W/R Equivalent Conicity and Clearance Effects on Hunting Speed 19
Figure 19. Hunting Speed Contour Chart for Representative Heavy Railcar 19
Figure 20. Existing and New Design Wheel Conicity (56.25-inch gage) 20
Figure 21. Existing and New Design Wheel Conicity (56.25-inch gage) 21
Figure 22. Truck Frame Accelerations of the Existing and New Design Wheel (56.25-inch gage) 21
Figure 23. Measured Rail Profiles in Curve 23
Figure 24. Contact Stress of the Existing and New Design Wheels on New Rails 23
Figure 25. Contact Stress of the Existing and New Design Wheels on Worn Rails 24
Figure 26. Track Curvature Distribution 24

Figure 27. Comparison of Wear Index for the Existing and New Design Wheel 25
Figure 28. Cylindrical Wheel Contact on a Worn Switch 26
Figure 29. Tapered Wheel Contact on a Worn Switch 26
Figure 30. A Worn Wheel Contact on a Worn Switch Point and Stock Rail 27
Figure 31. A Taper Wheel and Cylindrical Wheel Contact on a Frog 28
Figure 32. Switch Point Protector 28
Figure 33. A Larger Chamfer Wheel Contacts on a New Switch Point Guard 29
Figure 34. A Smaller Chamfer Wheel Contacts on a New Switch Point Guard 29
Figure 35. Spring Switch in a Light Rail Transit System 30
Figure 36. W/R Contact on Spring Switch Points 31
Figure 37. Wheel Diameter Difference (in the Same Axle) Effect on Hunting (56.25-inch gage) 32
Figure 38. Wheel Diameter Difference Effect on Wear Index 33
Figure 39. Wheel Diameter Difference Effect on Rolling Resistance 33
Figure 40. Wheel Diameter Difference Effect on Wheel L/V Ratio 34
Figure 41. Wheel Diameter Difference Effect on Wheel Lateral Force 34
Figure 42. Wheel Diameter Difference Effect on Wheel Unload 35
Figure 43. Measured New and Worn Wheel Conicity, Track Gage 56.25 inches 36
Figure 44. Hunting Speed Estimation for a Car Equipped with Measured New and Worn Wheels 37
Figure 45. Truck Frame Accelerations of a Car Equipped with Measured New and Worn Wheels (56.25-Inch Gage) 38
Figure 46. Measured New and Worn Wheel Conicity, Track Gage 56.5 inches 38
Figure 47. Measured New and Worn Wheel Conicity, Track Gage 57 inches 39
Figure 48. Wheel Wear Effect on Hunting 39
Figure 49. Effect of Wheel Wear on Ride Quality 40
Figure 50. No. 20 Turnout Frog Profiles 41
Figure 51. W/R Impact Loads on a New Frog 41
Figure 52. New and Worn Wheel Wear Index in Curves with New Rails 42
Figure 53. New and Worn Wheel Lateral Forces in Curves with New Rails 43

List of Tables

Table 1. Case Study Parameters..... 22

Summary

Transportation Technology Center, Inc., (TTCI), a wholly owned subsidiary of the Association of American Railroads (AAR), was contracted by the Transit Cooperative Research Program (TCRP D-07, Task Order 20) to develop wheel profile maintenance guidelines for rail transit operations.

The effects of wheel profile and wheel/rail (W/R) interaction on car dynamic performances, including lateral stability, curving, W/R contact stress, wear and performances in special trackwork, have been investigated using NUCARS®[1] simulations. The following guidelines were developed from this study:

- Both W/R contact conicity and W/R gage clearance have significant and complex effects on car lateral stability (hunting), especially as the wheels and rails wear. A new method for evaluating the combined effects of these two parameters was developed using Hunting Speed Contour (HSC) charts. To demonstrate the new method, two HSC charts were developed for a representative heavy railcar and a representative light railcar. The charts were used to generate the following guidelines for wheel profile design and maintenance:
  - Hunting speed generally decreases (car becomes more unstable) with the increase of both conicity and W/R clearance.
  - Wheel and rail wear increases W/R clearance, and its effect on hunting depends on wear pattern:
    - Worn wheels with high conicity and wide W/R clearances cause the hunting speed to decrease quickly
    - Worn wheels with low conicity and wide W/R clearances cause the hunting speed to decrease slowly, but may result in sudden onset of hunting instability
  - Hunting speeds for high conicity wheels are more sensitive to W/R clearance variations than for low conicity wheels.
  - HSC charts may be used to evaluate new wheel profile designs and also to evaluate worn wheels (and rails), and develop wear and gage clearance tolerances. To provide specific conicity and gage clearance guidelines for a particular vehicle in a rail transit system, a new HSC chart would need to be developed using simulations for the particular case.
- Increasing the maximum flange angle can effectively reduce flange climb derailment risk. American Public Transportation Association (APTA) recommends a 72-degree (with tolerance +3 degrees and -2 degrees) flange angle wheel for use in commuter railcars. However, a wheel profile with a flange angle less than 72 degrees (but high enough to prevent flange climb) can also be adopted to provide a smooth transition from an existing low flange angle wheel profile to a new design with high flange angle wheel profile.
- Wheel profiles (new and worn) should be compatible with special trackworks:
  - Impact forces on the switch frog nose generally increase with wheel wear.
  - Wheels with profiles that are incompatible with the frog generate significant impact on the switch frog.
  - High flange angle wheels can reduce flange climb derailment risk and reduce excessive switch point tip wear in spring switches.
- Wheel diameter differences on an axle can improve hunting performance because of the decrease of W/R gage clearance when the axle shifts (moves laterally) from the track center position toward the smaller radius wheel. However, wheel diameter differences may result in poor curving performances, such as more wear and larger lateral forces on high rails, which may cause gage spreading.

[1] NUCARS® is a registered trademark of Transportation Technology Center, Inc.

  - Systems with many curves may need tighter tolerances on wheel diameter differences than systems with few curves and mostly straight track.
- Wheel wear has significant effects on both hunting speed and switch frog impact. Wear limits on wheel treads and flanges can be determined by the HSC chart and impacts with switch frogs.

On-track tests are recommended to further validate these guidelines.

CHAPTER 1

Introduction

The Transportation Technology Center, Inc. (TTCI) is developing "Wheel Profile Maintenance Guidelines" under Project D-7, Task 20, for the Transit Cooperative Research Program (TCRP) to help transit systems minimize maintenance costs and maximize system performance. The objectives of this study are to:

- Investigate the effects of wheel profiles (include both new and worn profiles) on rail transit vehicle performance (safety and ride quality)
- Develop wheel profile maintenance guidelines for rail transit operations (light rail and heavy rail systems)
- Develop guideline implementation procedures demonstrated with examples

The tasks of this project include:

- Task 1 – Survey current wheel profiles and maintenance practices
- Task 2 – Develop wheel profiles maintenance guidelines
- Task 3 – Demonstrate wheel maintenance guideline implementation procedures

This report presents the development of wheel profile maintenance guidelines for rail transit operations. The optimum wheel and rail profiles are to provide:

- Stable performance over the range of normal train speeds
- Safety from derailment under adverse but realistic operating conditions
- Maximized wheel and rail life

Wheel and car performances are generally evaluated in the following two aspects for safety operations:

- Hunting (lateral stability) performance and ride quality
- Curving performance

In addition, the following aspects should be addressed for wheel profile design and optimization:

- W/R contact stress and wear
- Compatibility with special trackwork, including frog, switch, and switch point protector

Requirements from these aspects often conflict with each other. Wheel profile design and maintenance guidelines have been developed in this report to compromise these different requirements for an overall optimum solution.

CHAPTER 2

Development of Wheel Profile Design and Maintenance Guidelines for Rail Transit Operation

Wheel profile shape has significant effects on rail vehicle and track performances. Wheel and rail profile optimizations have been investigated intensively to improve car performances with the increase of car running speed and axle load, as described in the Task 1 literature review report for this study (Shu 2014). Different optimization approaches and concepts have been developed by researchers for specific or general objectives.

Various guidelines for wheel profile design and maintenance have been used or proposed for railroad and rail transit systems. Some guidelines have been commonly accepted by the industry, such as use of high flange angle wheels to reduce flange climb derailment risk and low tread conicity wheels to prevent hunting. However, some guidelines remain controversial, especially for hunting performance. A high equivalent conicity can lead to wheelset and truck hunting, whereas a very low conicity can lead to combined oscillation of the vehicle body and trucks due to a resonance between the truck waving movement and an eigenmode (natural frequency) of the vehicle body (Polach 1009, Smith and Kalousek 1991).

Dynamic simulation programs provide useful tools to improve vehicle and track design. Car curving performance predictions are more consistent with tests than that of hunting. Curving simulation results usually follow certain trends, while uncertainties exist among hunting simulation results because of the hunting sensitivity to nonlinear parameters in a vehicle and track system. This uncertainty is so strong that from an academic point of view, a researcher has asked: “Does a critical speed for railroad vehicles exist?” (True 1994)

However, car hunting is such a persistent dynamic behavior that railroads worldwide have adopted safety standards to prevent hunting. This study intends to re-examine the hunting related criteria and to provide a W/R contact geometry based hunting criterion for wheel profile design and maintenance.

2.1 Wheel Profile Design Considerations

Wheel profile shape is one of the fundamental aspects for new transit system design and existing system maintenance. Changing wheel profile shape is a common practice for a rail transit system to resolve vehicle and track dynamic performance issues. Derailment is the leading reason for changing wheel profiles especially for a system with low flange angle wheels. Other reasons may include poor ride quality, corrugation, and excessive wheel and rail wear.

The objective of changing an existing wheel profile is to not only fix specific problems but also to improve overall vehicle and track dynamic performances.

Wheel maximum flange angle has a significant effect on flange climb derailment. The derailment risk decreases with the increase of flange angle. The experiences of Massachusetts Bay Transportation

Authority's Type 8 car demonstrated that derailment accidents were significantly reduced by increasing wheel maximum flange angle from 63 to 75 degrees (Griffin 2006).

In addition to the maximum wheel flange angle, wheel tread taper is another parameter for wheel profile design and maintenance. The hunting speed (speed at which a railcar bogie or bogies begin to hunt) generally increases with the decrease of equivalent conicity. The equivalent conicity generated from the modified wheel profile and existing rail profile has to be designed to work with the car suspension system to ensure the hunting speed is higher than the current operation speed.

Once the maximum flange angle and tread taper are determined, the flange root that connects the wheel tread and flange could vary with different shapes. The flange root shape has significant effects on both curving (especially shallow curves) and hunting performances. Compromise on these two aspects (curving and hunting) is needed for optimal performance. A rule of thumb for flange root design is to start from the existing worn flange root shape and further modify it to optimize the curving and hunting performances. A worn flange root shape is usually conformal to the majority of existing worn rails and generates low contact stresses and less wear.

Other parts of a wheel that have potential contact with rails, such as the wheel flange back, tread end near the field side, and the wheel face, also have to be compatible with special trackwork, such as switches, frogs, guardrails, and switch point protectors. Incompatible wheel shapes and contacts with special trackworks not only generate high W/R impact forces and excessive wear on wheels and rails, but also could result in derailment.

The following subsections demonstrate with examples how all these aspects can be addressed comprehensively, and how new guidelines were developed for new wheel profile design and worn wheel maintenance.

2.2 Guidelines for Improving Curving Performance

Wheel wear on a representative heavy rail transit system was investigated, and an improved wheel profile was designed. The existing new wheels on this system are designed with a flange angle of 63 degrees. Rail transit systems using low flange angle (60 to 63 degrees) wheels often experience flange climb derailments on yard track and small number turnouts. The desirable wheel flange angle is above 72 degrees because a higher flange angle gives a higher wheel lateral force to vertical force (L/V) ratio limit required for wheel climb based on the Nadal criterion (Shu 2014).

Measurements showed the wheels and rails in the investigated rail transit system wore into a relatively consistent flange/gage face angle about 70 degrees, as Figure 1 shows. Adopting the existing 70-degree worn flange angle will provide a higher wheel L/V ratio limit to reduce the risk of wheel flange climb and achieve a smooth transition from existing low flange angle wheels.

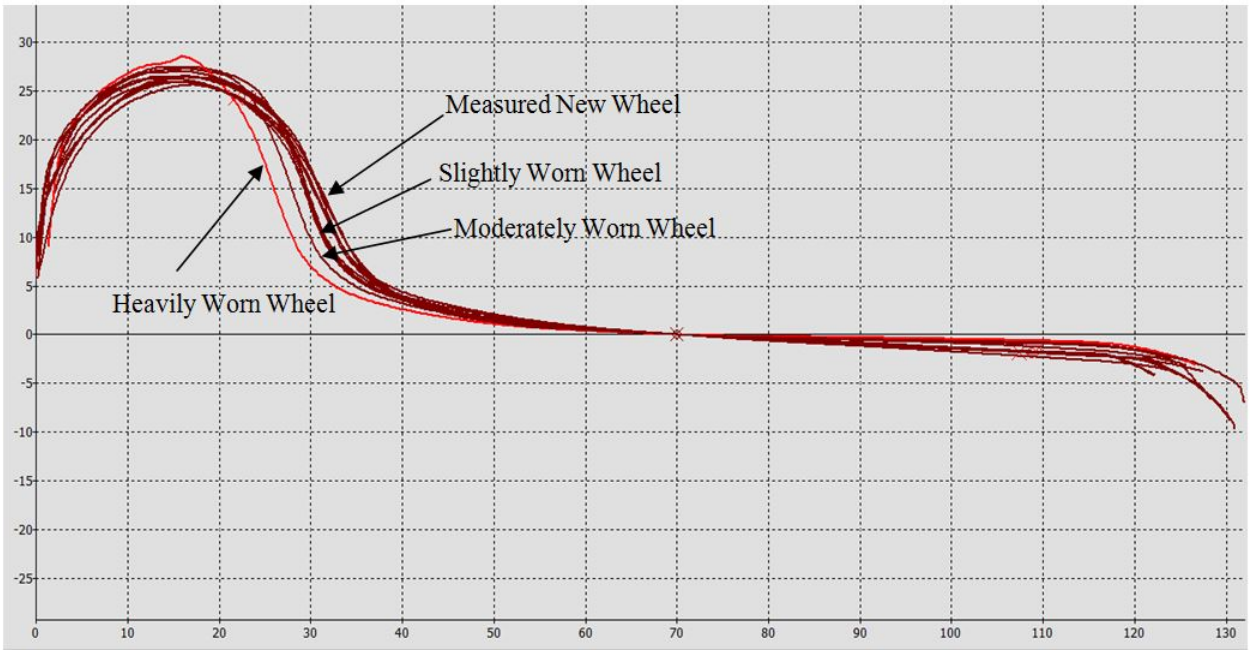

Figure 1. Measured Wheel Profiles

If wheels with a flange angle greater than 70 degrees are directly introduced, such as the 75-degree flange angle wheel that has been commonly adopted for many newly built transit systems, the resulting incompatible contact pattern with the existing worn rails will require aggressive wheel truing and rail grinding. The new improved design wheel profile thus uses a 70-degree flange angle and similar flange root shape of the worn wheels, as Figure 2 shows.

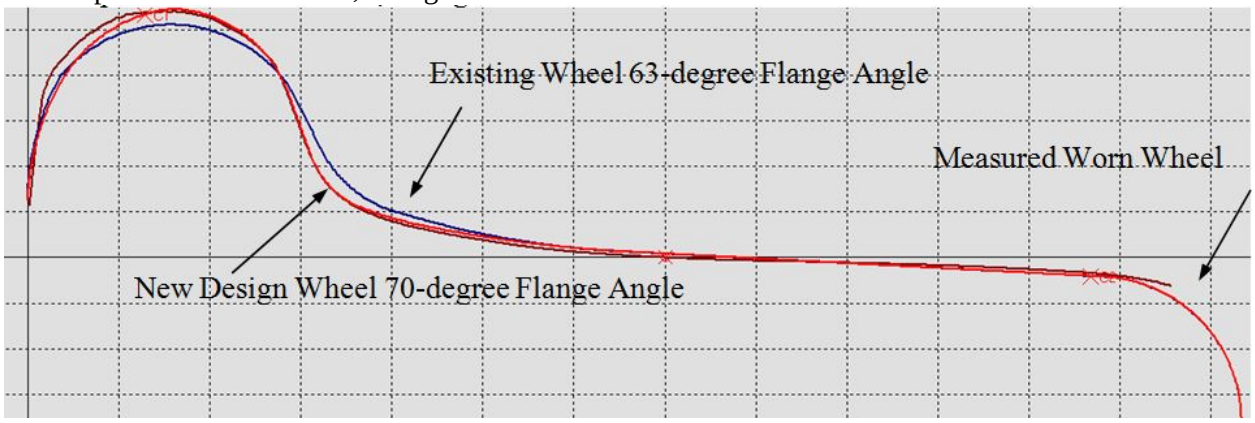

Figure 2. Existing and New Design Wheel Profiles

Computer simulations were conducted to evaluate the performance of the improved wheel profile in comparison to the existing wheel profiles. A typical heavy rail vehicle model with the following specifications was used in this study:

- Cylindrical bushing primary suspension
- Four-point air spring leveling secondary suspension system
- Lateral and vertical damper in secondary suspension
- Articulated truck frame
- Axle spacing: 7.5 feet

- Truck Center Spacing: 52 feet
- Wheel load: 9.45 kips
- Wheel diameter: 27 inches

Vehicle model parameters were measured through characterization tests. The measured primary suspension longitudinal and lateral stiffness and damping were reduced by half to simulate a worn truck condition. Measured track geometries, the standard American Railway Engineering and Maintenance of Way Association (AREMA) 115RE rail profile, and 0.5 W/R friction coefficient representing dry W/R contact conditions were used in the simulations.

A number of yard track geometries, all without restraining rails, were included in the simulations to compare the curving performances of the current 63-degree flange angle new wheel and the improved new design 70-degree flange angle wheel. These were:

- A 755-foot radius curve with 1-inch superelevation, 56.5-inch gage and 100-foot spirals.
- A 500-foot radius curve with 1-inch superelevation, 56.5-inch gage and 100-foot spirals.
- A 320-foot radius curve with 1-inch superelevation, 57.0-inch gage and 100-foot spirals.
- A 250-foot radius curve with 1-inch superelevation, 57.0-inch gage and 100-foot spirals.
- A No. 8 turnout with no superelevation and 56.5-inch gage.

The track geometries were represented as design case smooth track geometry with no track irregularities for yard curves, and a “Down-and-Out” perturbation for the No.8 turnout. The Down-and-Out perturbation consisted of a combination of track geometry irregularities that were of a magnitude at the limit stated in the transit system’s track standard. This consisted of a downward vertical cusp of 1.25-inch amplitude on the high rail combined with a 2-inch outward lateral alignment cusp on the high rail and an inward cusp on the low rail of a magnitude sufficient to ensure that the maximum permitted gage was not exceeded. These irregularities were of 31-foot wavelength with a haversine (1-cosine) shape.

In all cases, the vehicle speed was 15 mph, which is the speed limit for yard track. The W/R friction coefficient is also a factor that has a large effect on the potential for derailment. Therefore, all simulation cases were carried out for W/R friction coefficients of 0.3, 0.4, 0.5, and 0.6.

All of the simulation cases were modeled using TTCI’s NUCARS vehicle dynamics simulation program. The results are presented as graphs of the maximum wheel L/V ratio as a function of W/R friction coefficient. The maximum W/R L/V ratio was evaluated by using FRA’s *Code of Federal Regulations*, Track Safety Standards, Part 213, Subpart G, Section 213.333” (FRA March 2013).

Also plotted on the graphs is a line representing the Nadal limit for the particular W/R profile combination. Where the simulation results closely approach or cross this line indicates the potential for a flange climb derailment.

Figure 3 show the results for the cars equipped with the existing 63-degree wheel profiles running on new rails. The maximum L/V ratios on curves with 250- and 320-feet radii were close to the limit at 0.5-friction coefficient; the car derailed at 0.6-friction coefficient conditions even without any track perturbation. Figure 4 shows the significant improvement on curving for the car equipped with the 70-degree flange angle wheel; the maximum L/V ratios on curves with 250- and 320-feet radii were close to the limit at 0.6, but no derailments occurred.

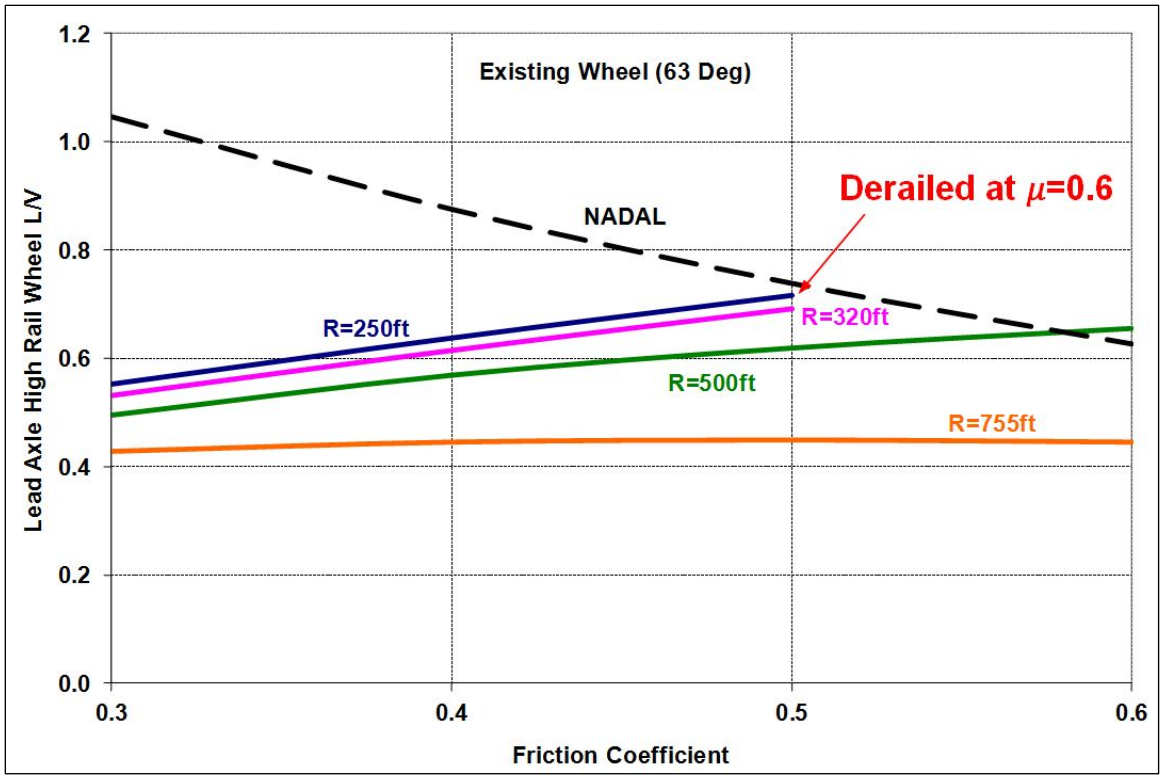

Figure 3. L/V Ratio, Existing 63-degree Wheel on New Rail, No Track Perturbations

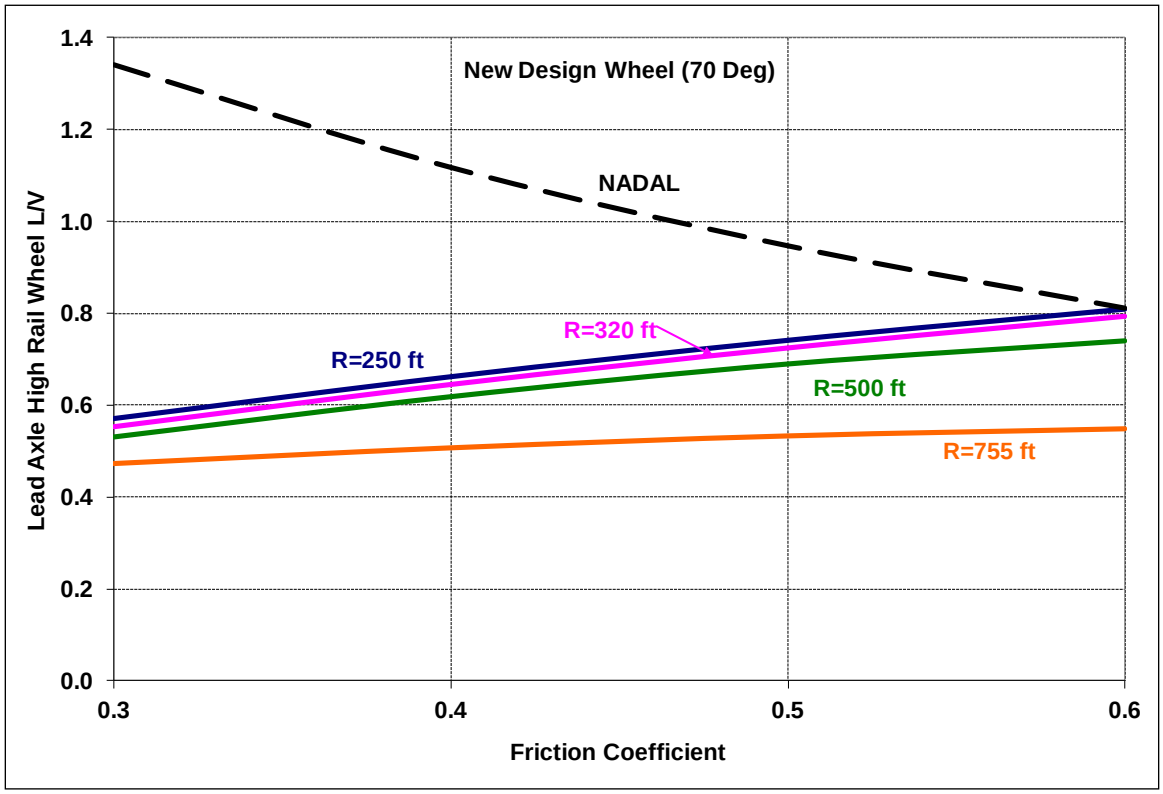

Figure 4. L/V Ratio, New Design 70-degree Wheel on New Rail, No Track Perturbations

Figure 5 shows the car with the 63-degree flange wheel exceeding the L/V ratio limit at 0.5-friction coefficient, derailing at 0.5-friction coefficient on a No. 8 turnout. Figure 6 shows that even though the maximum L/V ratio of the 70-degree flange angle wheel exceeded the limit at 0.6-friction coefficient, no derailment occurred on the No.8 turnout.

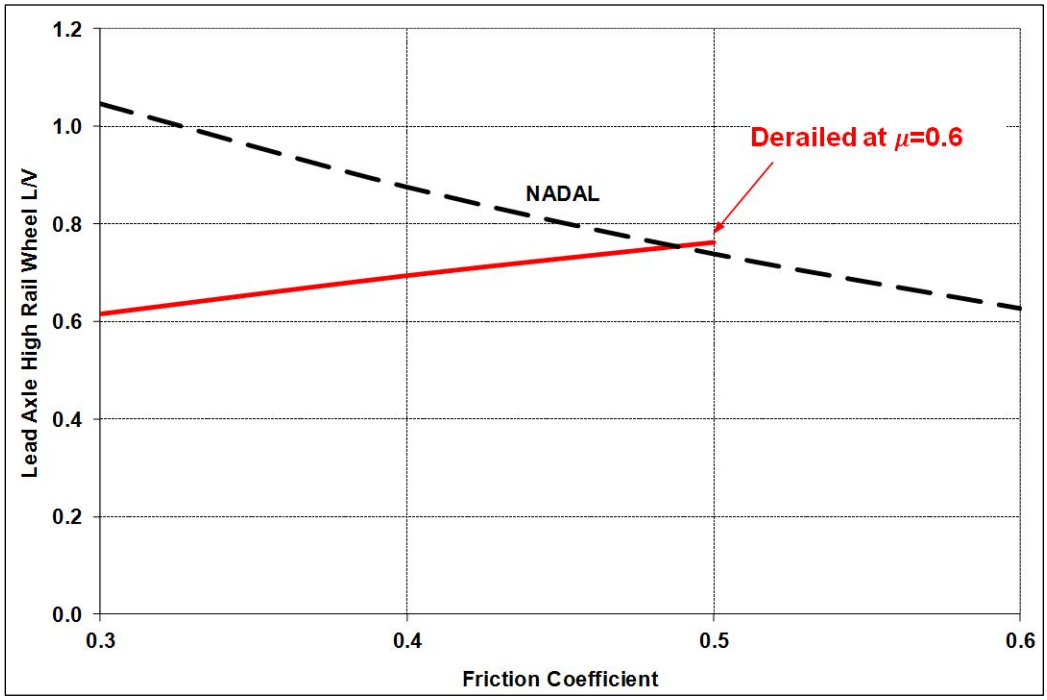

Figure 5. L/V Ratio, Existing 63-degree Wheel on New No. 8 Turnout, Down-and-out Track Perturbations

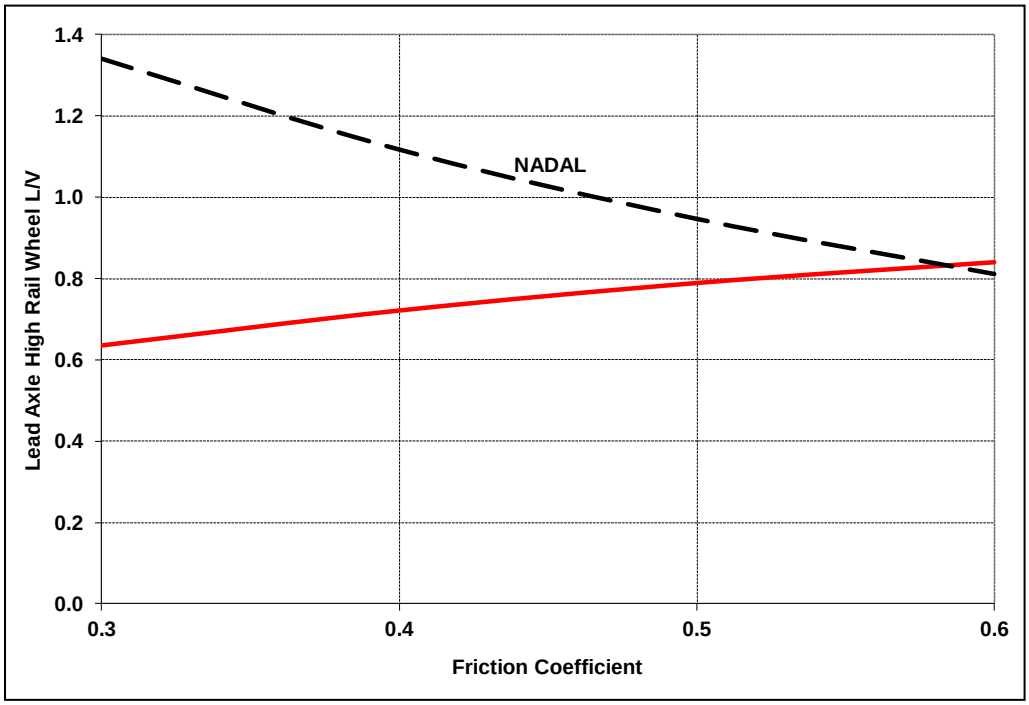

Figure 6. L/V Ratio, New Design 70-degree Wheel on New No. 8 Turnout, Down-and-out Track Perturbations

Increasing the maximum flange angle can effectively reduce flange climb derailment risk. APTA recommends a 72 degree (with tolerance +3 degrees and -2 degrees) flange angle for wheels used in passenger railcars. However, wheel profiles with flange angles less than 72 degrees (but high enough to prevent flange climb) can also be adopted for a smooth transition from low flange angle wheels.

2.3 Guidelines for Improving Hunting Performance

2.3.1 Hunting and Safety Criteria

Lateral instability or hunting is an inherent characteristic of rail vehicles with solid axles and noncylindrical wheel profiles. The tapered wheel profile results in coupled axle lateral and yaw movements. With increasing speed, axle hunting, characterized by sustained flange-to-flange lateral motion, will occur as the energy from forward motion is transferred to the axle oscillation.

Hunting has been a core topic of W/R interaction research. The critical speed is sensitive to not only the car suspension parameters but also the track perturbations in terms of both the shape and amplitude. A railcar's suspension system deteriorates over time in service, and track geometries also degrade over time and vary along the track. These parameters change so dramatically in vehicle and track systems that the critical speed also changes from case-to-case.

The maximum wheel flange angle is a simple geometry index for evaluating wheel profile effects on flange climb derailment. Similarly, researchers also hope to find a simple geometry index to evaluate wheel profile effects on hunting. So far, the most promising index appears to be the conicity.

For a constrained single axle with a conical wheel without a flange, as Figure 7 shows, an analytical formula can be derived as Equation 1. NUCARS simulations using the transit car model with conical wheels without a flange validated that the hunting speed is inversely proportional to square root of conicity, as Figures 8 and 9 show. The parameter varied solely in the model is the conical wheel profile with different tread slopes (conicity).

However, wheels must have flanges for safe operation. Once the wheel flange is introduced, the relationship between the hunting speed and conicity becomes much more complicated and cannot be expressed in a simple analytical equation.

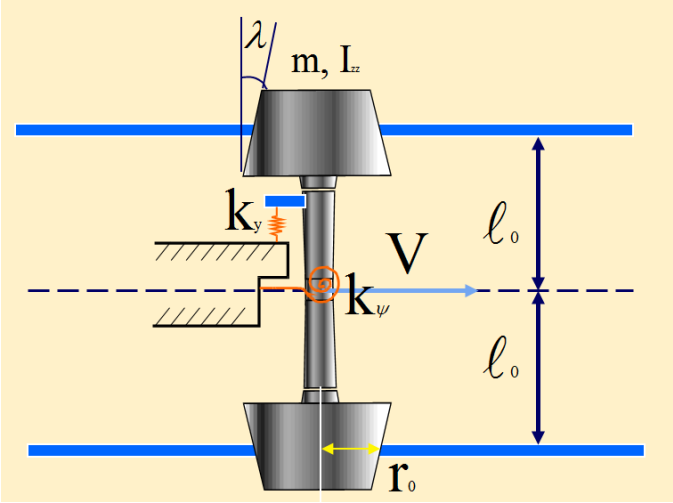

Figure 7. A Constrained Single Axle with Conical Wheel

$$\text{Hunting Speed } V_C = \sqrt{\frac{r_0 \ell_0 (k_\psi + \ell_0^{\,2} k_y)}{\lambda (I_{zz} + \ell_0^{\,2} m)}} \qquad (1)$$

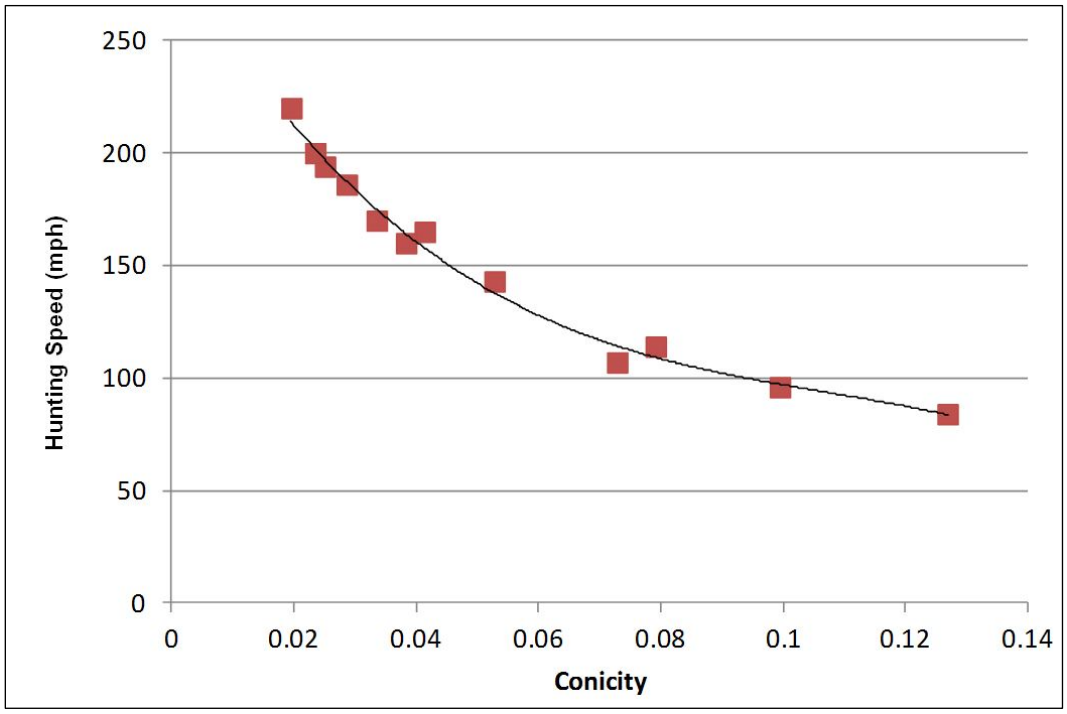

Figure 8. Effect of Conical Wheel Conicity on Hunting Speed

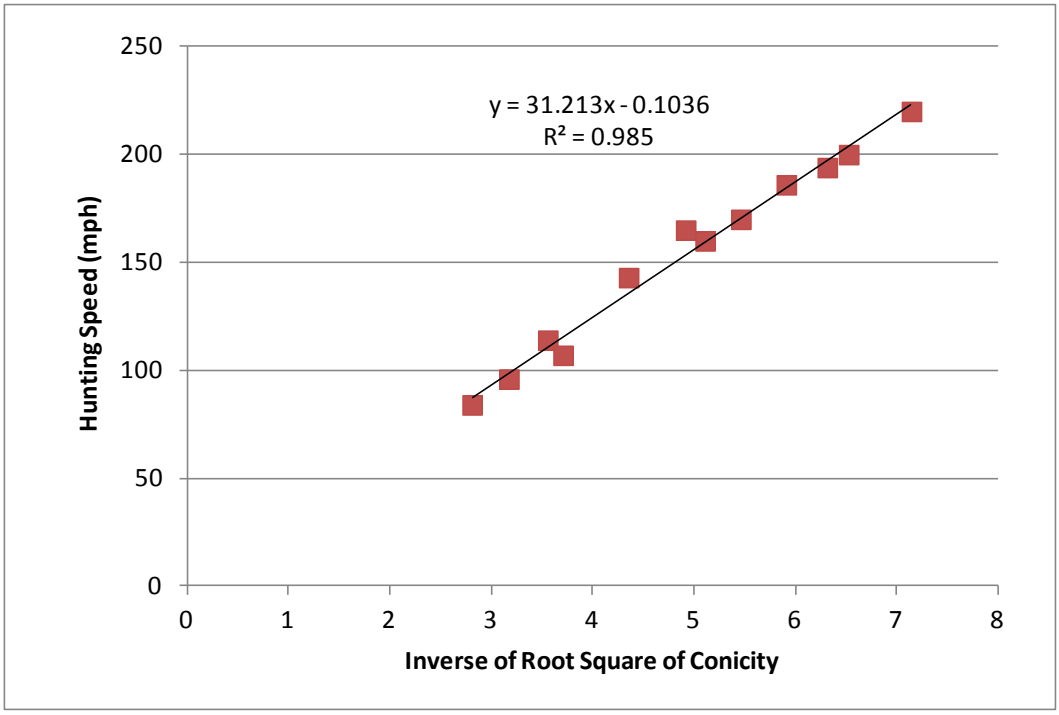

Figure 9. Relationship between Hunting Speed and Root Square of Conicity

The hunting criteria adopted by the railroad industry are different from that in academic research. The hunting speed in Figures 8 and 9 was defined as the speed at which the axle lateral motion starts to increase without damping after the excitation of track perturbations, as Figure 10 shows. Figure 11 shows the axle movement was stable at 64 mph (blue line, converged to track center position) but unstable (hunting) at 65 mph and reached a stable limit cycle over certain distances.

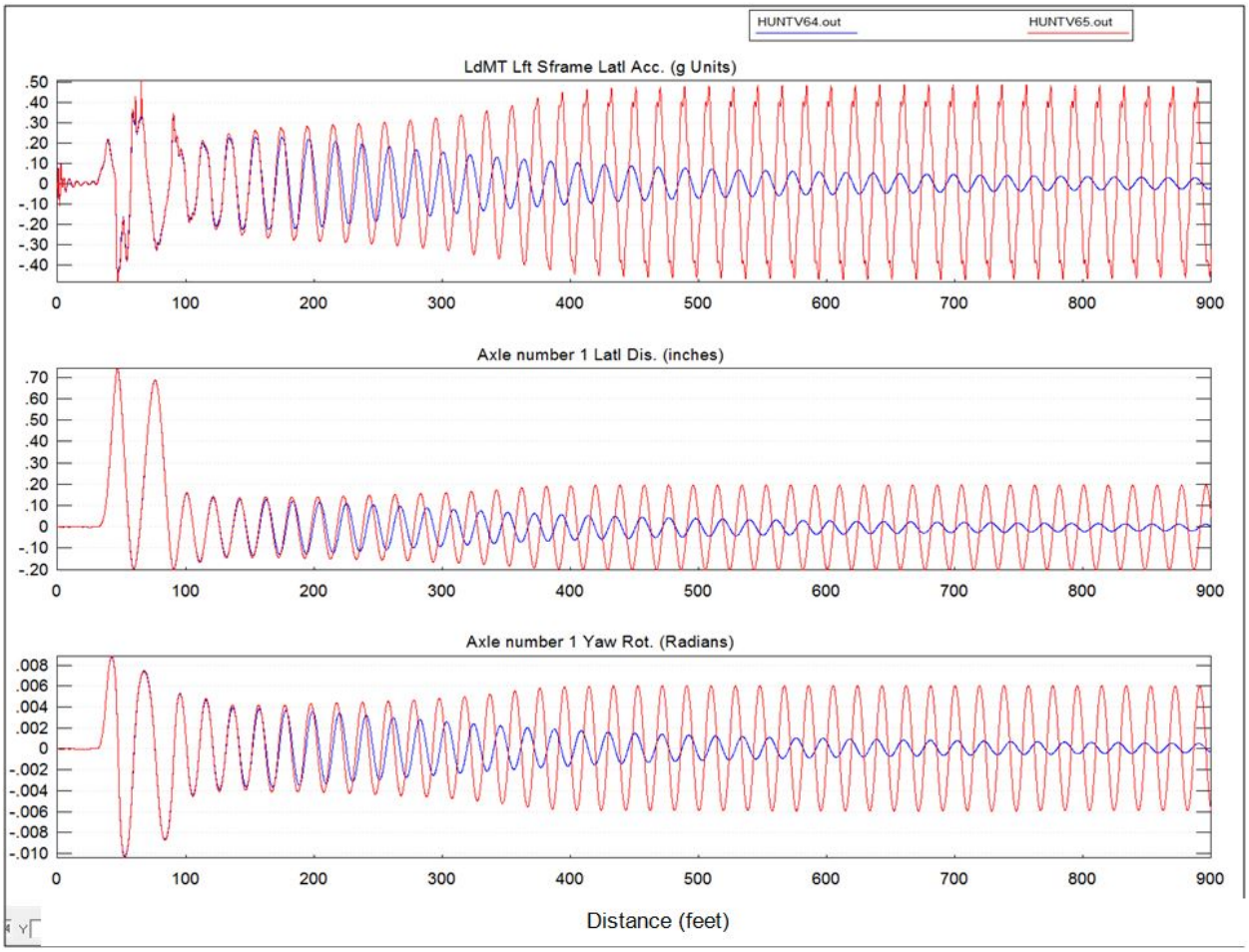

Figure 10. Time History Comparisons of Conical Wheel Hunting (65 mph) and No Hunting (64 mph)

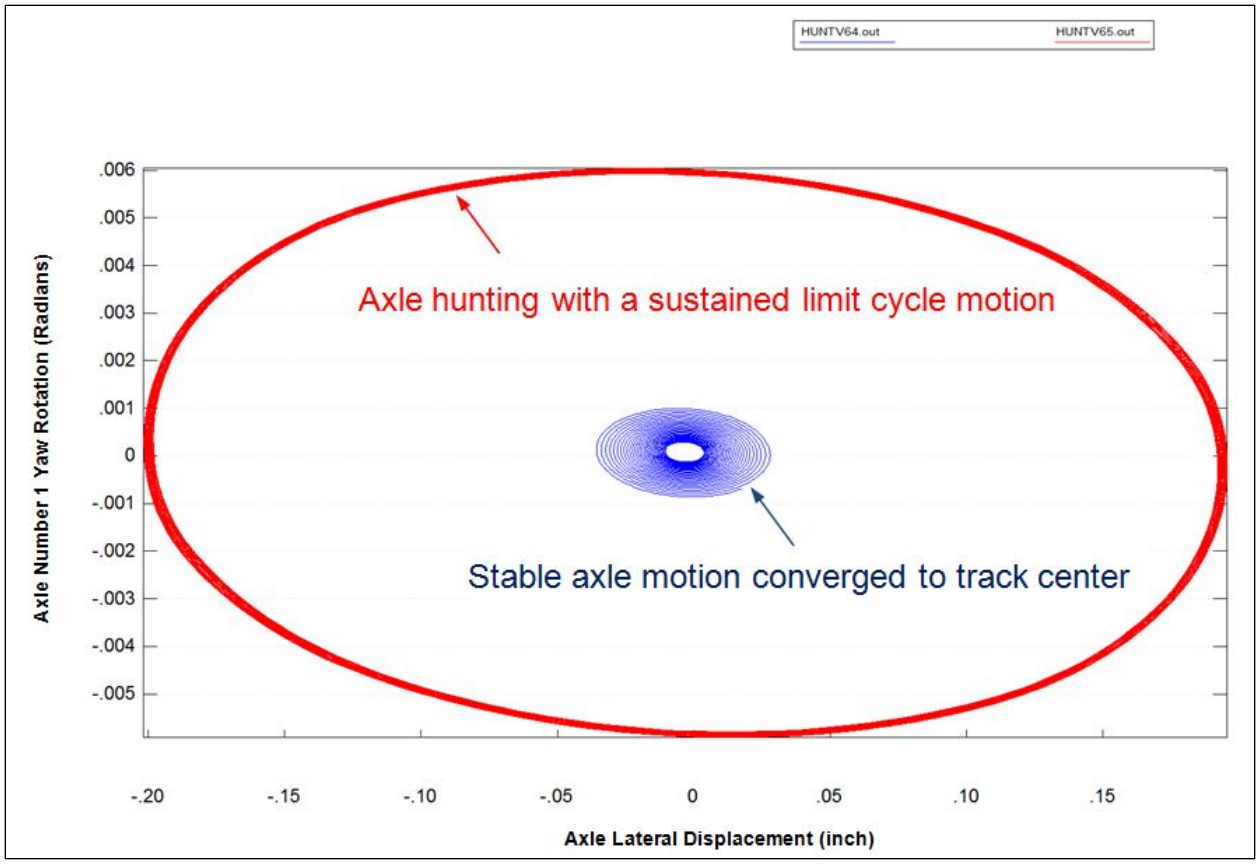

Figure 11. Limit Cycle Movements of Conical Wheel Hunting (65 mph) and No Hunting (64 mph)

From an academic point of view, the hunting speed was reached when the real part of the eigenvalue of a linear system changed to positive from negative, with the calculated hunting speed referred to as "linearized critical speed." However, the vehicle and track system is strongly nonlinear. Therefore, the linearized critical speed calculated by eigenvalue analysis usually does not match test results very well.

The "nonlinear critical speed" is usually calculated through parametric study by using dynamic simulations. The critical speed is defined as the speed at which the amplitude of axle lateral oscillation (coupled with axle yaw motion) starts to increase and may reach a stable limit cycle motion. The axle limit cycle motion is not necessarily involved with flange contact. It may be stable with or without flange contact, and it may also burst into an instable state and result in derailment. The critical speed must be judged case-by-case.

The nonlinear critical speed simulation requires a large amount of work because there are many vehicle and track parameters influencing hunting and each parameter can vary in certain ranges. The lowest of critical speed from all these parametric variation cases was defined as the hunting speed (True 1994).

The hunting speed in the railroad industry is defined differently by using truck frame accelerations instead of axle movements, such as defined in the FRA 49 CFR Parts 213 Vehicle/Track Interaction Safety Standard (FRA March 2013) and UIC Leaflet 518, Testing and Approval of Railway Vehicles from the Point of View of Their Dynamic Behavior – Safety – Track Fatigue – Running Behavior (UIC Leaflet 518 2009). The FRA 213 standard defines truck hunting as: "Truck hunting is defined as a sustained cyclic oscillation of the truck evidenced by lateral accelerations in excess of 0.3 g root mean square (mean-removed) for more than 2 seconds (FRA March 2013)."

The industry uses an acceleration-based hunting speed criterion instead of an axle motion based criterion for the following reasons:

- It is difficult to measure the dynamic axle displacements in the field.
- The definition of hunting using axle motion is not clear; for some cases, the axle lateral motion bursts into hunting with hard flange contact, while for other cases, the axle lateral oscillation slowly grows into flange contact, while the truck and carbody accelerations may exceed safety limits before flange contact.
- The truck frame acceleration hunting criterion is more conservative because it provides a safety warning before the axle oscillates in full scale with hard flange impact.
- Truck frame acceleration is easy to measure and more sensitive to hunting movement. Earlier signs of hunting can be more easily captured by truck frame accelerations than axle lateral displacements, so an acceleration-based hunting criterion is more conservative than that based on axle lateral displacement.

2.3.2 Development of a W/R Contact Geometry Based Hunting Criterion

New cars fleets are required to meet vehicle and track safety standards through on-track tests. Hunting performance is usually evaluated through truck frame and/or carbody acceleration measurement. However, for daily vehicle and track maintenance, rail transit agencies prefer a W/R contact geometry based hunting criterion and guidelines because wheel and rail geometry measurement is easier than that of acceleration and, for a given rail transit system, the vehicle parameters are generally fixed, while wheel and rail wear, and track geometry can vary.

A W/R contact geometry based hunting criterion was developed through NUCARS simulations. Simple two-line wheel profiles were evaluated in the model to investigate the effects of flange angle, tread conicity, and track gage on hunting. The two-line wheel profile consists of two segments: tread and flange. The wheel tread and flange-segment profiles are two lines connected by a small arc at the flange root, as Figure 12 shows.

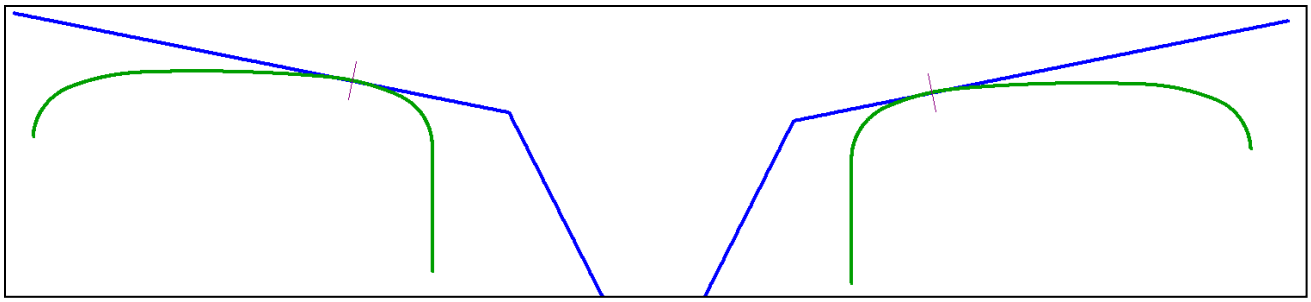

Figure 12. Two-line Wheels Contact on AREMA 115RE Rails Used for Hunting Simulations

The wheel tread conicity, flange angle, and track gage were varied in the parametric study:

- Wheel flange angle: 45, 63 and 70 degrees
- Tread conicity: 0.1, 0.2, 0.3 and 0.4
- Track gage: 56.1, 56.25, 56.5, and 57 inches

The Task 1 report described several definitions and methods for equivalent conicity calculation (Shu 2014). The equivalent conicity defined in UIC 519 (UIC Leaflet 519 2004) was used in this study.

Figure 13 shows two types of hunting responses: the subcritical and supercritical Hopf Bifurcations. The Hopf bifurcation theory and methodology have been used to investigate nonlinear dynamic system stability for decades (Strogatz 1994). At a critical state, a nonlinear dynamical system could lose stability

in two different trends, namely supercritical and subcritical Hopf bifurcation. Hopf bifurcations occur when a railway vehicle runs above a critical speed (True 1994).

An unstable vehicle with supercritical Hopf bifurcation generally has the following characteristics:

- High conicity, usually with high flange angle or negative slope of equivalent conicity
- Limit cycle of wheelset movements (sustained wheelset lateral displacement and yaw) with amplitudes growing with running speed
- Limit cycle starts at low speed and may not exceed safety limit

An unstable vehicle with subcritical Hopf bifurcation generally has the following characteristics:

- Low conicity, usually with low flange angle and positive slope of equivalent conicity
- Sudden occurrence of a limit cycle with large amplitudes that exceed safety limits
- No limit cycle movements until a critical speed was reached

Figure 13 shows the truck frame acceleration root mean square (rms) value for the car equipped with a 45-degree flange angle running on 56.25-inch gage track. The wheelset accelerations jumped to 1.4 g at 75 mph, demonstrating a typical subcritical Hopf bifurcation instability. However, the truck frame acceleration RMS value for the car equipped with 63-degree flange angle running on 57-inch gage track gradually increased with running speed, demonstrating a typical supercritical Hopf bifurcation instability.

Based on a hunting defined as flange-to-flange contact axle oscillation, it is clear the hunting speed for the car with the 45-degree wheels is about 75 mph since the truck frame acceleration suddenly increased, indicating the wheel flange contact. However, the hunting speed is unclear for the car equipped with 63-degree wheels, because it is unclear at which speed the flange-to-flange contact axle oscillation occurred.

Application of an acceleration-based hunting criterion, such as the 0.3 g rms FRA 213 track safety standard, is straight forward. For the simulated cases, the hunting speed for the car equipped with 63-degree wheel running on 57-inch gage track is about 66 mph, and the hunting speed for the car equipped with 45-degree wheel running on 56.25-inch gage track is about 71 mph.

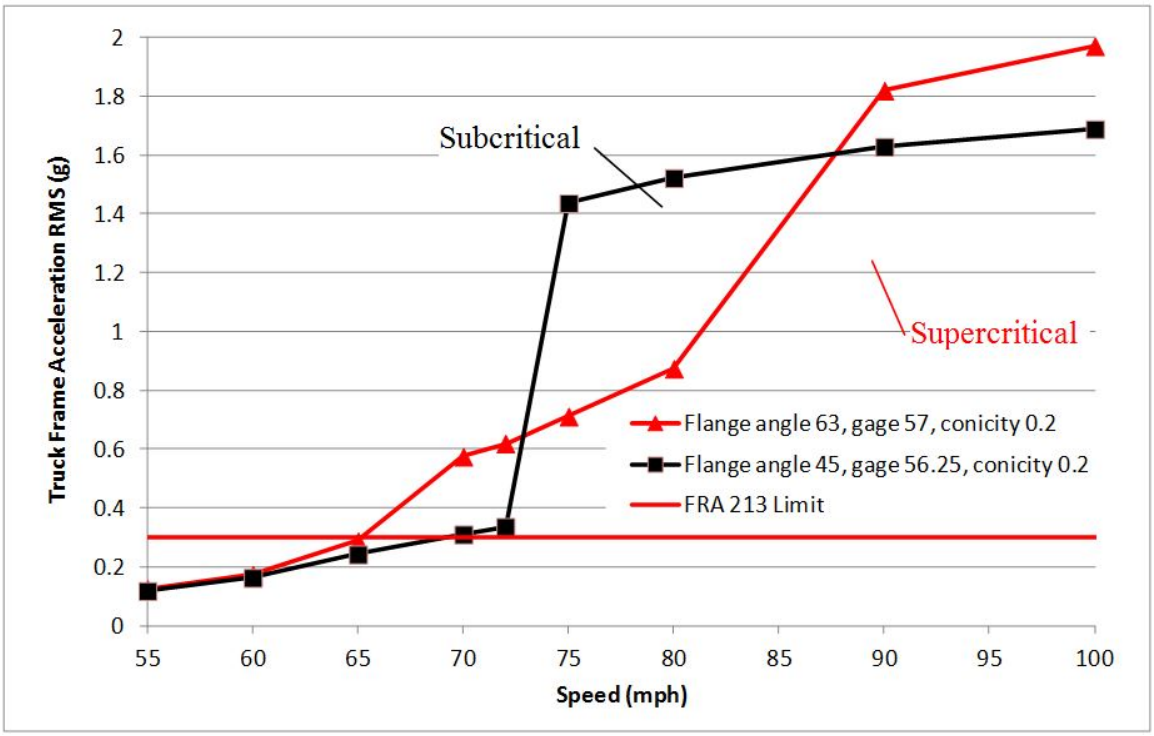

Figure 13. Subcritical and Supercritical Hunting Cases

Figure 14 shows the ride quality of the simulated car equipped with 45-degree wheels is better than that with 63-degree wheels at speeds lower than 79 mph, which is consistent with their hunting performances (the hunting speed of the car equipped with 45-degree wheels is higher than that with 63-degree wheels).

The examples in Figure 14 demonstrate that an acceleration-based hunting criterion is adequate for hunting performance evaluation.

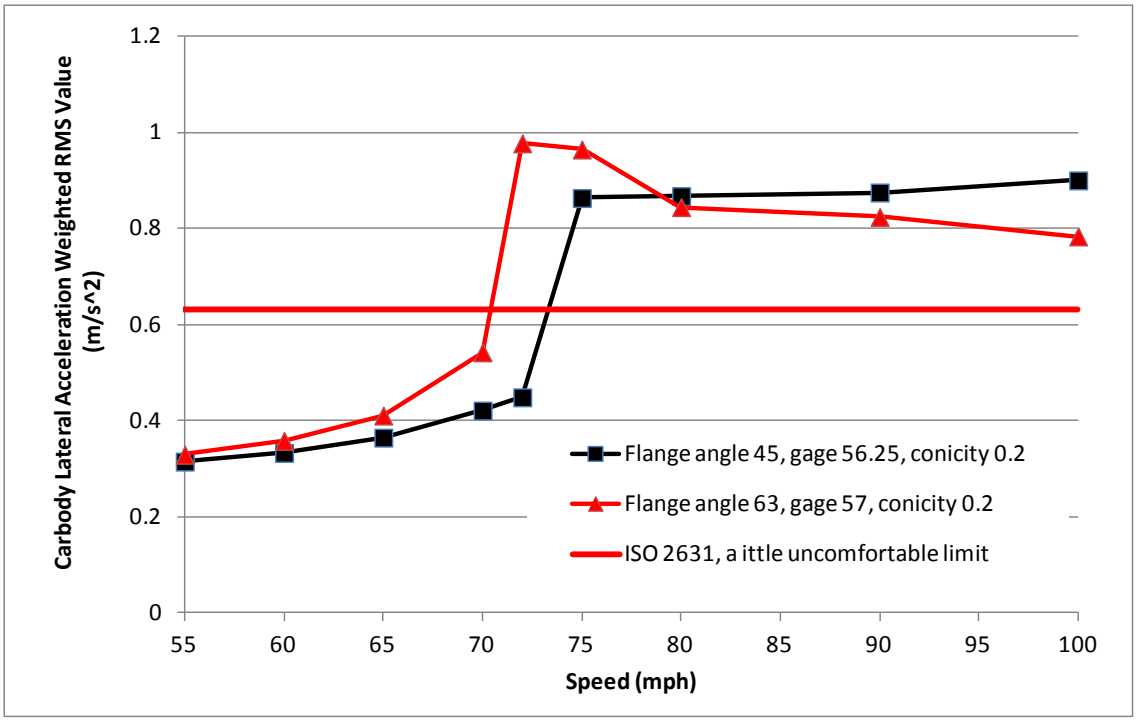

Figure 14. Ride Quality of Subcritical and Supercritical Hunting

Figures 15 through 17 show the truck frame acceleration rms values at different speeds for the car equipped with 45-, 63- and 70-degree flange angles and different conicity wheels running on measured track geometry from Transportation Technology Center's hunting test track (Railroad Test Track) with different track gages. Simulation speeds were from 50 mph to 120 mph to determine the hunting speed at which truck frame lateral acceleration values reach 0.3 g rms. Each graph shows results for several combinations of gage and conicity. For example, the line marked g561, 0.1 is for 56.1-inch track gage with 0.1-tread conicity.

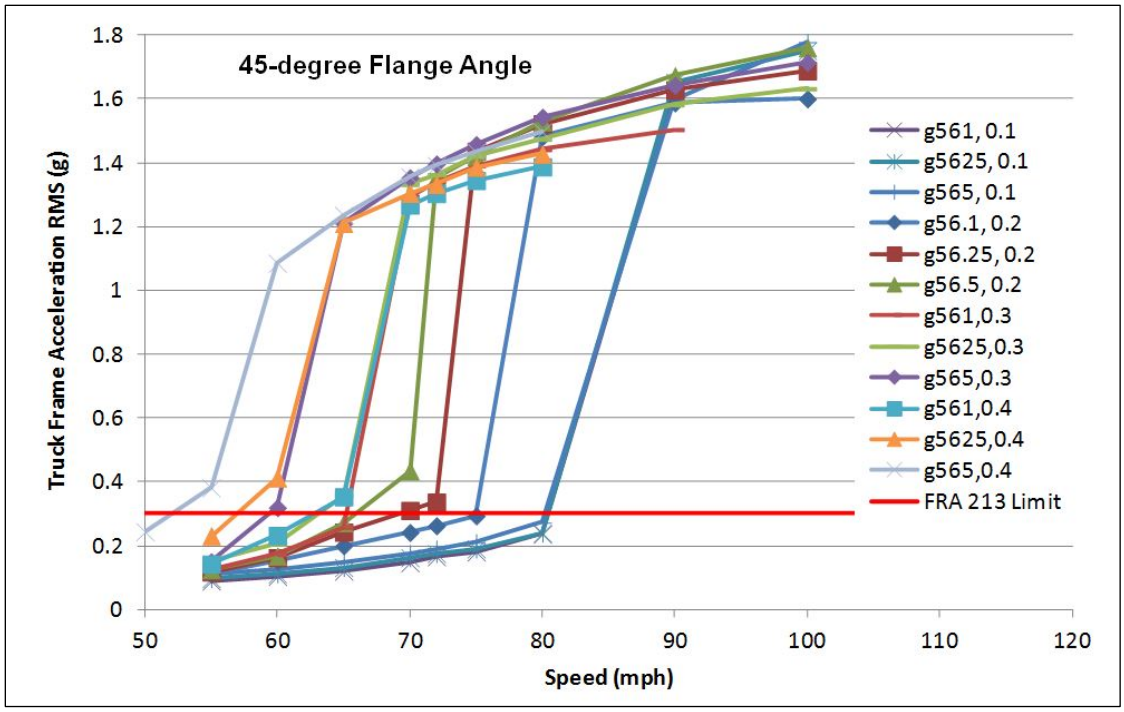

Figure 15. Truck Frame Accelerations at Different Speeds (45-degree flange angle wheel)

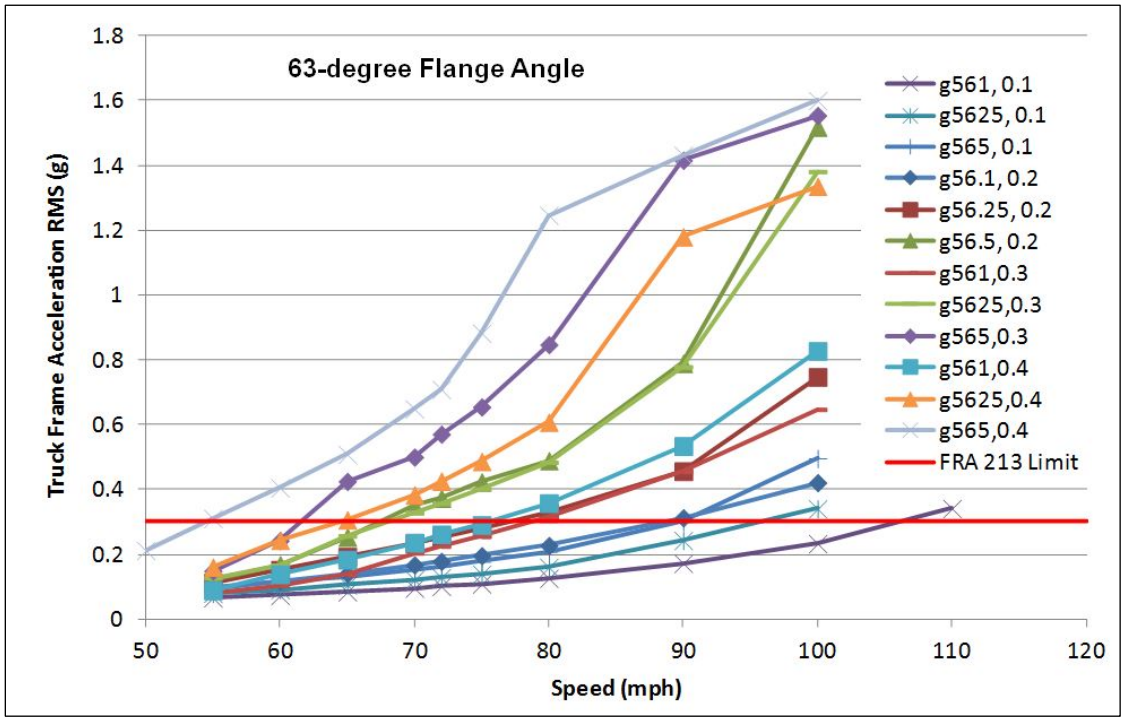

Figure 16. Truck Frame Accelerations at Different Speeds (63-degree flange angle wheel)

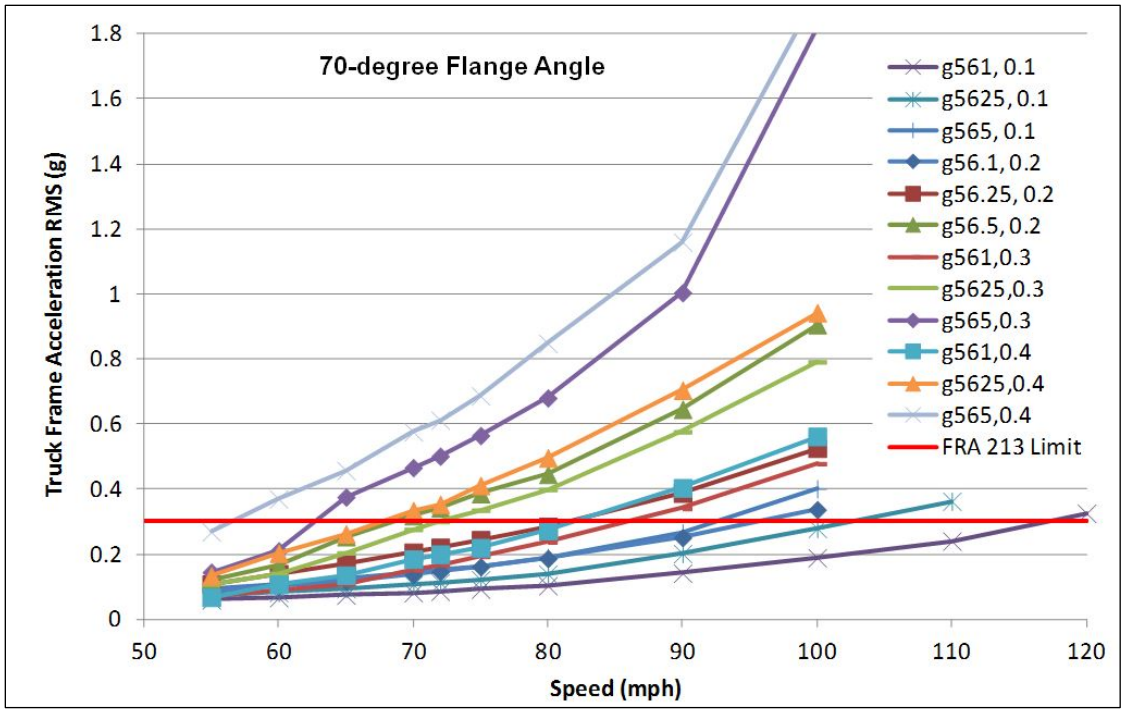

Figure 17. Truck Frame Accelerations at Different Speeds (70-degree flange angle wheel)

Figures 15 through 17 appear to show that the highest hunting speed increases with flange angle. But the flange angle effects on hunting are different for subcritical (such as in Figure 15) and supercritical (such as in Figures 16 and 17) hunting.

In comparison to the flange angle, the conicity and track gage effects on hunting are more consistent. The hunting speed decreased with the increase of conicity and track gage, regardless of subcritical or supercritical hunting responses.

The question is how to quantify the relationship between the hunting speed and these varied parameters. The first step used in this study is to prioritize the parameters based on their effects, then combine multiple parameters into one parameter if possible using multiple parameter regression analysis. The fewer the parameters are, the easier the analyses is.

Wheel flange angle and track gage variations result in different W/R clearances. The clearance was defined as the axle lateral shift from track center to the position where the wheel contacts the rail at maximum flange angle.

Because the hunting speed was defined based on truck frame acceleration rms values, the W/R contact clearance was more relevant to the hunting speed than wheel flange angle. The wheel flange angle and track gage effects on hunting can be replaced by one parameter, the W/R clearance.

In Figure 18, the simulation results were regrouped based on conicity. For each group with the same conicity, the hunting speed and the W/R clearance was fitted with an exponential function. The r-square quality of fit for each group is above 0.97.

The fitting results were interpolated to obtain the same hunting speed for each conicity group. A group of hunting speed contour (HSC) functions, with two W/R contact geometry parameters, the conicity and W/R clearance, was developed by using the interpolation results, as Figure 19 shows.

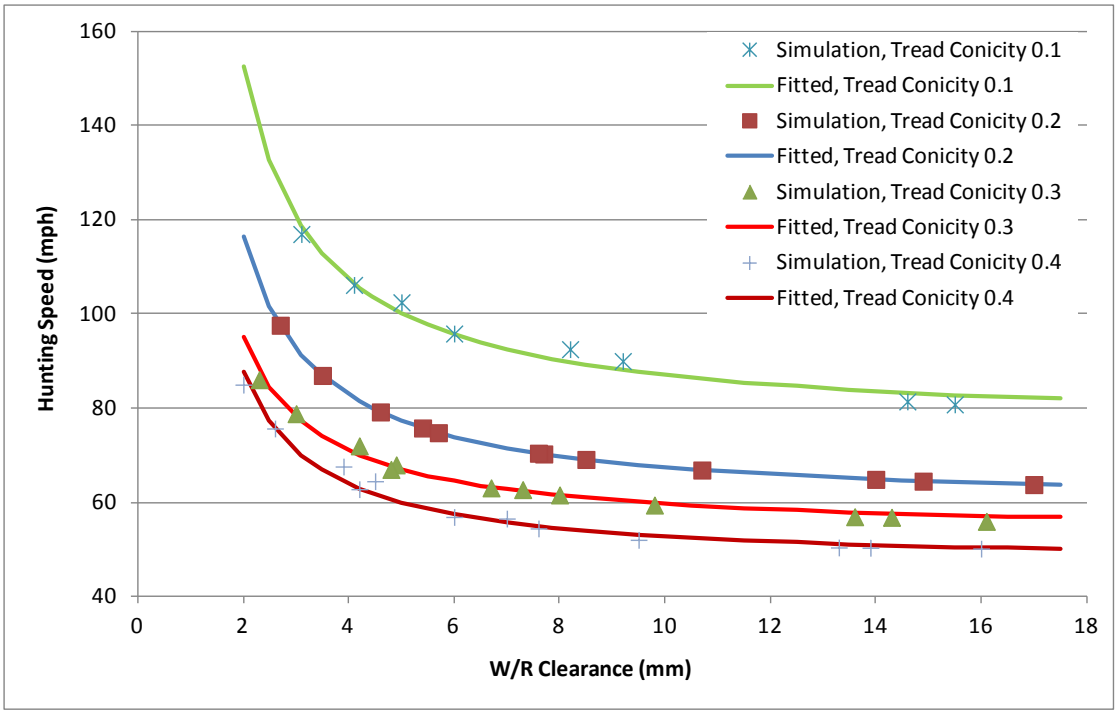

Figure 18. W/R Equivalent Conicity and Clearance Effects on Hunting Speed

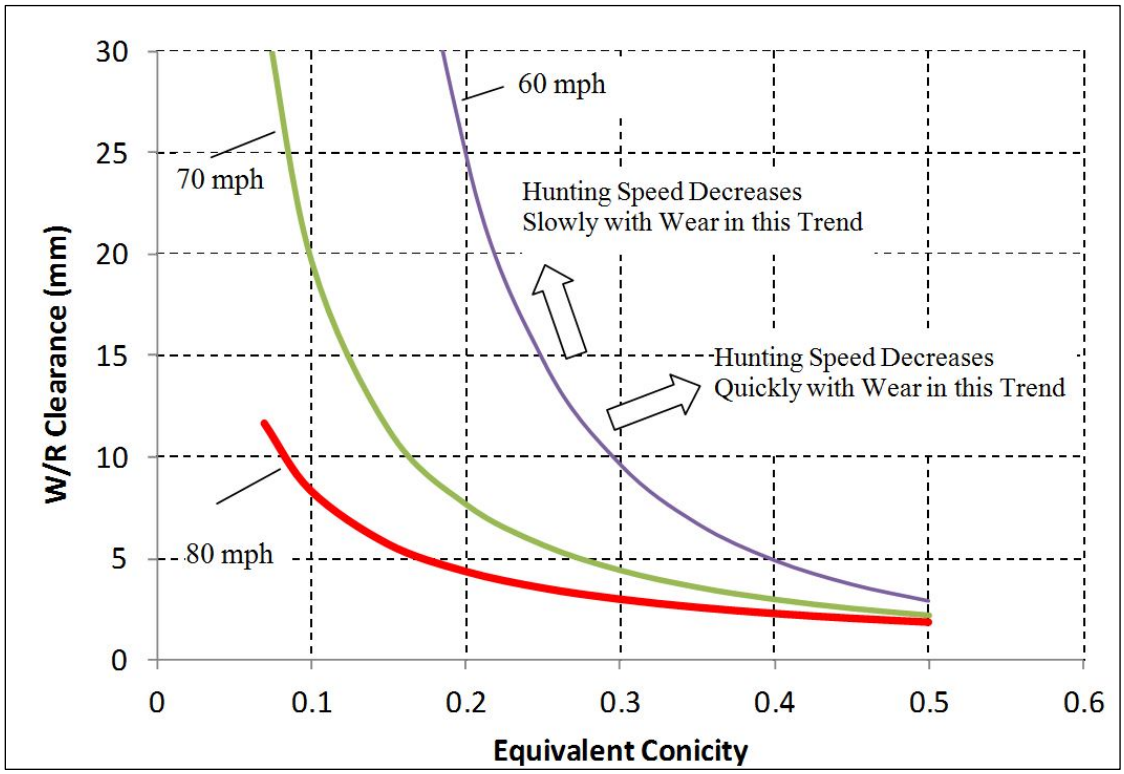

Figure 19. Hunting Speed Contour Chart for Representative Heavy Railcar

The HSC chart in Figure 19 was developed based on a specific type of transit car model. It can be used to determine the hunting speed of this type of transit car with new and worn wheels. This chart provides the following guidelines:

- The same hunting speed can be achieved by using either a high conicity with tight W/R clearance or a low conicity with wide W/R clearance.
- The hunting speed generally decreases with the increase of conicity and W/R clearance.
- Wheel and rail wear increase W/R clearance, so the worn wheel hunting speed decreases quickly as a wheel wear into high conicity and wide W/R clearance.
- The worn wheel hunting speed decreases slowly when wheel wear results in low conicity and wide W/R clearance.
- High conicity wheel hunting speeds are more sensitive to W/R clearance variation than that of low conicity wheels.

2.3.3 New Design Wheel Hunting Performance Evaluation

The hunting performances of the existing and new design wheels were evaluated by using the HSC chart. Figure 20 shows the conicity of the existing 63-degree wheel and the new design 70-degree wheel with 56.25-inch gage, which was standard on tangent track in the transit system studied by TTCI.

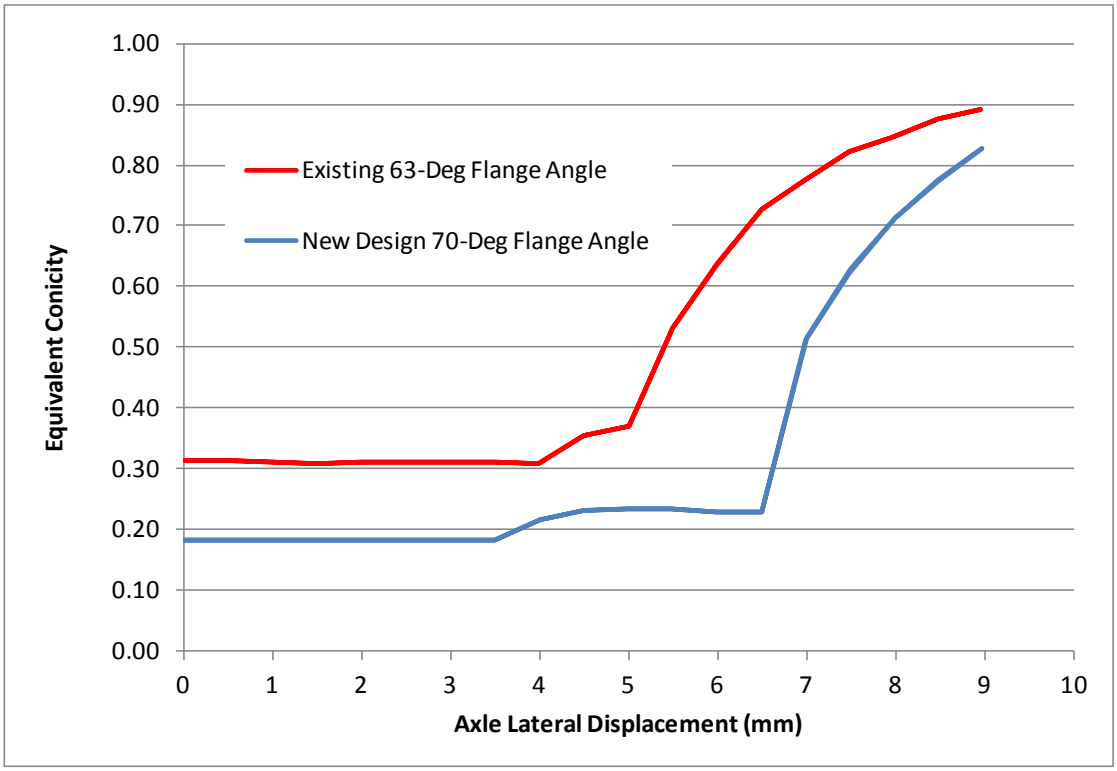

Figure 20. Existing and New Design Wheel Conicity (56.25-inch gage)

The existing 63-degree wheel and AREMA 115RE rail generate 0.37 conicity (before contact at maximum flange angle) and 4.94-millimeter (0.19 inch) W/R clearance; the new design 70-degree wheel and AREMA 115 RE rail generate 0.22 conicity and 6.73-millimeter (0.26 inch) W/R clearance. The new design 70-degree wheel generates lower conicity but wider W/R clearance than the existing 63-degree wheel. By plotting these parameters in the HSC chart in Figure 21, the hunting speeds of these two

wheels were estimated to be 70 mph and 65 mph for the new design 70-degree wheel and existing 63-degree wheel, respectively.

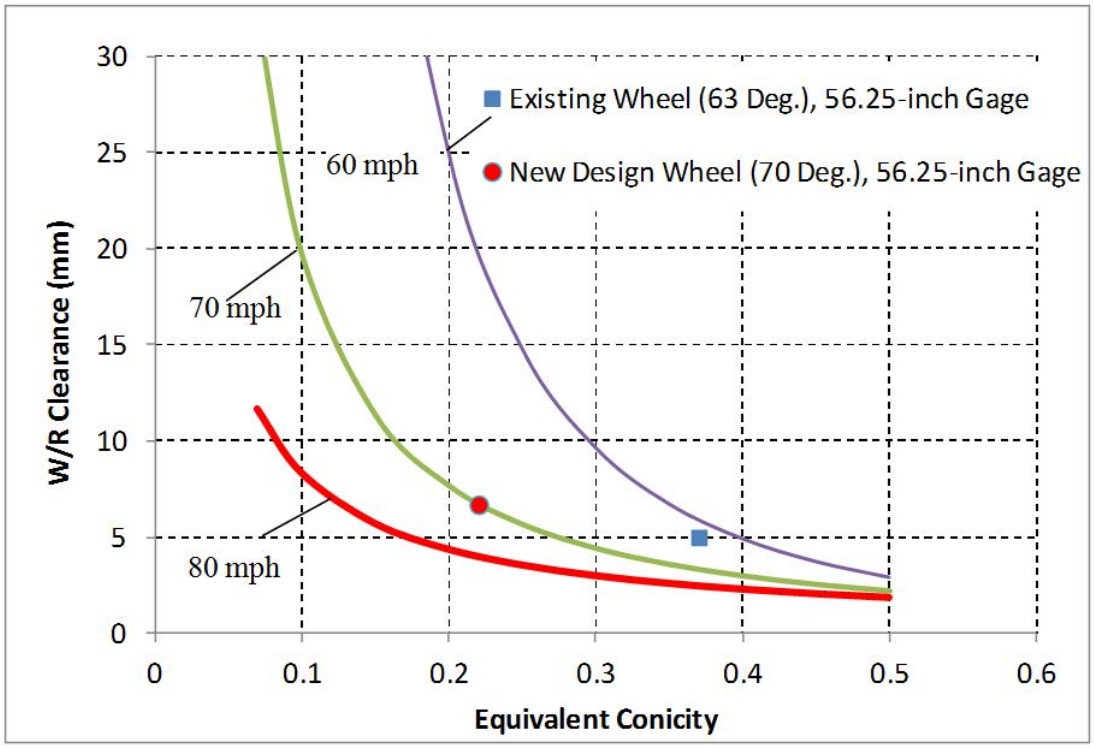

Figure 21. Existing and New Design Wheel Conicity (56.25-inch gage)

Based on the HSC chart, the new design 70-degree wheel will improve car lateral stability. This was validated through simulations using these two types of wheels, as Figure 22 shows.

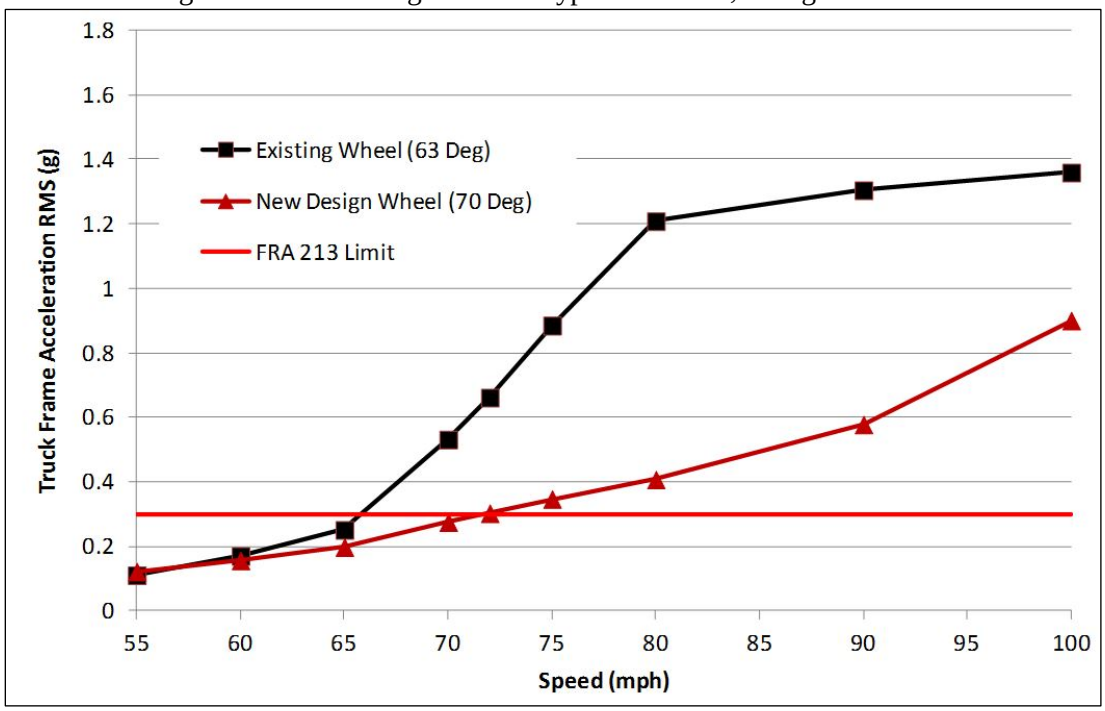

Figure 22. Truck Frame Accelerations of the Existing and New Design Wheel (56.25-inch gage)

The application of the HSC chart includes the following steps:

- Generate a HSC chart for a representative type of car:
  - Build the car model by using parameters measured through characterization test
  - Generate a series of simplified wheel profiles consisting of tread (with different tread slopes) and flange (with different flange angles) lines
  - Conduct W/R contact geometry analysis by using a simplified wheel profile and a representative rail profile to obtain W/R conicity and clearance
  - Conduct simulations using these simplified wheel profiles at different speeds with track gage variations
  - Conduct regression analysis between the predicted hunting speed and W/R contact geometry parameters in terms of conicity and W/R clearance
  - Interpolate the fitting results to obtain a group of HSC functions with W/R conicity and clearance parameters
- Validate the HSC chart through simulation or test
  - Measure wheel and rail profiles
  - Conduct W/R contact geometry analysis on measured wheel and rail profiles to obtain conicity and clearance
  - Estimate the hunting speed from the HSC chart by using the measured W/R conicity and clearance
  - Conduct simulations by using wheel and rail profiles and track geometry, or conduct on-track test to measure hunting performances
  - Validate the HSC chart by comparing the estimated hunting speed to the hunting speed measured from tests or predicted from simulations.
- Evaluate the car stability by using the HSC chart and W/R contact geometry parameters based on the guidelines described in subsection 2.3.2.

2.4 Guidelines for Contact Stress and Wear Performance

Table 1 lists the curvatures, track superelevation, and running speed used in the wear analysis simulations. The speeds correspond to 1-inch cant deficiency for the curve.

Table 1. Case Study Parameters

Case	Curve Radius (feet)	Curvature (degree)	Superelevation (inch)	Speed (mph)	Track Gage (inch)
1	250	22.92	0	7.87	57
2	500	11.46	0	11.12	56.5
3	750	7.64	4	30.66	56.5
4	817	7.01	4	32.00	56.5
5	955	6.00	4	34.60	56.5
6	1,145	5.00	4	37.88	56.5
7	1,430	4.01	4	42.34	56.5
8	1,910	3.00	4	48.93	56.25
9	2,864	2.00	4	59.91	56.25
10	5,729	1.00	1.5	59.83	56.25

New and worn rail profiles were used in the simulations. The worn rails were measured on curves, as Figure 23 shows.

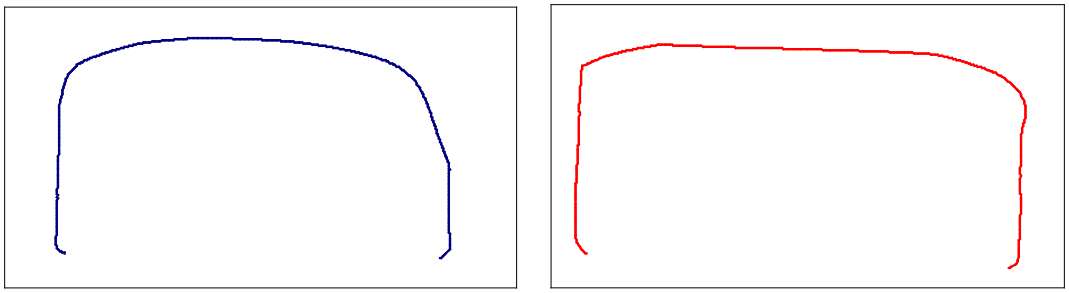

Figure 23. Measured Rail Profiles in Curve

Figure 24 shows the new design 70-degree flange angle wheel running on a new 115RE rail generates lower contact stress than that of the existing 63-degree flange angle wheel for almost all simulated curves. The maximum contact stress on tight curve was lowered by about 31 percent.

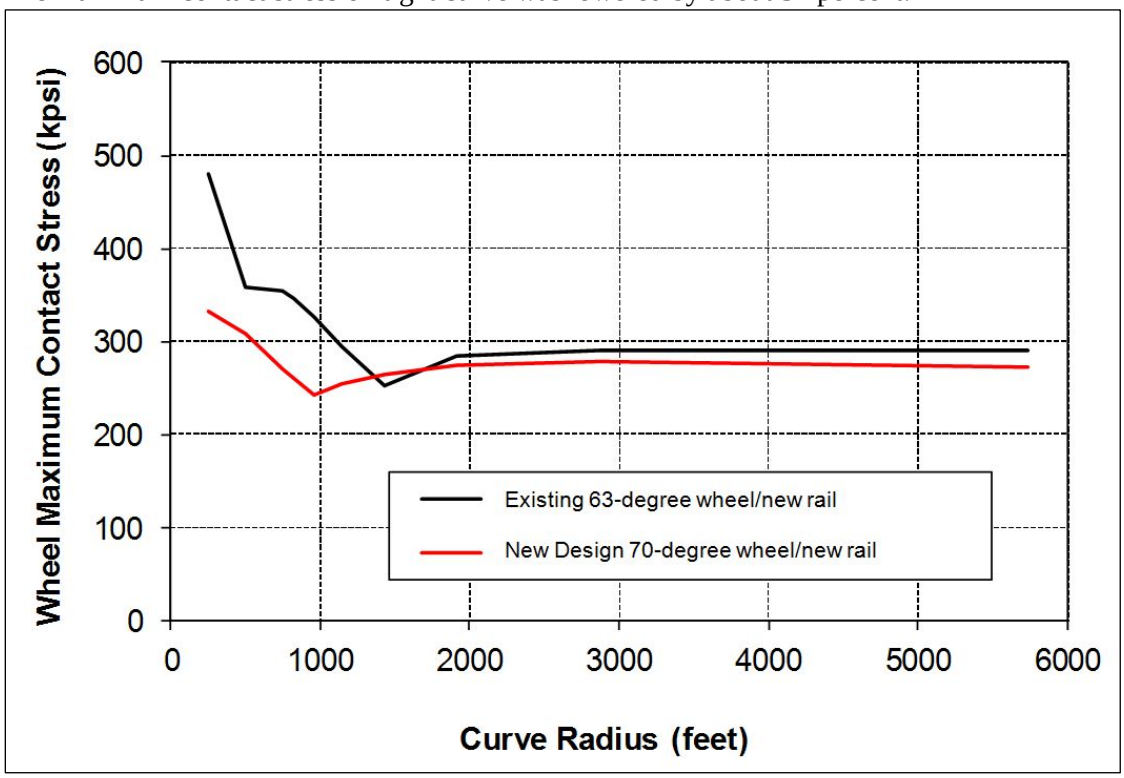

Figure 24. Contact Stress of the Existing and New Design Wheels on New Rails

Figure 25 shows that the new design 70-degree flange angle wheel running on a worn 115RE rail generates lower contact stress than that of the existing 63-degree flange angle wheel on tight curves (<955-feet curve radius, 6-degree curve) and curves with radii larger than 2,600 feet (2.2-degree curve). The maximum contact stress on tight curve was lowered by about 42 percent. The design wheel generates higher contact stress than the existing wheel on 2- to 6-degree curves. However, these curves only account for 12 percent of the total track length, as Figure 26 shows.

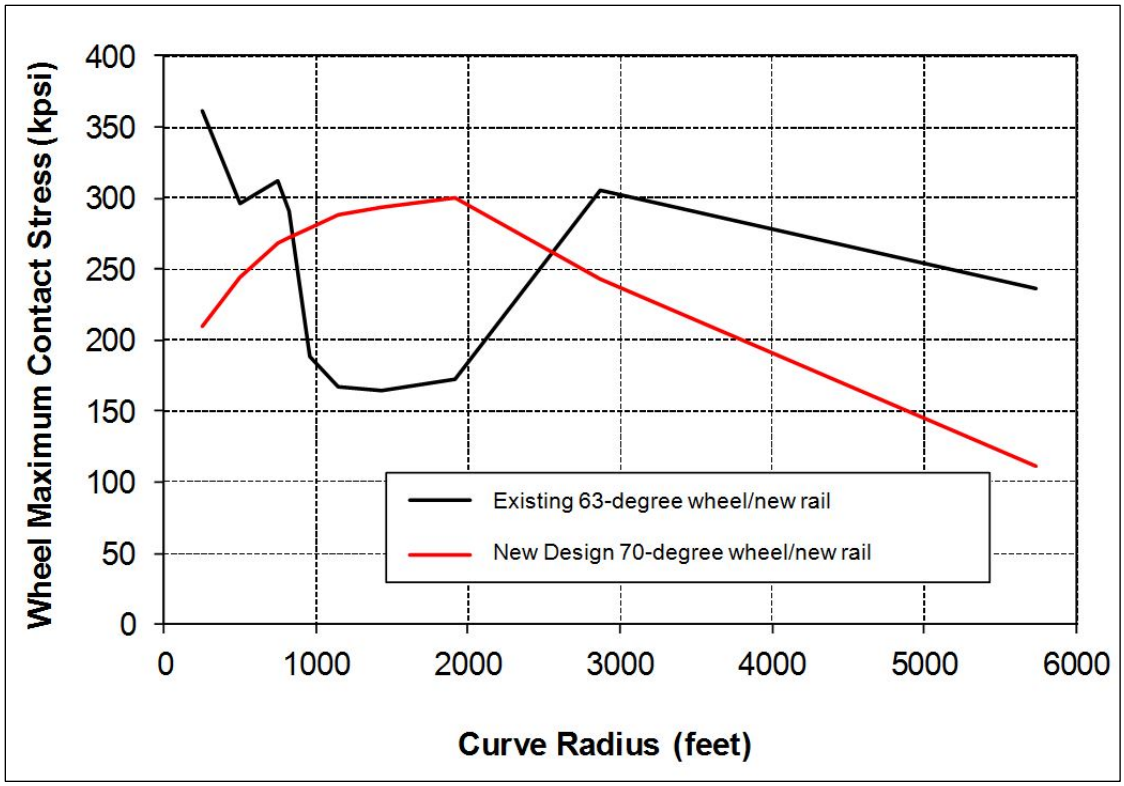

Figure 25. Contact Stress of the Existing and New Design Wheels on Worn Rails

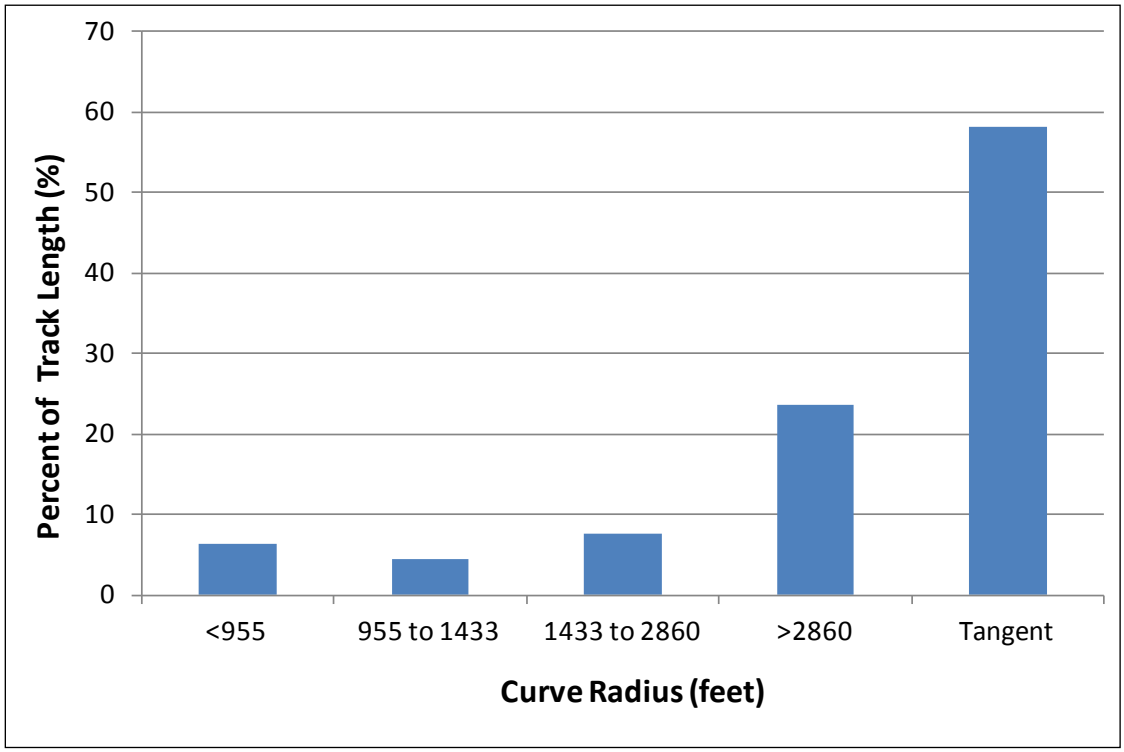

Figure 26. Track Curvature Distribution

The W/R wear was evaluated by using the wear index, defined in Equation 2. It is calculated as the sum of the tangential forces (T_x, T_y and M_z) multiplied by the creepages (γ_x, γ_y and ω_z) at the contact patch. Rolling resistance is defined as the sum of wear indices on all wheels in a car. High rolling resistance can induce either RCF or high rates of wear. It is also an indicator of the energy consumption at the W/R interface.

$$Wear\ Index = \sum_{n} T_x\gamma_x + T_y\gamma_y + M_z\omega_z \qquad (2)$$

Figure 27 shows the wheel wear index of the wheel with 70-degree flange angle is slightly higher than that of the 63-degree wheel on curves with radii less than 750 feet, but a little lower on curves with radii from 750 to 1,430 feet. Sharp curves with radii smaller than 750 feet are generally in the yards in the system that was investigated. The yard tracks were designed to 4.5-inch underbalance speed operation. Because all simulations were conducted with 1-inch overbalance, the actual wheel and rail wear on sharp curves (radii less than 750 feet) is expected to be lower than the simulation results. Since the curve radii on the mainline are mostly above 750 feet, the rate of W/R wear of the proposed 70-degree wheel profile will be similar to the existing 63-degree wheel profile.

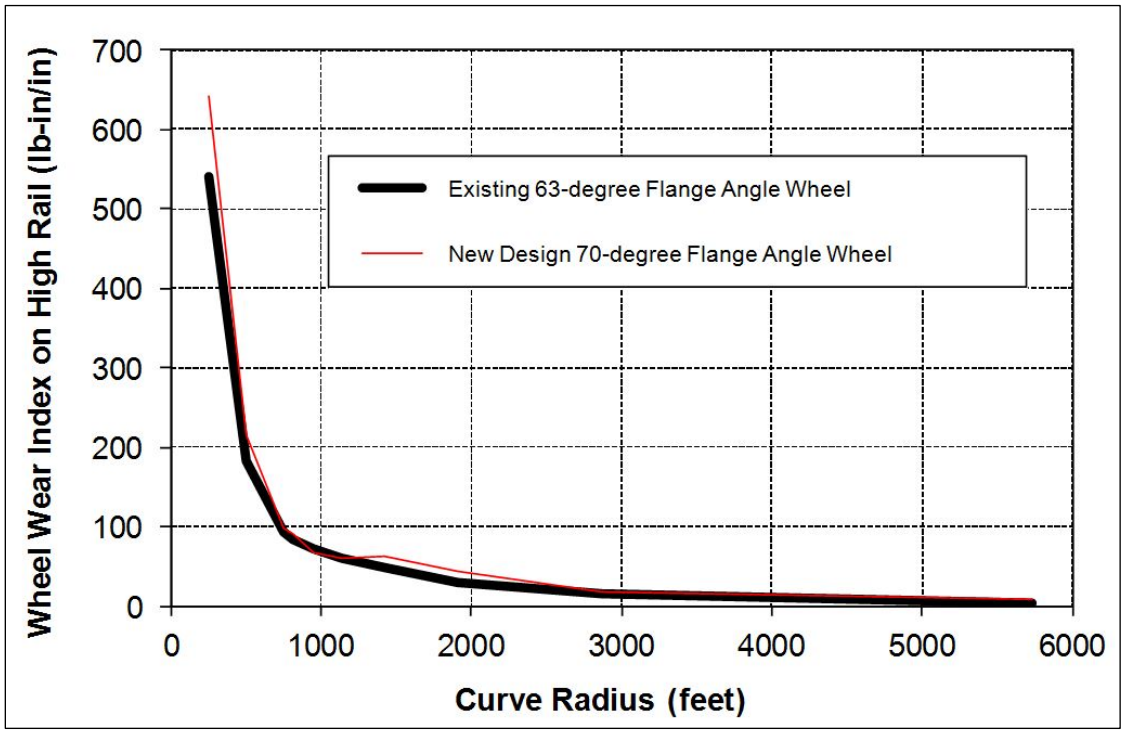

Figure 27. Comparison of Wear Index for the Existing and New Design Wheel

Using high flange angle wheels may increase wheel and rail wear, especially when the new design wheel flange angle is higher than the maximum flange angle on worn wheels and rails. Adopting new design wheel with a flange angle close to that of the worn wheel can smooth the transition by reducing the cost from wheel truing and rail grinding.

2.5 Guidelines for Compatibility with Special Trackwork

2.5.1 Turnouts

2.5.1.1 Switch Points

Wheel profile changes have significant effects on existing special trackwork because the special trackwork has been either worn or adjusted into shapes compatible with existing wheels.

To avoid derailments on worn switches, the new design wheel has to be checked against worn switches to make sure the new wheel profile will not increase flange climb derailment risk.

Figure 28 shows an existing cylindrical wheel contact on a worn switch point; the contact angle on the switch point is about 52 degrees. Figure 29 shows an example candidate new design tapered wheel profile[2] contacting on the same worn switch point; the contact angle is about 23 degrees and the lower contact angle cannot effectively resist wheel climbing in a small number switch. The existing cylindrical wheel maximum flange angle is 68 degrees, while the new design tapered wheel maximum flange is 66 degrees, so the candidate new design wheel flange climb derailment risk could be higher than the existing cylindrical wheel in the worst-case scenario.

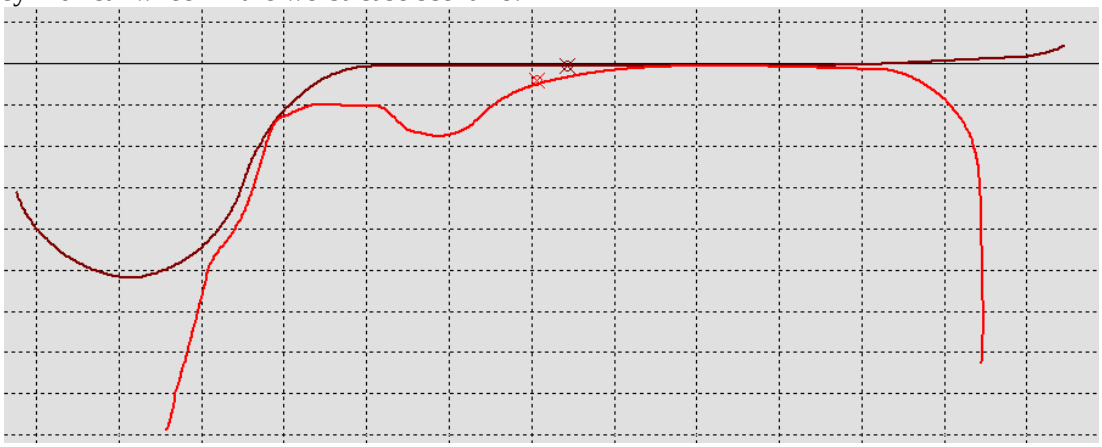

Figure 28. Cylindrical Wheel Contact on a Worn Switch

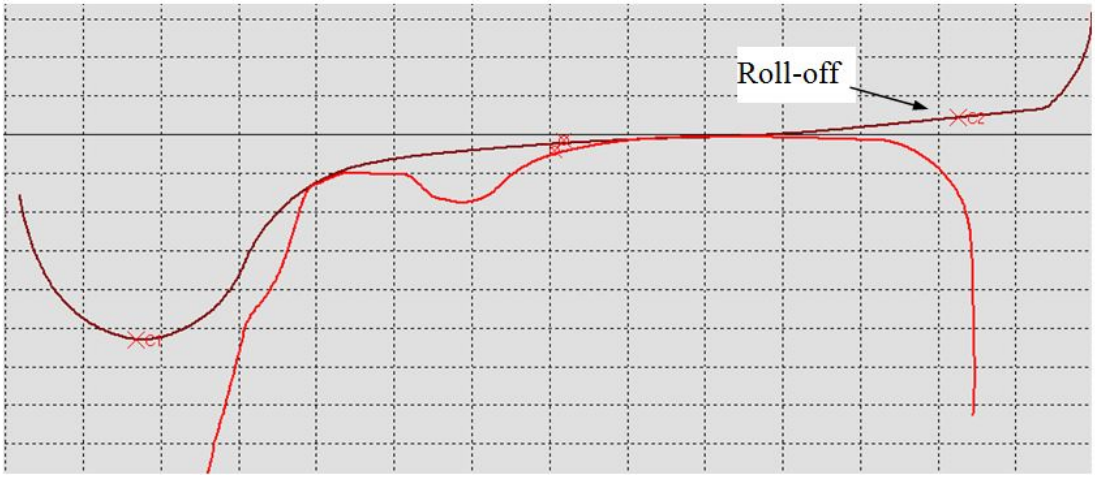

Figure 29. Tapered Wheel Contact on a Worn Switch

[2] Not the same new design profile as used for the curving (Section 2.2) and hunting (Section 2.3)analyses

It is a common practice in European railroad and rail transit systems to add an increased taper roll-off segment to the wheel tread near the field side, as Figure 29 shows. Compared to the tapered wheels without the roll-off, the wheel tread roll-off provides additional rolling radius difference on curves where high rail contacts on the wheel flange and low rail contacts on the roll-off segment. The larger rolling radius difference promotes steering and improves curving performances. It also delays the onset of wheel hollowing as the wheels wear.

AREMA standard (AREMA 2009) requires that switch points rise up ¼ inch above stock rail top. The rise of the switch point is to prevent "false flange" contact on the field side of the wheel tread in the trailing point move. Figure 30 shows that the wheel flange face will contact the stock rail and push it outward if the switch point doesn't rise up. This is especially important for hollow worn wheels. However, the standard European switch design does not have such requirements; therefore, the switch point and stock rail tops are in the same plane. Instead of raising the switch point to prevent false flange contact, the European car manufacturers often design wheels with a roll-off segment on the tread near the field side, which has more taper than the main part of the tread.

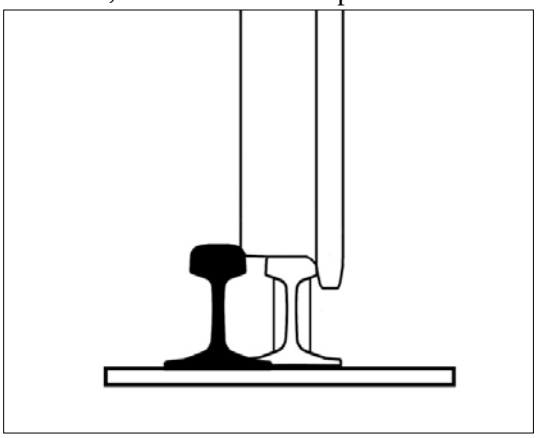

Figure 30. A Worn Wheel Contact on a Worn Switch Point and Stock Rail

It is not clear why these two switch standards are different. Historically, the European and North American (N.A.) rail networks evolved in two different directions. The N.A. system was based primarily on the reliable movement of heavy freight tonnage at the lowest cost, and the European system focused more on speed. A switch point rise will generate vertical track perturbations that have less of an effect on car performances at low speeds than at high speeds. Both AREMA and European recommended types of switches can meet the dynamic performance requirements for rail transit service because the transit car running speeds are relative low. However, wheel profile design requirements for running on these two different types of switches may need to be different. European car manufacturers usually design wheels with tread roll-off, which is necessary for European types of switches, but the benefits of the roll-off need to be justified for N.A. rail transit systems using AREMA recommended switches because:

- High contact stress and rolling contact fatigue could occur near the area where the roll-off segment connects the main part of wheel tread with a sudden change of slope.
- The roll-off segment further increases wheel tread slope, which may not be compatible with frog design as discussed in the following subsection.

2.5.1.2 Switch and Crossing Frogs

W/R impact on frogs is very sensitive to wheel profile shapes. Most rail transit systems in N. A. have adopted the standard AREMA frog, which was designed for tapered wheels. For transit systems using cylindrical wheels, the standard frog nose is often welded back to be level with the wing rail to be

compatible with cylindrical wheels. A new design wheel with a tapered tread will bluntly strike the existing frog nose and result in a depressed nose, as Figure 31 shows. The added taper on the field side exacerbates the problem. To avoid damage, the frog noses would need to be ground accordingly before the new candidate tapered wheels are introduced into service.

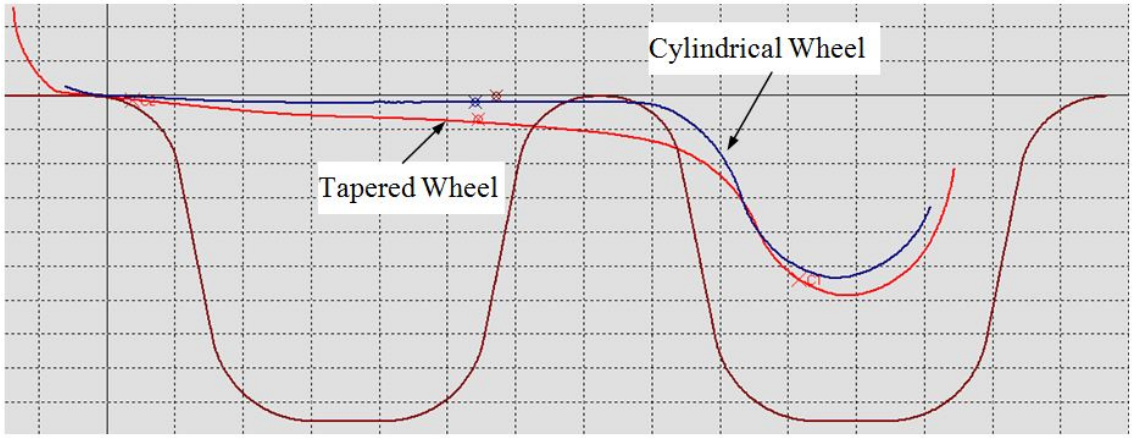

Figure 31. A Taper Wheel and Cylindrical Wheel Contact on a Frog

2.5.2 Switch Point Protectors

Figure 32 shows a typical switch point protector implemented in a yard switch. A recent study showed that wheel tread chamfers on locomotive wheels likely contributed to switch point derailments due to contact between wheel chamfer and the guard (Wilson et al. 2010).

Figure 32. Switch Point Protector

Figure 33 shows the wheel with a large chamfer (45 degrees) contacting on a new switch point guard at about a 78-degree contact angle. Figure 34 shows the wheel with smaller chamfer contacting on the vertical surface of the guard with a 90-degree contact angle. Both wheels are standard AAR S-622 cylindrical tread narrow flange wheels. The large chamfer (0.8839 inch length, 5/8 inch depth) wheels were permitted to be used prior to 2007. The small chamfer (0.4375 inch long) is currently the largest chamfer allowed in AAR M-107.

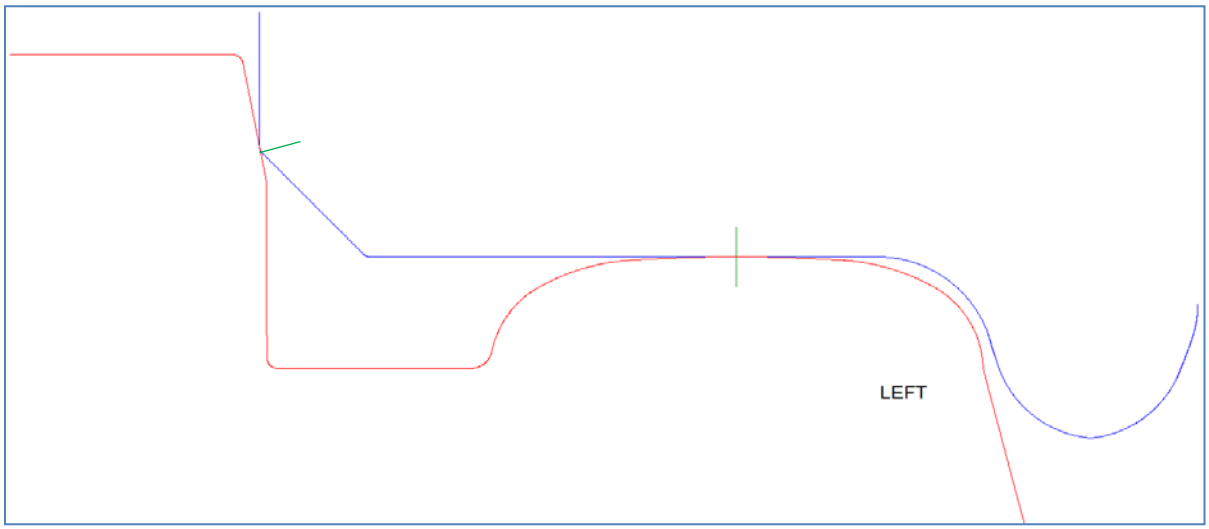

Figure 33. A Larger Chamfer Wheel Contacts on a New Switch Point Guard

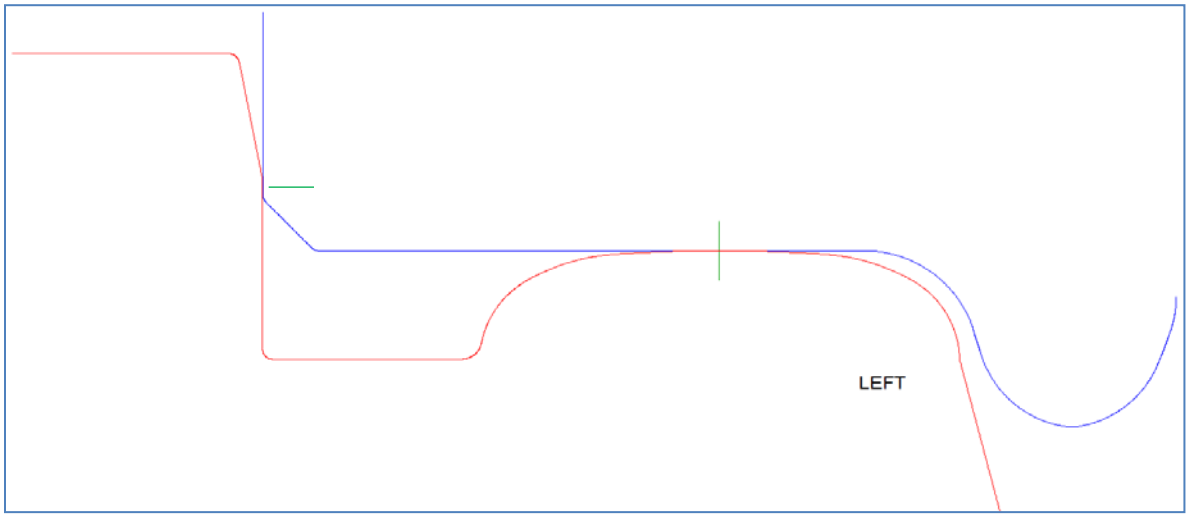

Figure 34. A Smaller Chamfer Wheel Contacts on a New Switch Point Guard

The contact angle of the larger chamfer wheel on the guard could be lower than 78 degrees as the switch point protector guard wears out. The low contact angle between the larger chamfer and the worn guard facilitates wheel climb. Wheel profiles that include a wheel chamfer need to be carefully designed with consideration of special trackwork compatibility.

2.5.3 Spring Switches

Spring switches are often used in light rail transit systems, especially in urban city areas. They lower costs by using a mechanical device (spring or retard) instead of a throw motor. It is automatically operated by mechanical devices located under road surface, which also eliminates the safety hazard caused by switch stand. Figure 35 shows a typical spring switch used in a light rail transit system.

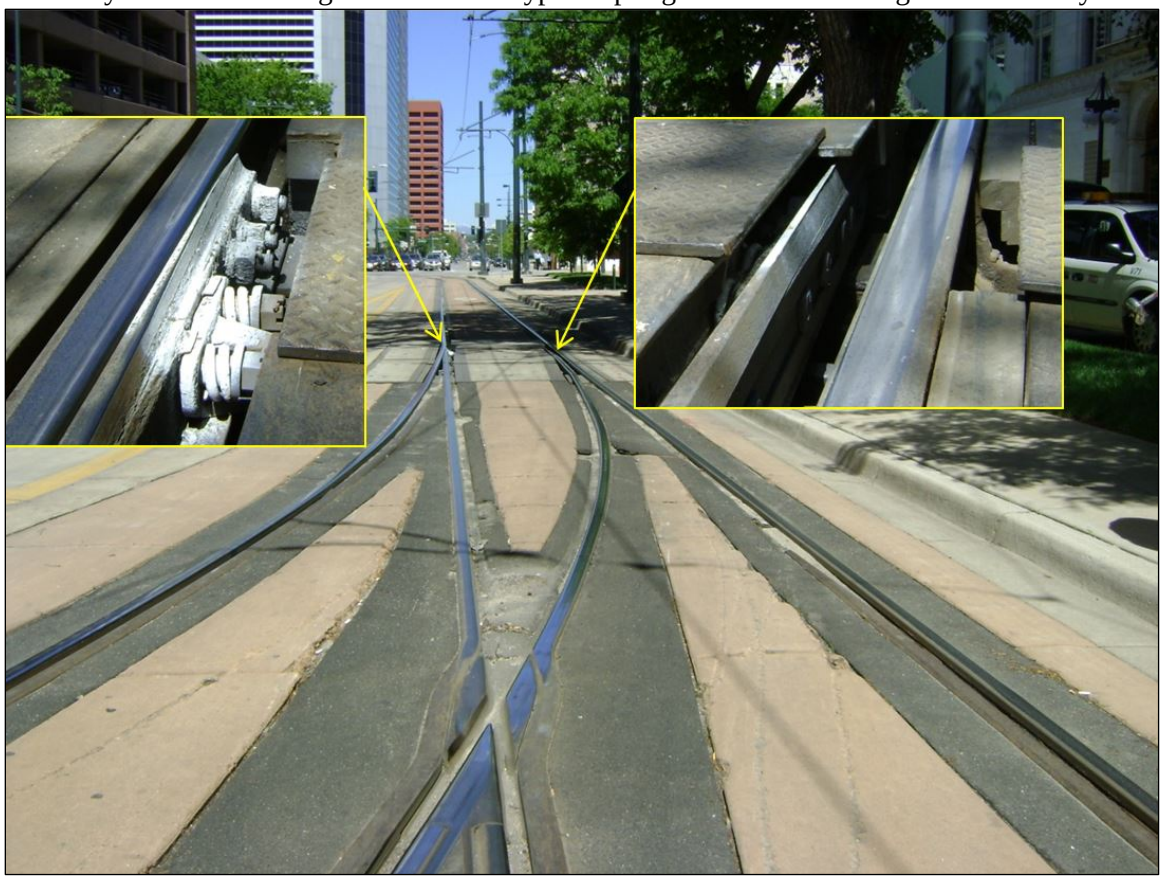

Figure 35. Spring Switch in a Light Rail Transit System

In Figure 35, the mainline switch point is closed. In the trailing move direction of the branch line, the switch point is opened by the wheels; after the wheels pass the switch point, it is closed by the spring force. The spring force must meet requirements from two aspects:

- The force has to be big enough to close the point for main line movement.
- The force cannot be too high. The high spring force resists the wheel opening the switch point in the trailing move direction for branch-line movement, which may cause flange climb derailment.

Figure 36 shows the W/R contact and spring force in a spring switch. To avoid flange climb derailment in a spring switch, the following criterion must be met:

$$\mu_2 + \mu_3 + \frac{F}{V_2} < \frac{\mu_1 + \tan\alpha}{1 - \mu_1 \tan\alpha} \qquad (3)$$

Where, α is the maximum wheel flange angle, μ_1 is the left side W/R friction coefficient, μ_2 is the right side W/R friction coefficient, μ_3 is the friction coefficient between the rail base and the sliding plate underneath the switch point, V_2 is the right side vertical wheel load, and F is the spring force.

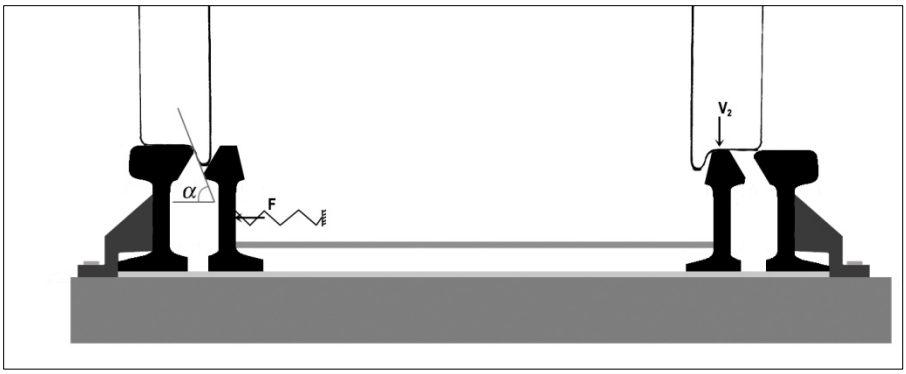

Figure 36. W/R Contact on Spring Switch Points

While the friction coefficient μ_3 can be decreased as low as possible by using grease to ease the sliding movement of the switch point on the plate, the W/R friction coefficient μ_2 cannot be controlled because of environmental changes. Lubrication on the switch point is limited by operation. The weather, wheel, and rail surface conditions can dramatically change the W/R friction coefficient. For a rusty switch point top and a new trued wheel, the friction coefficient could easily reach 0.6. Flange climb derailment could occur if the criterion in Equation 3 is not met because of high friction coefficients and low wheel flange angle. Another issue of spring switches is excessive wear occurring on the open point tip (right side switch point tip in Figure 36, which is open for facing movement). The wear was generated during trailing point movement when the wheel opened the switch point on the left side and pushed the right switch point towards the stock rail.

A gap between the right side switch point tip and the stock rail exists because of the resistant spring force F and the friction resistance forces in a spring switch. The wheel not only wears out the switch point tip but also bends it towards the stock rail due to the gap. This type of unusual wear does not occur in a regular switch operated with a manual or motor switch machine, where the switch point was hidden under the stock rail without any gap. A wheel with a shallow flange angle (<70 degree), which usually has a larger radius flange root, could generate more wear and metal flow on a spring switch point tip than a wheel with high flange angle (>72 degree).

Adopting high flange angle (>70 degree) wheels and lubricating new trued wheels and switch point top can reduce derailment risk and excessive wear in a spring switch. However, because use of lubrication is not failsafe, design and maintenance guidelines should assume dry, high friction conditions.

2.6 Wheel Profile Maintenance Guidelines

Wheel maintenance is critical for rail vehicle safety and ride quality. Effects of wheel diameter differences and wheel wear on car performances were investigated in the following subsections to develop wheel profile maintenance guidelines.

2.6.1 Wheel Diameter Difference

2.6.1.1 Effect on Hunting

Wheel diameter difference in an axle is usually caused by asymmetric wear or malfunction of a wheel truing machine. Figure 37 shows the effect of wheel diameter difference in the same axle on hunting performance. The wheel profile used in the simulations was the existing new 63-degree wheel profile.

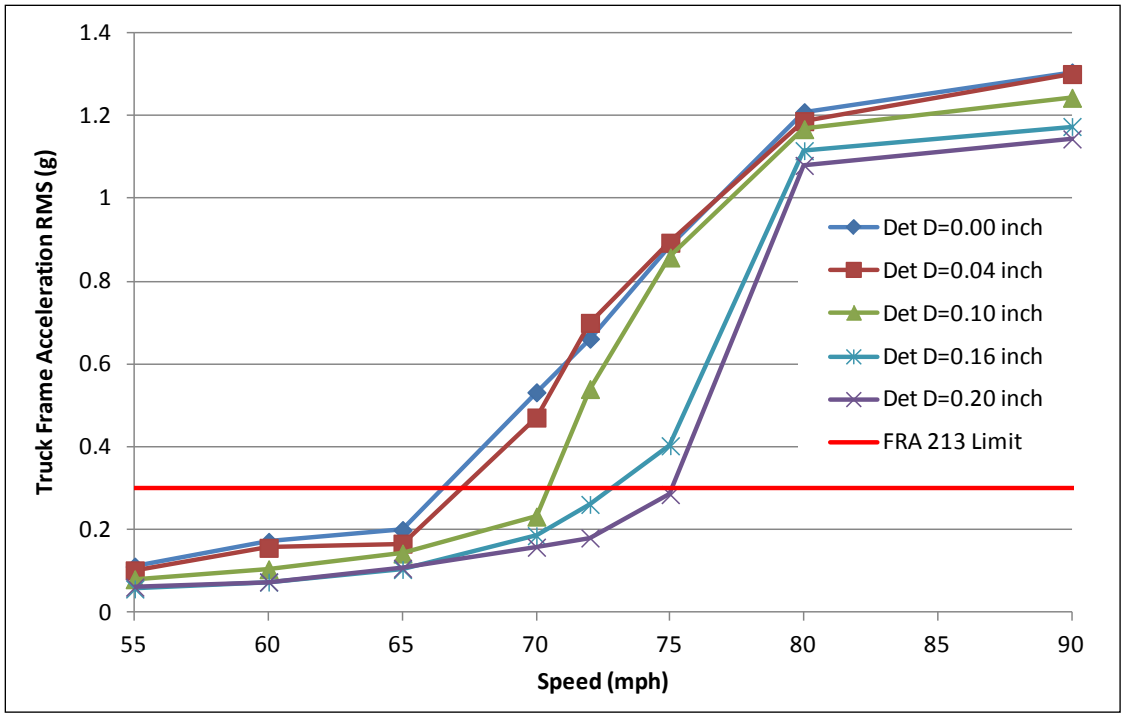

Figure 37. Wheel Diameter Difference (in the Same Axle) Effect on Hunting (56.25-inch gage)

Figure 37 shows that the hunting speeds increased with wheel diameter differences. Wheel diameter differences in an axle cause the axle to shift away from the track center towards the wheel with smaller diameter, which decreases the W/R clearance between the smaller diameter wheel and rail. The HSC chart in Figure 19 shows that the hunting speed increases with the decrease of W/R clearance when the conicity stays the same. This conclusion only applies for new wheel profiles with diameter differences, because wheel diameter difference does not change conicity. For worn wheels with different diameters, both the conicity and clearance will change because of wear and diameter difference. Therefore, for worn wheels the hunting performance has to be evaluated based on the HSC chart.

2.6.1.2 Effect on Wear and Curving Performance

For curving simulation, the smaller diameter wheel was implemented on the high rail to simulate the worst curving scenario for a car with wheel diameter differences. Figures 38 and 39 show that the wheel wear index and rolling resistance generally increase with wheel diameter differences on curves. Diameter differences from 0 inch to 0.2 inch (5.08 mm) were simulated.

Figures 40 and 41 show that the wheel L/V ratios and lateral forces significantly increase with wheel diameter difference on curves.

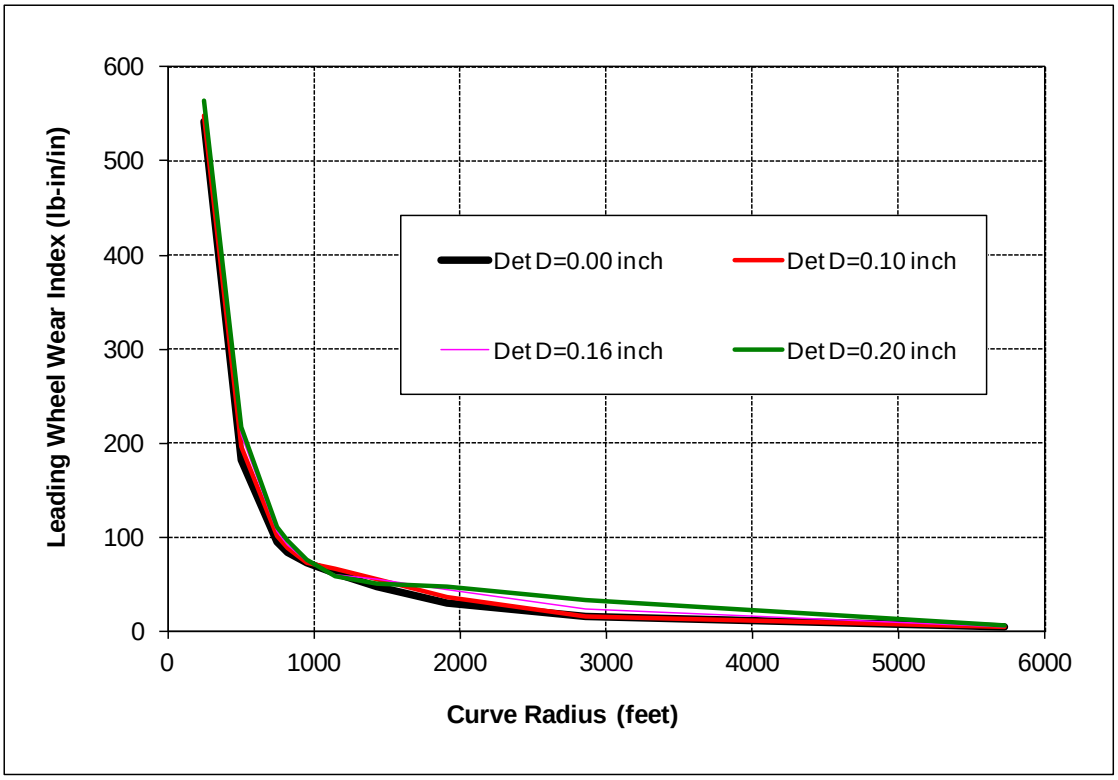

Figure 38. Wheel Diameter Difference Effect on Wear Index

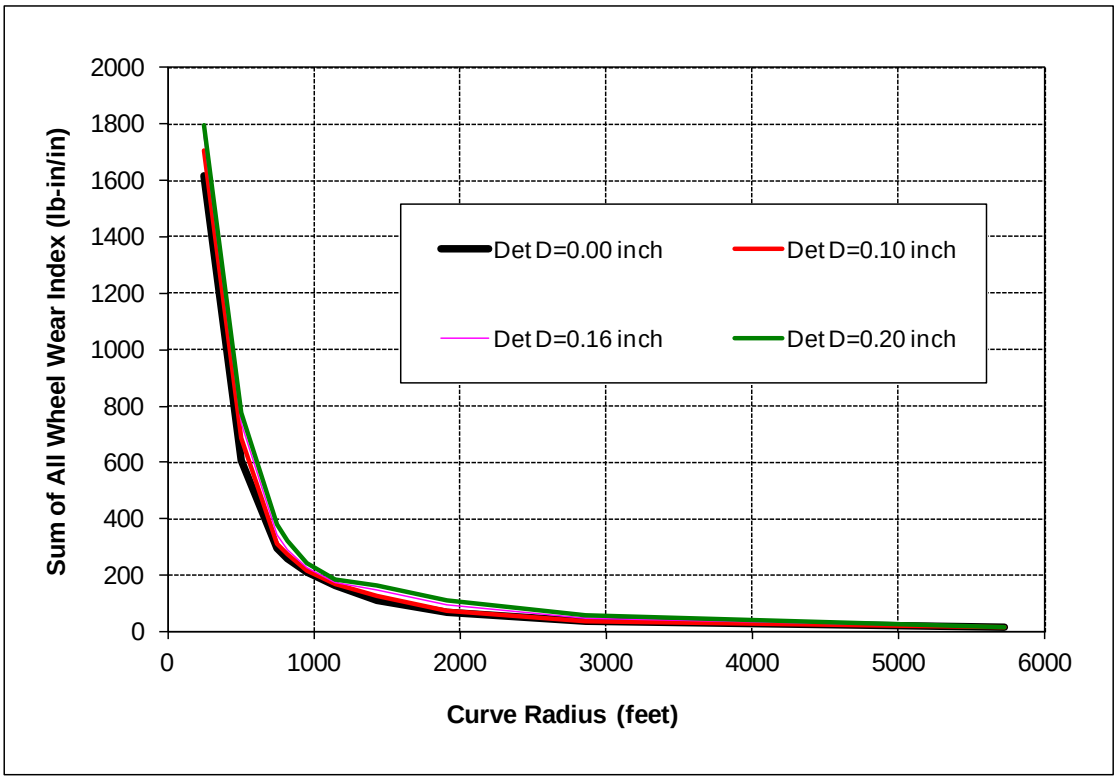

Figure 39. Wheel Diameter Difference Effect on Rolling Resistance

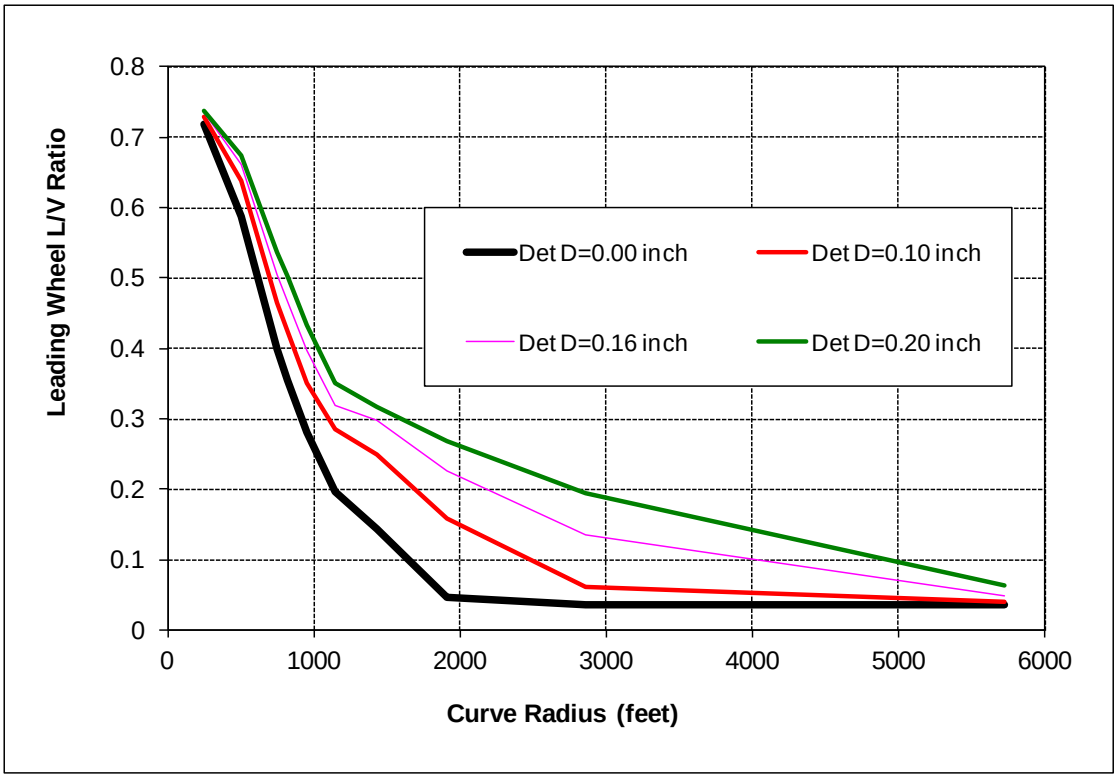

Figure 40. Wheel Diameter Difference Effect on Wheel L/V Ratio

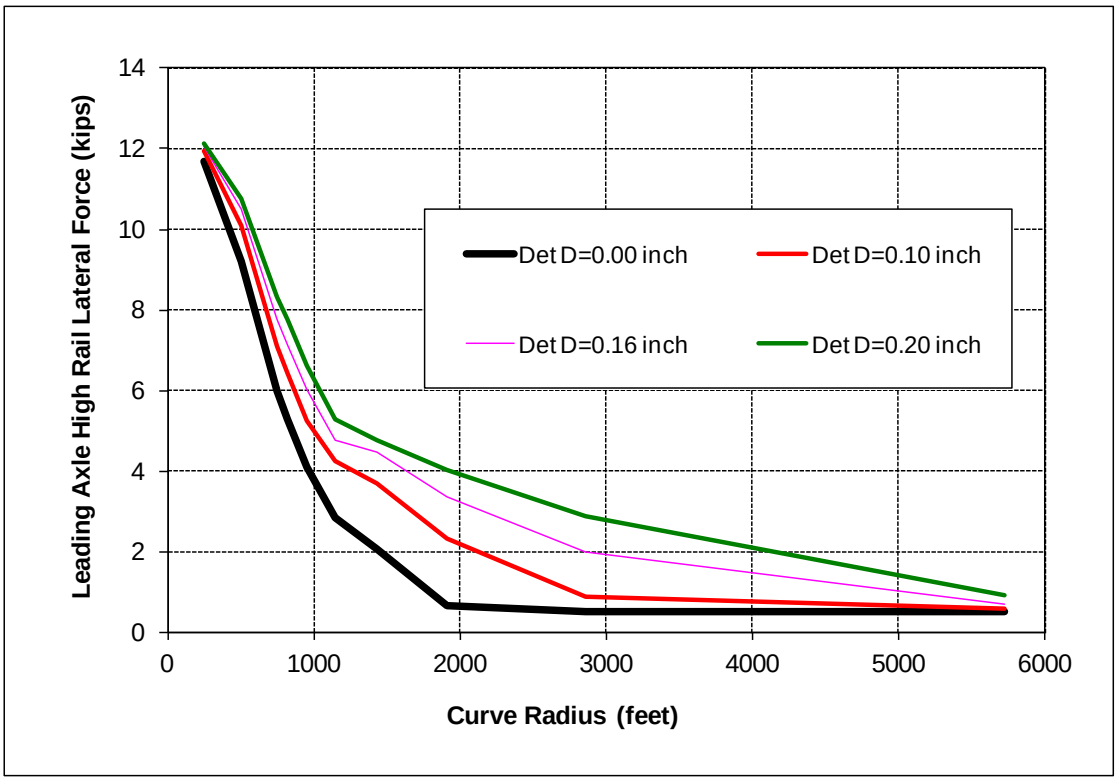

Figure 41. Wheel Diameter Difference Effect on Wheel Lateral Force

2.6.1.3 Effect on Wheel Unloading

Wheel diameter difference effects on vertical wheel unloading were investigated by running the car through measured pitch and bounce track perturbations (AAR Chapter 11, Pitch and Bounce track perturbations, 39-feet wave length and maximum ¾-inch amplitude) at different speeds. Figure 42 shows that the wheel diameter difference effect on the wheel unloading ratio is negligible.

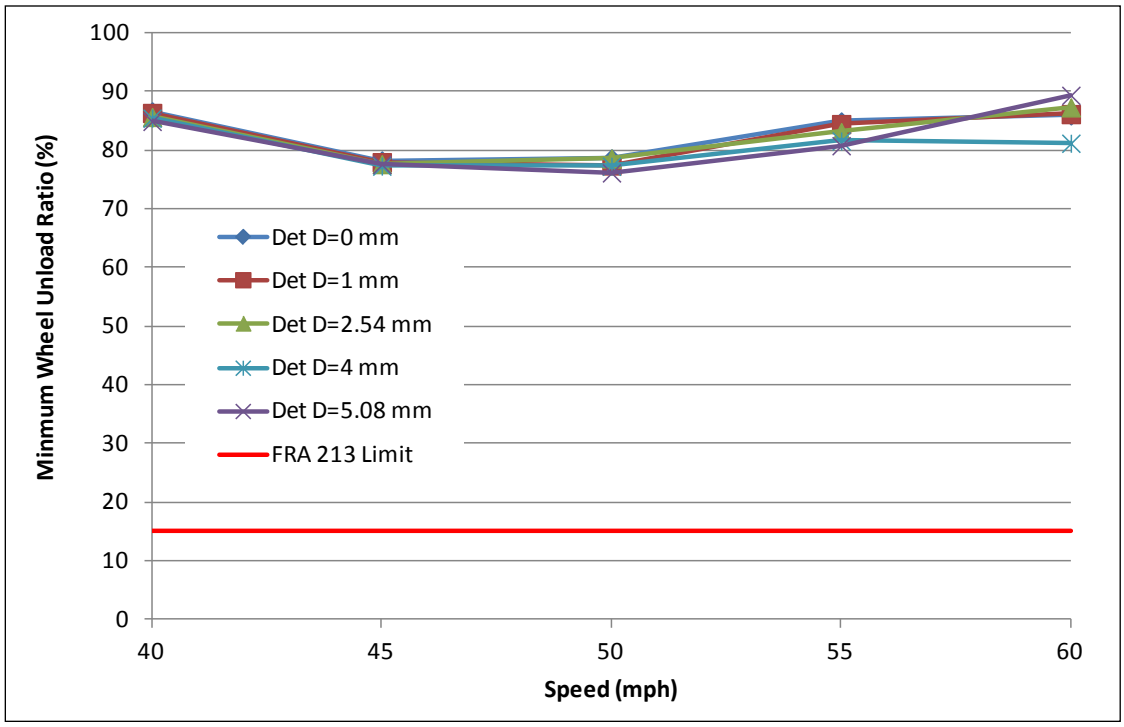

Figure 42. Wheel Diameter Difference Effect on Wheel Unload

2.6.1.4 Effect on Vertical Wheel Load Equalization

The maximum wheel unloading for a car equipped with axles with 0.25-inch wheel diameter difference between left and right wheels is 8 percent at 2.5-inch wheel drop. The maximum wheel unloading for car equipped with axles with 1.0-inch wheel diameter difference between leading and trailing axle in a truck is 7 percent at 2.5-inch wheel drop, both are well below the 65-percent limit for APTA Class G and R passenger equipment (APTA SS-M-014-06 2007). Wheel diameter difference effects on load equalization should be small as long as the static primary suspension deflection is larger than the wheel diameter difference in an axle.

2.6.1.5 Wheel Diameter Difference Summary

In summary, wheel diameter differences on new or freshly turned wheels improve hunting performance due to the decrease of W/R clearance when the axle shifts from the track center position towards the smaller radius wheel. However, wheel diameter differences resulted in poor curving performances, such as more wear and larger lateral forces on high rails, which may cause gage spreading. Wheel diameter differences between axles and trucks may lead to components interfering or fatigue, which will have to be addressed case-by-case.

2.6.2 Wheel Wear

2.6.2.1 Effect on Hunting and Ride Quality

Transit agencies usually adopt wear limits on wheel and rail wear to maintain acceptable vehicle and track performances. A new wheel quickly wears into a shape conformal with existing rails, which decreases contact stress, but may deteriorate car ride quality as it becomes heavily worn.

Wheel wear may result in hollow treads and thin flanges. Wheel wear was usually well controlled by wear limits on tread, flange, and flange height. Transit wheel tread wear depth (hollowness) is usually less than that in freight railroads. In addition to flat wheels, worn wheels with thin and tall flanges exceeding limits are usually corrected through wheel truing. The flange thicknesses for the measured new, slightly worn, moderately worn, and heavily worn wheels from the representative heavy rail transit system in Figure 1 were 34, 32, 30 and 28 millimeters (1.7,1.3,1.2,1.1 inches), respectively.

Figure 43 shows the conicities of these measured wheels on a new 115RE rail with 56.25 inch track gage. The conicity increased with wear for slightly and moderately worn wheels, but decreased when the wheel became heavily worn. W/R clearance increased consistently with wear as the flange wore out.

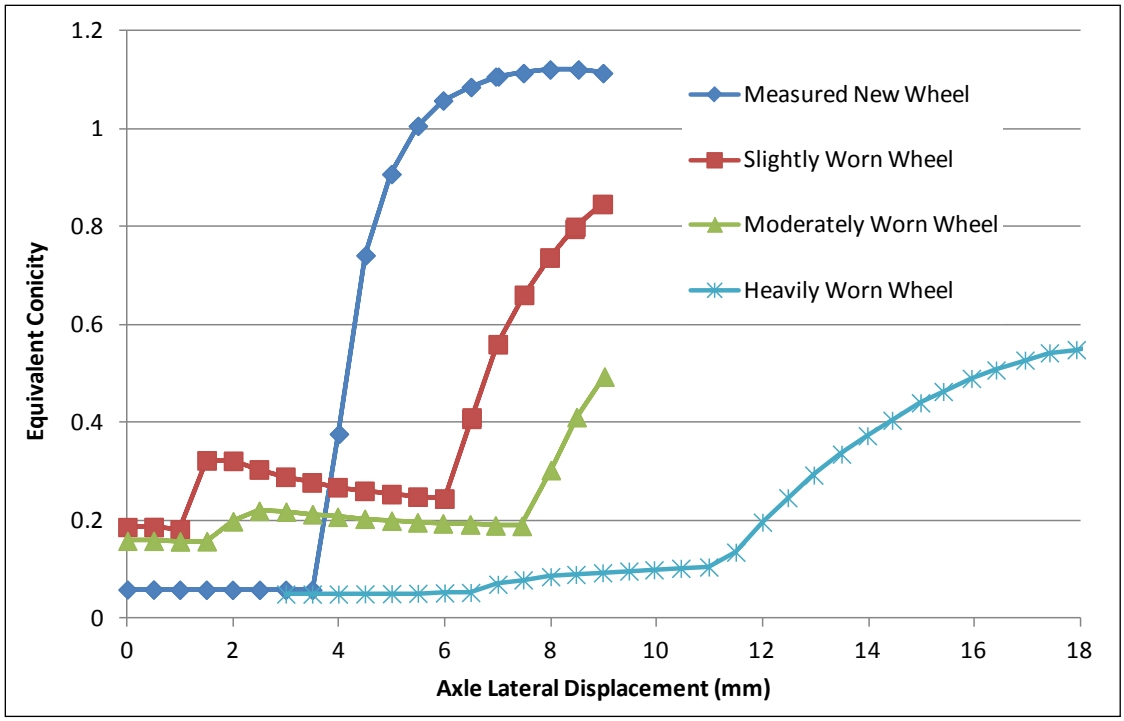

Figure 43. Measured New and Worn Wheel Conicity, Track Gage 56.25 inches

The calculated W/R conicity and clearance were plotted on the HSC chart for hunting performance evaluation, as Figure 44 shows. The estimated hunting speed for the new measured wheel is above 80 mph, while the hunting speeds for the worn wheels are about 70 mph.

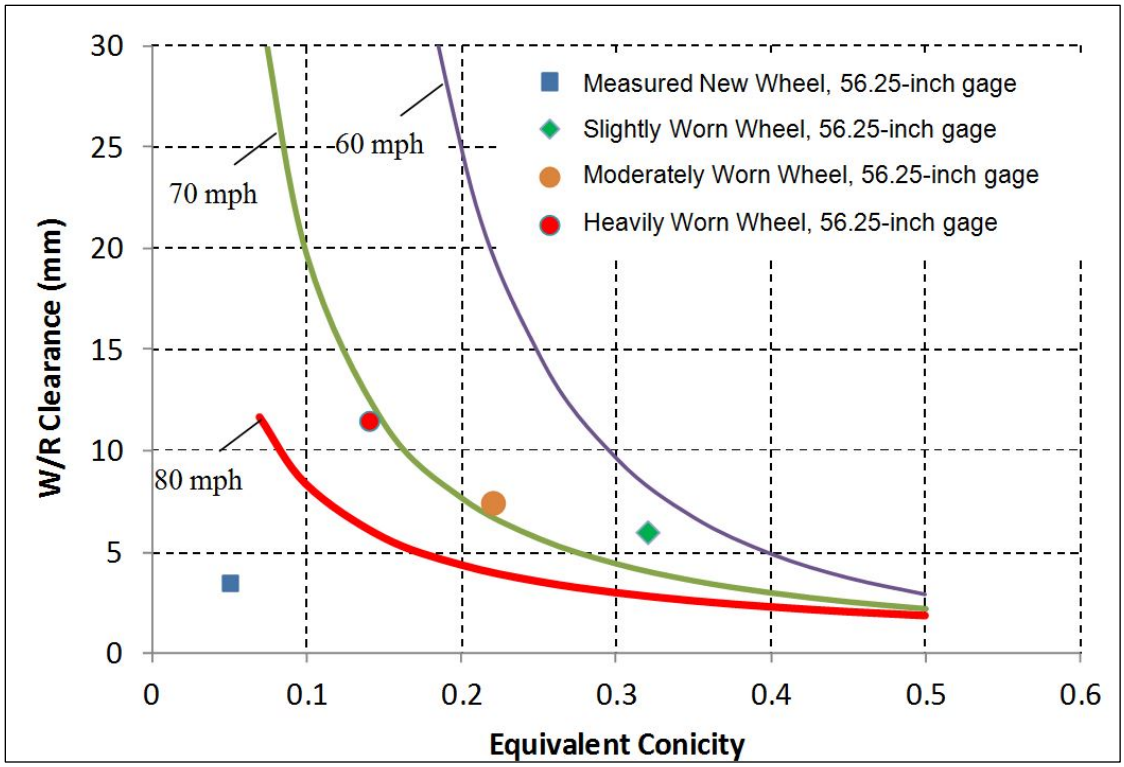

Figure 44. Hunting Speed Estimation for a Car Equipped with Measured New and Worn Wheels

Figure 45 shows the predicted car hunting speeds. The car equipped with new wheels has the highest hunting speed (about 81 mph), the hunting speeds with worn wheels decrease to about 67 mph, although the heavily worn wheel's hunting speed is a little higher than the slightly and moderately worn wheel because of its lower conicity. The estimated hunting speeds from the HSC chart are generally consistent with the predicted hunting speeds from the simulations.

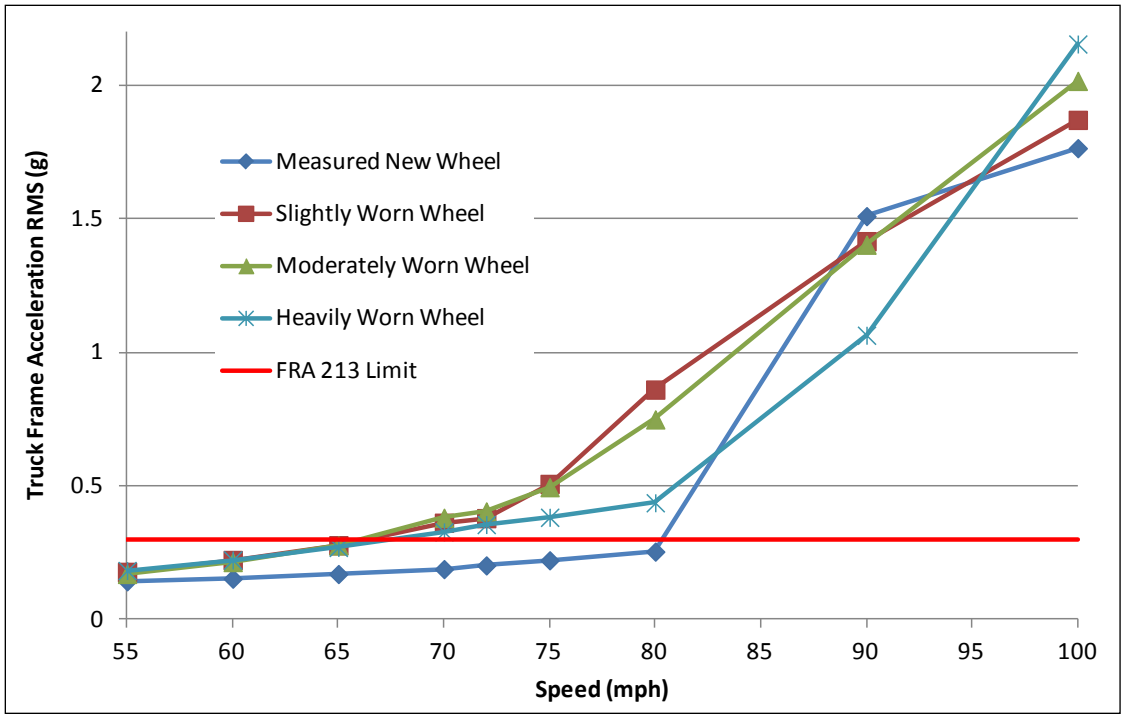

Figure 45. Truck Frame Accelerations of a Car Equipped with Measured New and Worn Wheels (56.25-Inch Gage)

Figures 46 and 47 show the conicities of these measured wheels with 56.5- and 57-inch track gages, which were used in shallow curves and tight curves, respectively. The conicity decreased and clearance increased with the increase of track gage. Figure 48 shows that the hunting speeds of measured wheel with track gage variations can be estimated from the HSC chart based on their conicity and clearance.

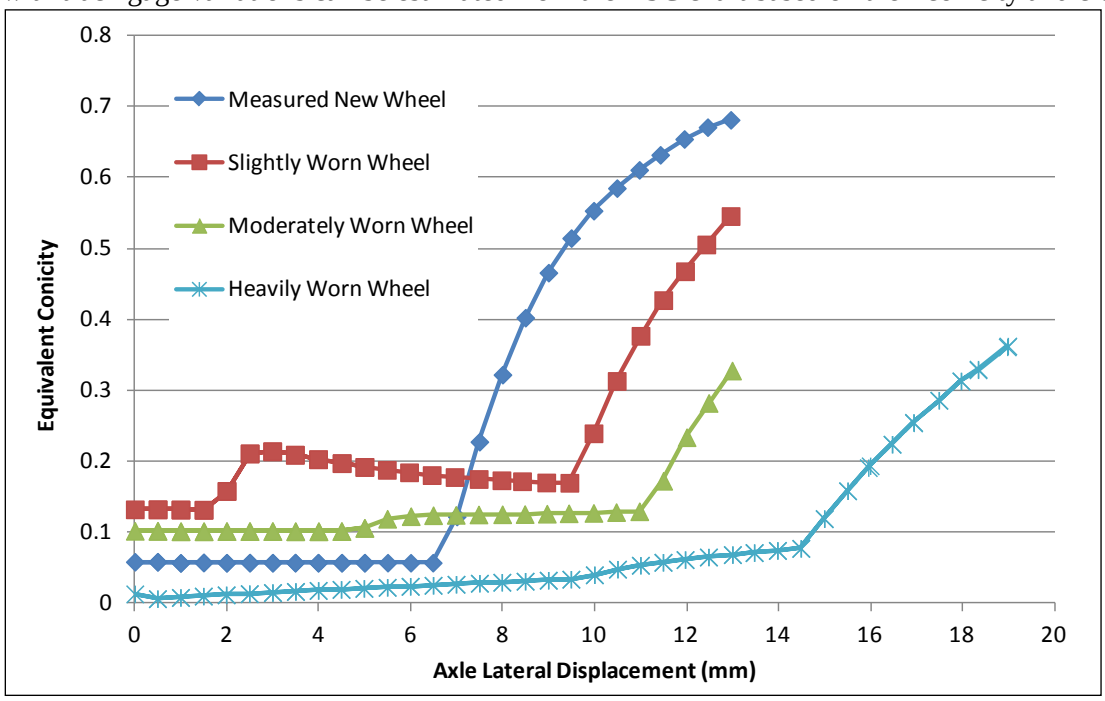

Figure 46. Measured New and Worn Wheel Conicity, Track Gage 56.5 inches

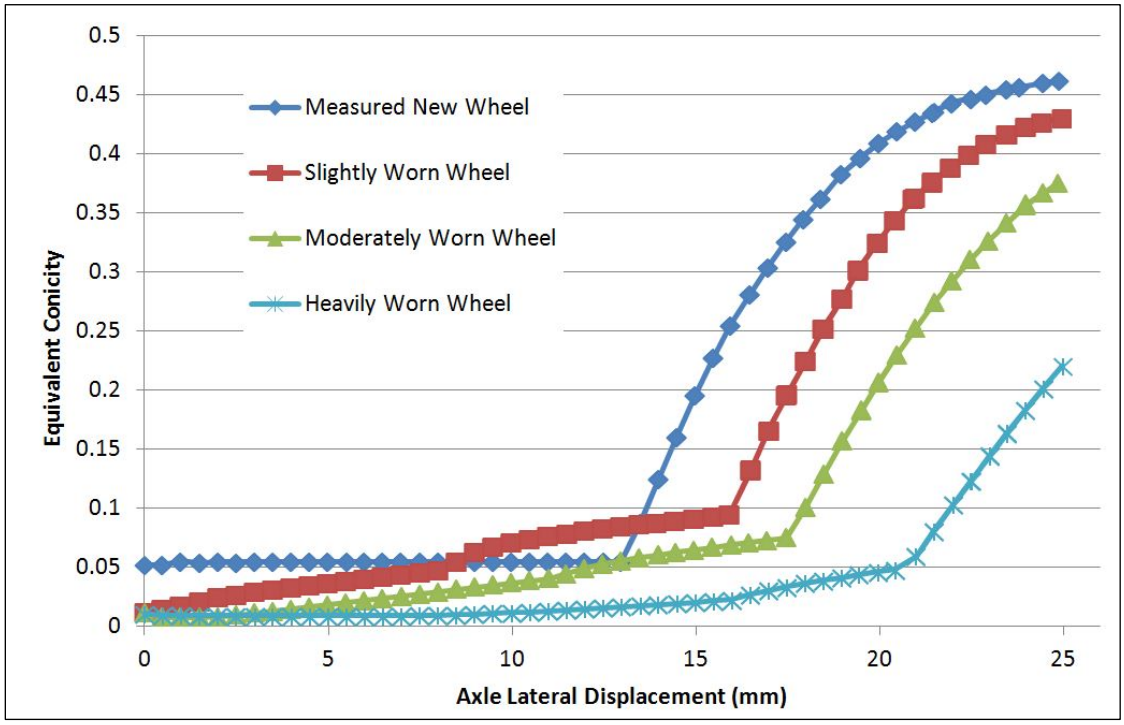

Figure 47. Measured New and Worn Wheel Conicity, Track Gage 57 inches

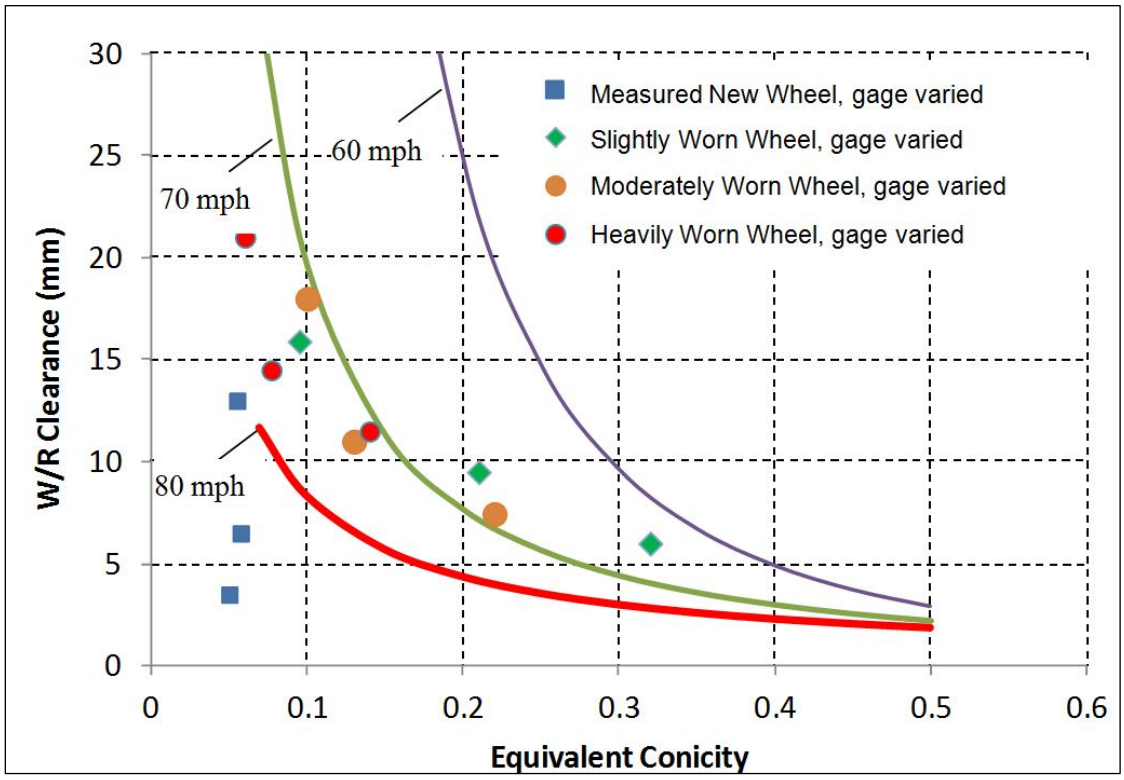

Figure 48. Wheel Wear Effect on Hunting

The car hunting speeds of new measured wheels with track gage variations are higher than that of worn wheels. However, the heavily worn wheel wore the tapered tread into a flat shape, which lowered the conicity. So, the car stability with heavily worn wheel is even better than slightly and moderately worn wheel due to its lower conicity.

Wheel wear may increase or decrease conicity depending on the wheel and rail geometry parameters, wear patterns, and operation conditions. Traditional wheel wear limits on tread and flange are not directly related with car hunting performances. The proposed W/R contact geometry based HSC chart provides a useful tool to control the car hunting speed with worn wheels above the operational speed.

Even though the hunting speed of the heavily worn wheel was similar to that of slightly worn and moderately worn wheels, Figure 49 shows that the low conicity heavily worn wheel with large W/R clearance has a negative effect on ride quality, probably due to the resonance response from carbody. Similar phenomena were observed in tests as described by Polach 2009 and Smith and Kalousek 1991. Further research on secondary suspension and carbody vibration modes is needed to investigate low conicity effect on ride quality.

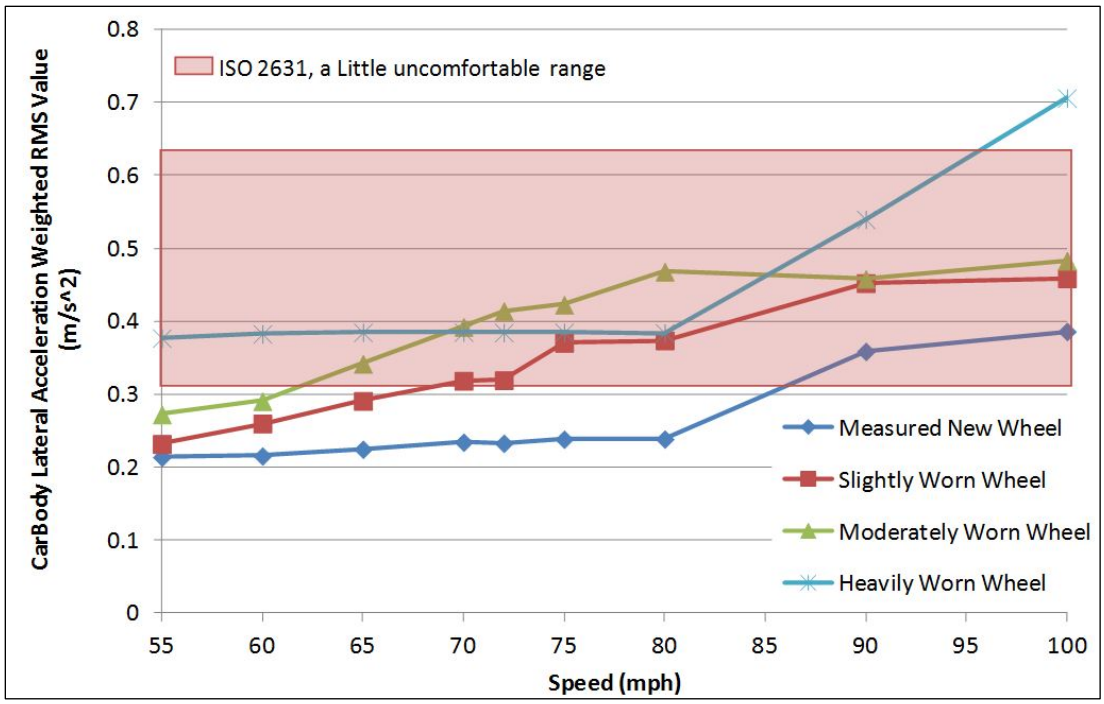

Figure 49. Effect of Wheel Wear on Ride Quality

Even though the measured new wheel profile generates low conicity, its maximum flange angle is still 63 degrees; therefore, it still has higher flange climb derailment risk than that of the new design wheel (with 70-degree flange angle). The new design wheel was optimized for both curving and hunting performances.

2.6.2.2 Effects on Frog Impact

Figure 50 shows four frog cross section profiles at locations A, B, C, and D in a standard AREMA No. 20 turnout. The distances on the track at location B, C, and D were measured as 0.2, 0.8, and 4.58 feet from location A (frog nose), respectively.

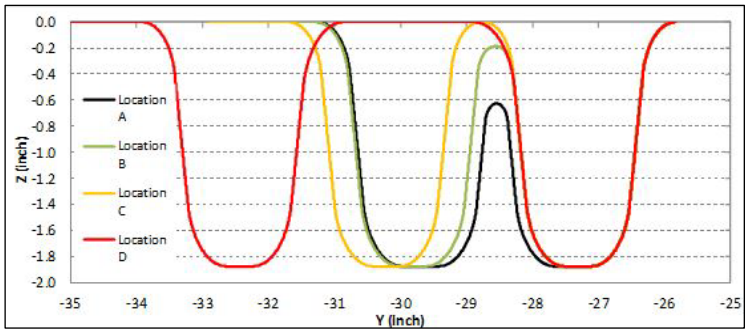

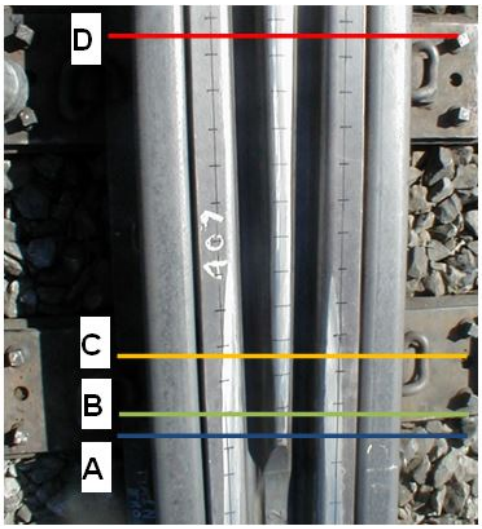

Figure 50. No. 20 Turnout Frog Profiles

Figure 51 compares the impact ratios predicted for the new and worn wheel profiles operating over a new No. 20 turnout frog. The impact ratio was defined as:

$$\text{Impact ratio} = \frac{\text{maximum impact force}}{\text{static wheel load}} \qquad (4)$$

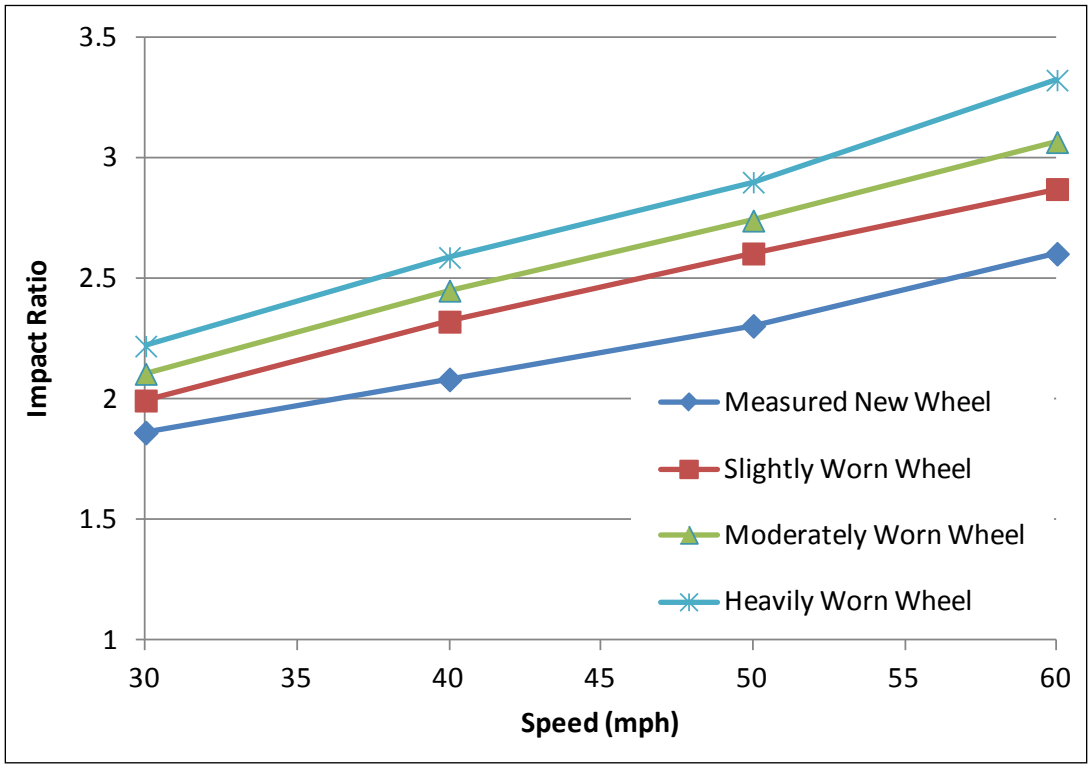

Figure 51. W/R Impact Loads on a New Frog

Figure 51 shows the impact ratio on frog nose increases with wheel wear and running speed. The heavily worn wheel impact ratio was increasing by about 25 percent compared to that of the new wheel. Heavily worn wheels have to be removed to prevent damage to the vehicle and frog. The wheel wear limit for removal can be set up based on the impact ratio.

2.6.2.3 Effect on Wear and Curving Performance

Figure 52 shows the wear index of the worn wheels increases on curves with radii from 800 to 2,000 feet, similar to new wheels on tight and shallow curves. Figure 53 shows a similar trend can also be found for lateral forces applied on high rail. Wheel wear effects on curving performances are relatively small compared to hunting and frog impact.

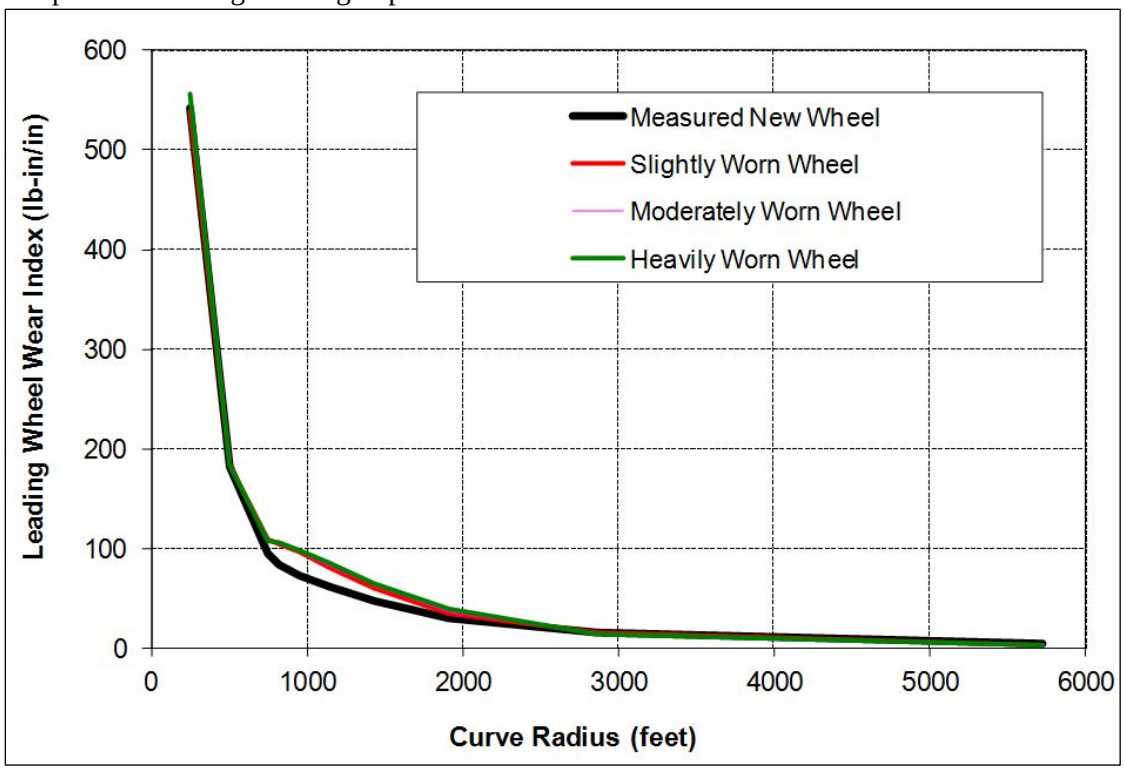

Figure 52. New and Worn Wheel Wear Index in Curves with New Rails

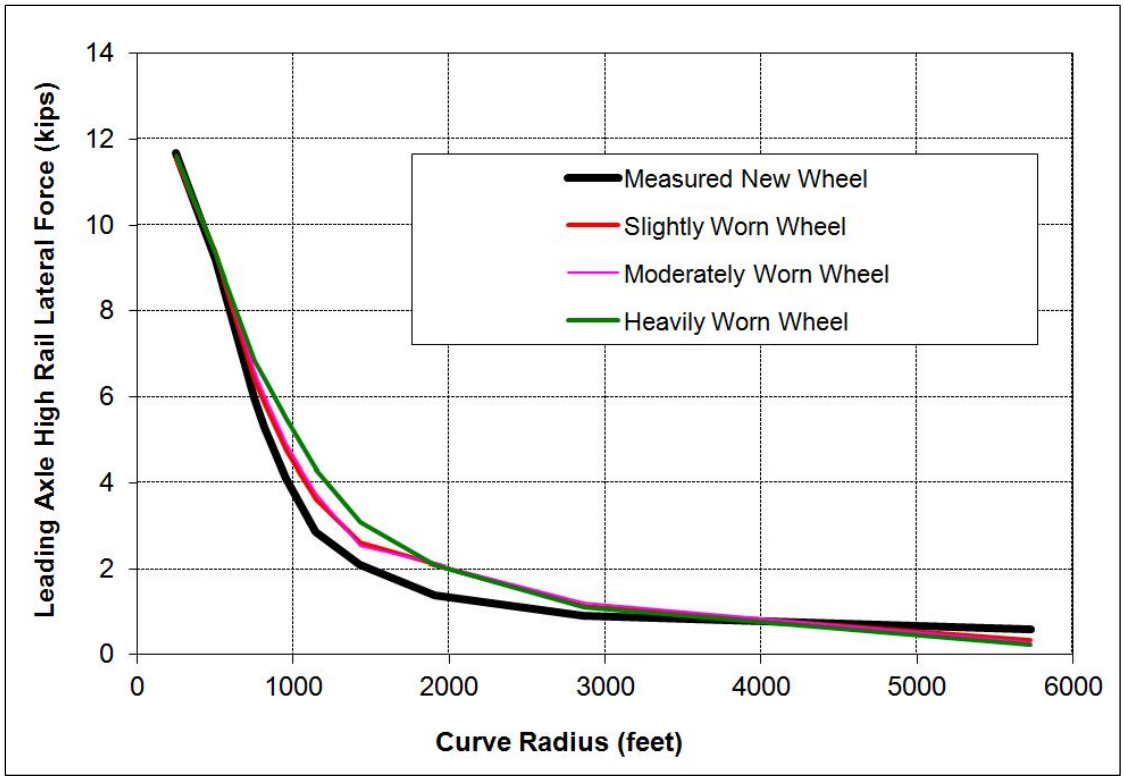

Figure 53. New and Worn Wheel Lateral Forces in Curves with New Rails

2.6.2.4 Wheel Wear Summary

Wheel wear effects on hunting performance depend on W/R wear patterns:

- If W/R wear results in high W/R conicity and larger gage clearance, a car may start hunting at speeds lower than that with new wheels and rails.
- If W/R wear results in low W/R conicity and larger gage clearance, car hunting stability needs to be evaluated by using the HSC chart.

Impacts on frogs increase with wheel wear. Wear limits on the wheel tread and flange can be set up based on W/R impacts, which also depend on frog wear conditions and running speeds.

CHAPTER 3

Conclusions and Recommendations

The following conclusions and recommendations are made from this study:

- Both W/R contact conicity and W/R gage clearance have significant and complex effects on car lateral stability (hunting), especially as the wheels and rails wear. A new method for evaluating the combined effects of these two parameters was developed using HSC charts. To demonstrate the new method, two HSC charts were developed for a representative heavy railcar and a representative light railcar. The charts were used to generate the following guidelines for wheel profile design and maintenance:
  - Hunting speed generally decreases (car becomes more unstable) with the increase of both conicity and W/R clearance.
  - Wheel and rail wear increases W/R clearance, and its effect on hunting depends on wear pattern:
    - Worn wheels with high conicity and wide W/R clearances cause the hunting speed to decrease quickly
    - Worn wheels with low conicity and wide W/R clearances cause the hunting speed to decrease slowly, but may result in sudden onset of hunting instability
  - Hunting speeds for high conicity wheels are more sensitive to W/R clearance variations than for low conicity wheels.
  - HSC charts can be used to evaluate new wheel profile designs and also to evaluate worn wheels (and rails), and develop wear and gage clearance tolerances. To provide specific conicity and gage clearance guidelines for a particular vehicle in a transit system, a new HSC chart would need to be developed using simulations for the particular case.
- Increasing the maximum flange angle can effectively reduce flange climb derailment risk. APTA recommends a 72-degree (with tolerance +3 degrees and -2 degrees) flange angle wheel for use in passenger railcars. However, a wheel profile with a flange angle less than 72 degrees (but high enough to prevent flange climb) can also be adopted to provide a smooth transition from an existing low flange angle wheel profile to a new design with high flange angle wheel profile.
- Wheel profiles (new and worn) should be compatible with special trackwork:
  - Impact forces on the frog nose generally increase with wheel wear.
  - Wheels with profiles that are incompatible with the frog generate significant impact on the frog.
  - High flange angle wheels can reduce flange climb derailment risk and reduce excessive switch point tip wear in spring switches.
- Wheel diameter differences on an axle can improve hunting performance because of the decrease of W/R gage clearance when the axle shifts from the track center position toward the smaller radius wheel. However, wheel diameter differences may result in poor curving performances, such as more wear and larger lateral forces on high rails, which may cause gage spreading.
  - Systems with many curves may need tighter tolerances on wheel diameter differences than systems with few curves and mostly straight track
- Wheel wear has significant effects on both hunting speed and frog impact. Wear limits on wheel treads and flanges can be determined by the HSC chart and impacts with frogs, which also depend on frog wear conditions and running speed.
- On-track tests are recommended to further validate these guidelines.

- Effects of wheel profiles with zero and negative W/R conicity (hollow worn wheels) on rail transit car hunting performance are recommended for further investigation.

References

American Public Transit Association. APTA SS-M-014-06, Standard for Wheel Load Equalization of Passenger Railroad Rolling Stock. Washington, D.C., 2007.

American Railway Engineering and Maintenance-of-Way Association. AREMA *Manual of Railway Engineering*, Vol. 1, Chapter 5, Track. Lanham, MD, 2006.

Federal Railroad Administration. 49 CFR Part 213, Track Safety Standards, Subpart G, Train Operations at Track Classes 6 and higher, 213.333 Automated Vehicle Inspection Systems, Washington, D.C., Amended March 13, 2013.

Griffin, T. *TCRP Report 114: Center Truck Performance on Low-Floor Light Rail Vehicles*. Transportation Research Board of the National Academies, Washington, D.C., 2006.

International Union of Railways. UIC Leaflet 518. Testing and Approval of Railway Vehicles from the Point of View of Their Dynamic Behavior – Safety – Track Fatigue – Running Behavior, 2009.

International Union of Railways. UIC Leaflet 519. Method for Determining the Equivalent Conicity, 2004.

Polach, O. "Wheel Profile Design for the Target Conicity and Wide Contact Spreading." *Proceedings of the 8th International Conference on Contact Mechanics and Wear of Wheel/Rail System*, Italy, 2009.

Shu, X. "Survey of Current Wheel Profiles and Maintenance Practices." Final Report, TCRP D-7 TASK 20 Task 1, Transportation Technology Center, Pueblo, CO, 2014.

Smith, R. E. and J. Kalousek. "A Design Methodology for Wheel and Rail Profiles for Use on Steered Railway Vehicles," *Wear*, Vol. 144, 1991.

Strogatz, S. H. *Nonlinear Dynamics and Chaos*. Addison Wesley Publishing Company, 1994.

True, H. "Does a critical speed for railroad vehicles exist?" RTD-Vol. 7, *Proc. Of the 1994 ASME/IEEE Joint Railroad Conference*, Chicago IL, March 22–24, 1994.

Wilson, N., D. D. Davis, and S. Anankitpaiboon. "Analysis of Contact Issues Between Locomotive Wheels and Switch Point Guards." *Technology Digest* TD-10-18, Association of American Railroads, Transportation Technology Center, Inc., Pueblo, CO, 2010.

APPENDIX

Light Railcar Hunting Speed Contour Chart

A.1 Vehicle Model

A typical light rail vehicle model consisting of two carbodies and three trucks with the following specifications was used in this study:

- Two carbodies articulate on the middle truck
- Primary Chevron suspension
- Secondary airbag suspension
- Lateral and vertical damper in secondary suspension
- Axle spacing: 6.3 feet
- Truck Center Spacing: 23 feet
- Wheel load: Mid truck: 5.2 kips, End truck: 8.2 kips
- Wheel diameter: 27 inches

Vehicle model parameters were measured through characterization tests. The measured primary suspension longitudinal, lateral stiffness, and damping were reduced by half to simulate a worn truck condition. The standard AREMA 115RE rail profile and 0.5 W/R friction coefficients representing dry wheel and rail contact condition were used in the simulations.

A.2 Hunting Speed Contour Chart

Hunting speeds of a light railcar with different wheel profiles were obtained through simulations by using the methodologies described in subsection 2.3 of this document. Figure A1 shows the hunting speed contour (HSC) chart for the simulated light railcar. Section 3 of this document discusses the guidelines for using the light rail HSC chart for new wheel design and worn wheel maintenance.

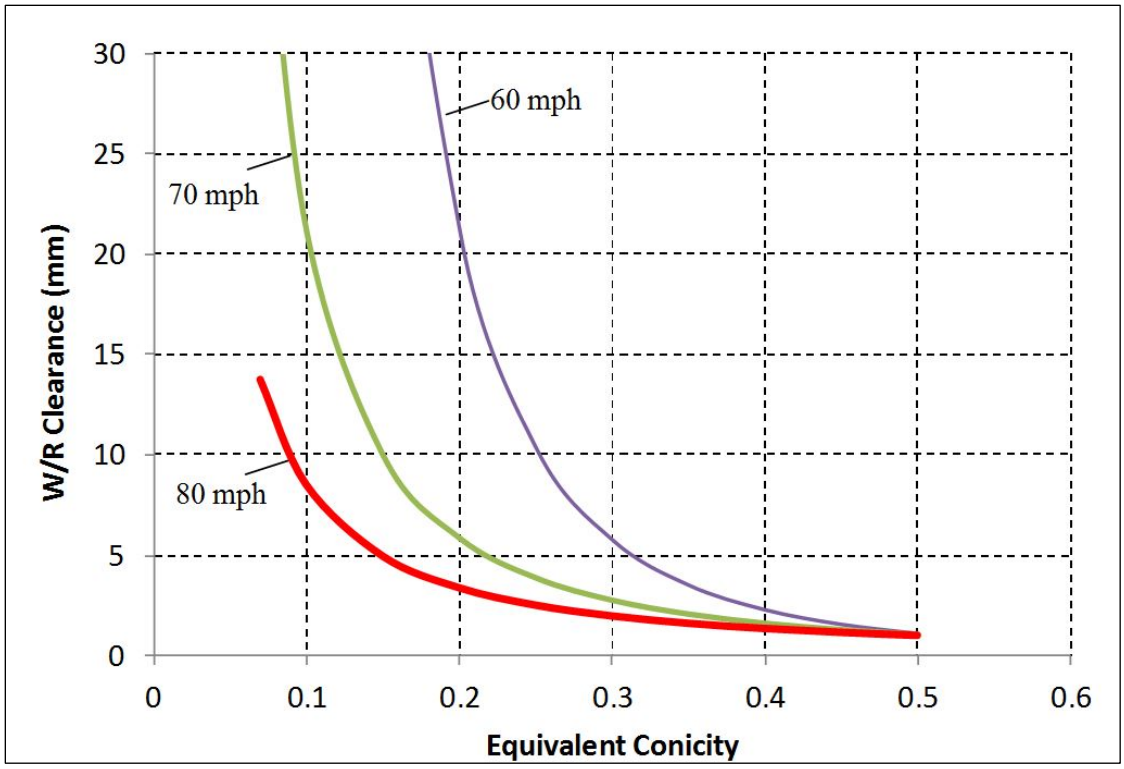

Figure A1. Hunting Speed Contour Chart for a Light Railcar

Wheel Profile Maintenance Guidelines

PART 3

Development of New Wheel Profiles for Port Authority Trans-Hudson

Table of Contents

TABLE OF CONTENTS i
LIST OF FIGURES ii
LIST OF TABLES iii
SUMMARY 1
CHAPTER 1 Introduction 2
CHAPTER 2 Methodology 3
CHAPTER 3 Review of Current Conditions 4
CHAPTER 4 Generation of Candidate Profiles 6
CHAPTER 5 Dynamic Performance Evaluation 9
5.1 Performance Criteria 9
5.2 Dynamic Modeling 9
5.3 Curving Analysis 10
5.3.1 Wear Index 10
5.3.2 Rolling Resistance 11
5.3.3 Contact Stress 13
5.3.4 Contact Angle 14
5.3.5 L/V Ratio 14
5.4 Stability Analysis 15
CHAPTER 6 Validation 22
CHAPTER 7 Conclusions and Recommendations 26
REFERENCES 27
APPENDIX A Proposed New Wheel Profile Arc Radius, Arc Center, and Segment Point Coordinates . 28
APPENDIX B Proposed New Wheel Profile (X,Y) Coordinates 29

List of Figures

Figure 1. Measured Newly Trued and Worn Wheel Profiles 4
Figure 2. Measured Rail Profiles 5
Figure 3. Existing Wheel Template and Worn Wheel Profiles 6
Figure 4. Existing and Proposed Wheel Template Profiles 7
Figure 5. Existing and APTA 240 Wheel Template Profiles 7
Figure 6. Contact between Worn Rail and Existing AAR S-622-78 Wheel Template Profiles 8
Figure 7. Contact between Worn Rail and Proposed Wheel Template Profiles 8
Figure 8. Wear Indices for Alternative Wheel and Rail Profiles – 147-foot Radius Curve 10
Figure 9. Wear Indices for Alternative Wheel and Rail Profiles – 300-foot Radius Curve 11
Figure 10. Rolling Resistances for Alternative Wheel and Rail Profiles – 147-foot Radius Curve 12
Figure 11. Rolling Resistances for Alternative Wheel and Rail Profiles – 300-foot Radius Curve 12
Figure 12. Contact Stresses for Alternative Wheel and Rail Profiles – 147-foot Radius Curve 13
Figure 13. Contact Stresses for Alternative Wheel and Rail Profiles – 300-foot Radius Curve 13
Figure 14. L/V Ratios for Alternative Wheel and Rail Profiles – 147-foot Radius Curve 14
Figure 15. L/V Ratios for Alternative Wheel and Rail Profiles – 300-foot Radius Curve 15
Figure 16. Truck Frame Lateral Acceleration for Alternative Wheel Profiles – New 100RB Rail 16
Figure 17. RRD for Alternative Wheel Profiles on New 100RB Rails 17
Figure 18. Comparisons of Axle and Truck Movement between APTA 240 and S-622-78 Wheels 18
Figure 19. Truck Frame Lateral Acceleration for Alternative Wheel Profiles – AREMA 115RE Rail 18
Figure 20. Comparison of Rail Profiles 19
Figure 21. Rolling Radius Difference for Alternative Wheel Profiles on New 115RE Rails 20
Figure 22. Truck Frame Lateral Acceleration for Alternative Wheel Profiles – Slightly worn Rail Measured on Tangent Track 20
Figure 23. Truck Frame Lateral Acceleration for Alternative Wheel Profiles – Moderately Worn Rail Measured on Tangent Track 21

Figure 24. Slightly Worn and Moderately Worn Rail Profiles Measured on Tangent Track 21
Figure 25. Measured Track Geometries 22
Figure 26. Car Response Time Histories of P5 Car running on Measured Track Geometry 23
Figure 27. Comparisons of Truck Frame Lateral Acceleration RMS Values 24
Figure 28. Comparisons of Wheel L/V Ratios 25
Figure A-1. Proposed New Wheel Profiles 28

List of Tables

Table 1. Curving Simulation Details 7

Summary

Transit Cooperative Research Program's project (TCRP D7 Task Order 20: wheel profile maintenance guidelines for transit systems) has an objective to demonstrate the application of guidelines and procedures developed in a selected transit system. As part of the project, Transportation Technology Center, Inc. (TTCI) has conducted a wheel/rail interaction study for Port Authority Trans-Hudson Corporation (PATH). A new wheel profile has been developed to decrease wheel and rail wear and to improve vehicle and track dynamic performances.

NUCARS® analyses were performed with a PA5 car operating on a variety of curved and tangent track. The analyses compared performances of four alternative wheel profiles: a new proposed profile, PATH's existing design (AAR S-622-78), APTA 240, and PATH worn wheels. Preliminary analysis has shown that the new proposed wheel profile provides overall best performance. The wheel wear index, contact stress, rolling resistance, and lateral/vertical (L/V) ratio of the proposed profile are lower than those of the existing cylindrical AAR S-622-78 wheel template profile. Trucks implemented with the proposed new wheel profiles would not hunt at speeds up to 80 mph for all simulated cases.

The APTA 240 wheel profile offers good curving capability with the lowest L/V ratio and rolling resistance, but its hunting speed is lowest among wheel profiles studied. There would be a higher risk of truck hunting if the APTA 240 wheel profile is used in the PA5 car, especially on tangent track with newly installed 100 RB rails.

It is recommended that the proposed wheel profile be tested in service. The test should include the following stages:

1. Manufacture templates for the wheel lathe to produce the proposed profile.
2. Lathe true four wheelsets using the new template and install them in a car.
3. True another set of four wheelsets using the existing wheel template and install them in another car.
4. Document two car numbers, wheel identification, and general conditions.
5. Conduct a revenue service test to measure truck and carbody accelerations according to the test plan TTCI submitted.
6. Analyze and compare the dynamic performances of the tested trucks.
7. Put the cars in revenue service and periodically (every 3 months) locate the two test cars, measure wheel profiles, and record surface conditions.
8. Document reasons for reprofiling the two test car wheels when this becomes necessary. True the wheels to the same profiles (proposed or existing template) as trued in the beginning of the test.
9. Analyze all test results and report on the findings.

It is anticipated that the wear monitoring test will be carried out over a period of one year.

Appendices A and B provide the geometric properties of the proposed wheel profile, in arc segment format and (X,Y) coordinates.

CHAPTER 1

Introduction

Transportation Technology Center, Inc. (TTCI) has been contracted under the Transit Cooperative Research Program (TCRP) to develop wheel profile maintenance guidelines for rail transit systems. One objective of this project is to demonstrate the application of guidelines and procedures developed from this study in a selected transit system.

TTCI has conducted a wheel/rail interaction study for Port Authority Trans-Hudson Corporation (PATH). A new wheel profile was designed to decrease wheel and rail wear and to improve vehicle and track dynamic performances.

In July 2012, TTCI visited PATH and measured wheel and rail profiles. A draft report was prepared and submitted to PATH in August 2012 to summarize wheel and rail profile measurements and findings (Madrill and Shu 2010). This report summarizes the development of the new wheel profile and recommendations.

CHAPTER 2

Methodology

The following methodology was used in the development of a new wheel profile:

1. Review of current wheel/rail interface issues
2. Generation of a new wheel profile
3. Analysis of the effect of the new proposed profile on vehicle dynamic performance by using TTCI's NUCARS® vehicle dynamic model
4. Evaluation of the new wheel profile through service tests

These steps are described in the following sections of this report.

CHAPTER 3

Review of Current Conditions

PATH has been operating PA5 cars in revenue service since 2009. The PA5 cars are 51 feet (16 meters) long and approximately 9 feet 2 3/4 inches (2.813 meters) wide. The maximum running speed is 55 mph. Each car seats 35 passengers on longitudinal seating, with a larger number of standees. PATH adopted the Association of American Railroads (AAR) S-622-78 cylindrical wheel profile for new car purchases and as the wheel truing template. Wheels are trued about every 3 years, using mill type and lathe type wheel truing machines. The average wheel life is about 8 years.

The infrastructure at PATH, including tunnels and tracks, was mostly built a century ago. The PATH system (ex-Hudson and Manhattan Railroad) was opened in 1907. 100RB rails were used for many years. In 2005, the rail manufacturer stopped fabricating 100RB rail and replaced it with 100-8 rail, which has a similar profile to American Railway Engineering Maintenance of Way Association (AREMA) 115RE rail. PATH continues to install the 100RB rail in stock, and has also started installing the standard AREMA 115RE rail.

Currently, the mainline track consists of 50 percent 100RB rail and 50 percent 115RE rail (including 100-8 rail). It will take time for the newly installed 100RB rail to be replaced.

In July 2012, 50 wheel profiles were measured in the PATH wheel shop, and 56 rail profiles were measured on revenue service track. All profiles were measured using MiniProf™ (Greenwood Engineering A/S, Denmark) profilometers.

Measured wheel profiles were selected from wheelsets in the workshop either just before or just after reprofiling. A few wheel profiles were measured on cars in the yard. Figure 1 shows the measured new and worn wheel profiles.

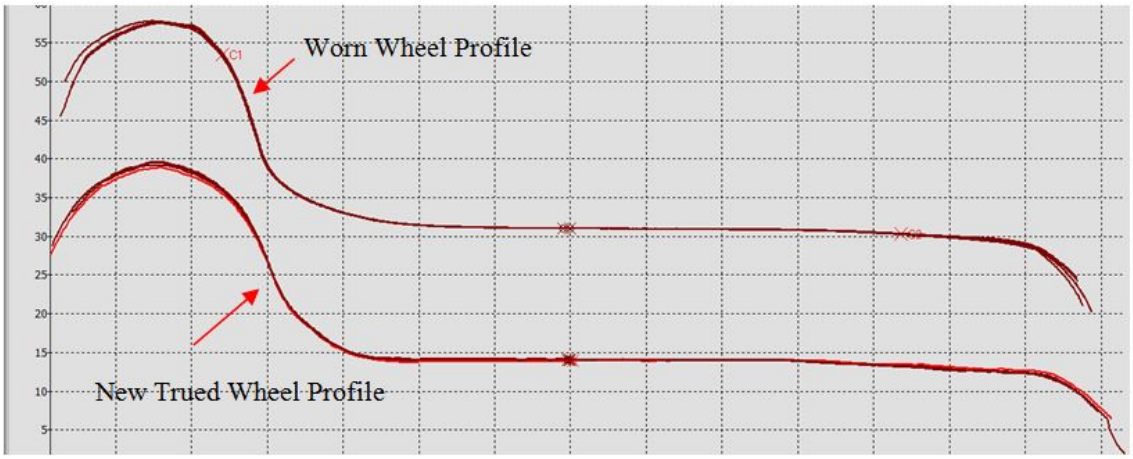

Figure 1. Measured Newly Trued and Worn Wheel Profiles

Figure 2 shows rail profiles that were measured on tangent tracks and curves at PATH. High wear rates were observed not only on high rails, but also on restraining rails adjacent to the low rails due to the small curve radii.

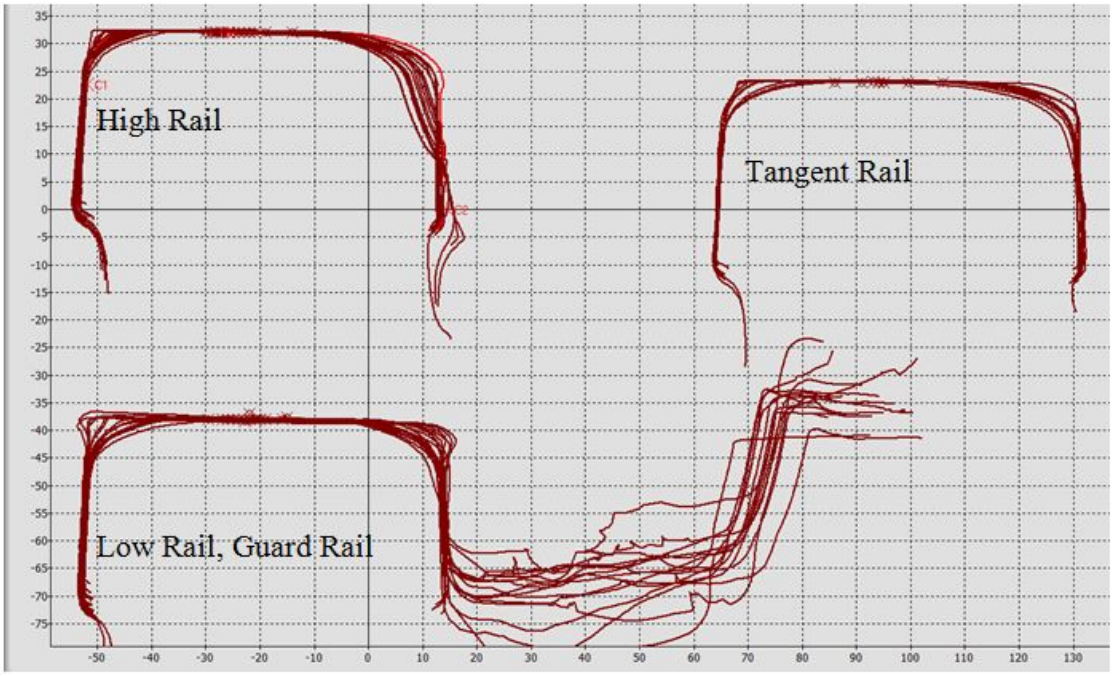

Figure 2. Measured Rail Profiles

All measurement results were provided by Madrill and Shu 2012. The following is a summary of the main findings and conclusions:

- Wheels and rails wear to a steeper contact angle of about 75 degrees.
- Wheels have high flange wear and slight tread hollowing.
- The high rails and the worn wheels wear into conformal shapes.
- The worn high rail/new wheel contact shows strong two-point contact.
- The low rails show flattening and hollowing on top of the rail due to contact with the cylindrical part of worn and new wheels.
- The 100RB rail and AREMA 115RE rail wear into similar shapes.

Controlling wheel and rail wear is one of the main tasks for wheel profile designs (Shu Part 1 2014). However, wheel profile changes are constrained by existing vehicle and track conditions. New wheel profile designs or truing templates should be optimized on the basis of existing rail wear conditions, vehicle design and maintenance standards, and special trackwork maintenance requirements (Shu Part 1 2014).

CHAPTER 4

Generation of Candidate Profiles

An optimized wheel profile should provide the following:

- Stable performance over the range of normal train speeds
- Safety from derailment under normal operating conditions
- Maximized wheel and rail life by decreasing wear

The following three general guidelines are used in wheel profile design:

- The wheel flange angle should be at least 72 degrees, preferably 75 degrees, to protect against flange climbing derailments.
- The slope of the wheel tread (tread taper) should produce a low conicity with different rail shapes in tangent track.
- The profile in the flange root should blend smoothly with the flange and tread. It should be close to the typical worn profile to give relatively conformal contact on rails, minimize the contact stress, and minimize the amount of metal removed during reprofiling.

The rail profiles used for the new wheel design include new 100RB rail profiles, new AREMA 115RE rail profiles, and measured worn rail profiles including slightly, moderately, and heavily worn shapes. The new rail profile is the standard 100RB and 115RE rail with 1:40 inclination. Typical worn profiles were measured on tangent tracks and curves on PATH.

A new wheel profile was designed using these guidelines and guidelines developed in the report for Part 2 of this project (Shu Part 2 2014). Figures 3 to 5 compare the new wheel profiles with a representative worn wheel profile, the existing template AAR S-622-78 wheel profile, and the APTA 240 wheel profile.

Figure 3. Existing Wheel Template and Worn Wheel Profiles

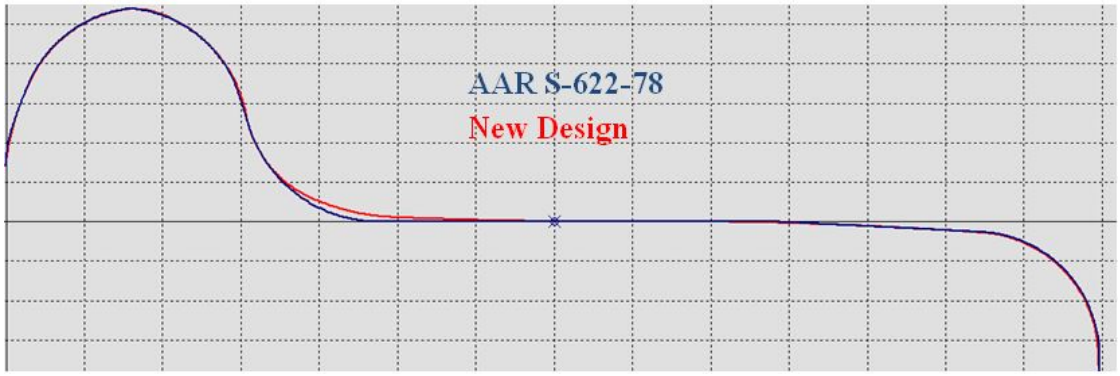

Figure 4. Existing and Proposed Wheel Template Profiles

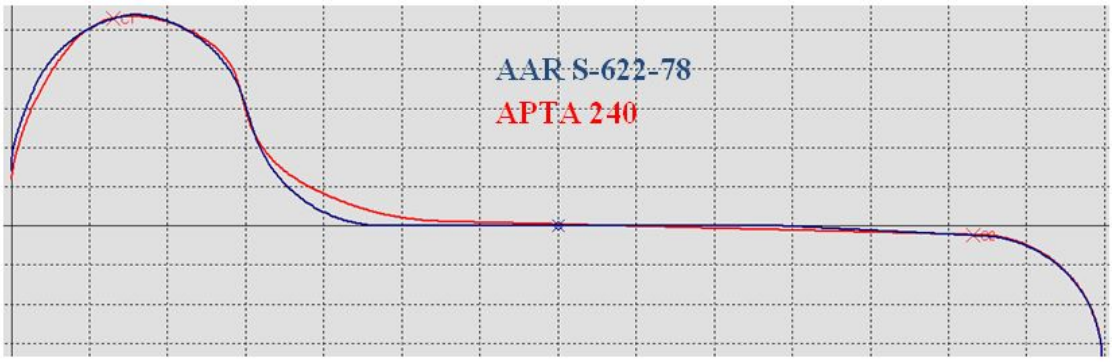

Figure 5. Existing and APTA 240 Wheel Template Profiles

Figure 3 shows that existing wheels mainly wore on the flange and flange root areas, with metal flow extending into the flange root. The new wheel profile design extends the flange root to the cylindrical tread with a larger arc radius than the existing wheel template, and increases the maximum flange angle to 75 degrees, as Figure 4 shows. The tread is slightly tapered, but close to cylindrical. The other parts of the proposed wheel profile are identical to the existing cylindrical wheel template.

APTA 240 wheel profile could be another potential candidate wheel profile, because it meets the requirements for rail transit cars (APTA SS-M-015-06, 2007). It has a 1:40 slope on tread, and a larger radius arc in flange root, as Figure 5 shows.

The wheel profile differences are most significant in the wheel flange root. Figure 6 shows that the AAR S-622-78 wheel profile contacts on the worn high rail. Because the arc radius on wheel flange root is much smaller than the radius of the gage corner of the high rail, it produces two points of contact – one on the top and the other on the gage face of the high rail. Severe two-point contact is known to cause large tangential forces between the wheel and the rail that increase wear and rolling contact fatigue (RCF).

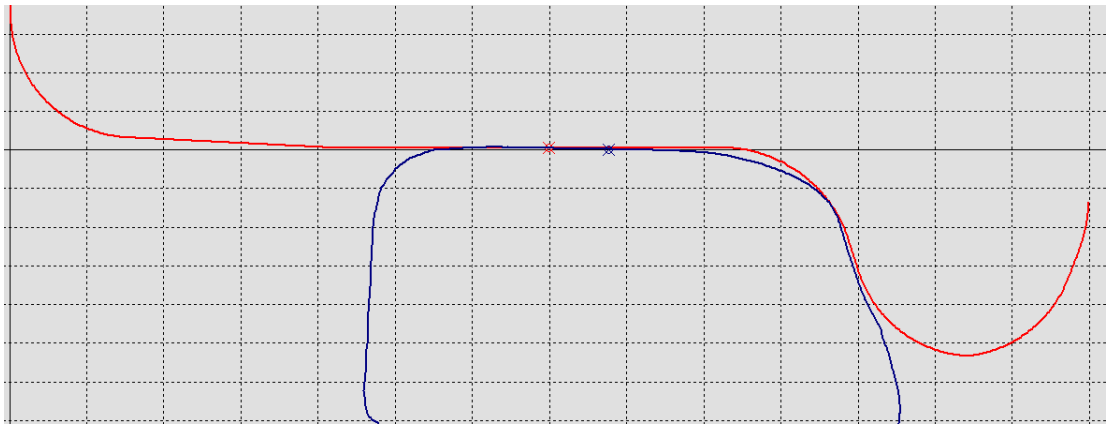

Figure 6. Contact between Worn Rail and Existing AAR S-622-78 Wheel Template Profiles

Figure 7 shows that the proposed wheel profile closely matches the worn rail profile with little gap in the gage corner to allow the wheels to quickly wear conformal to the rails.

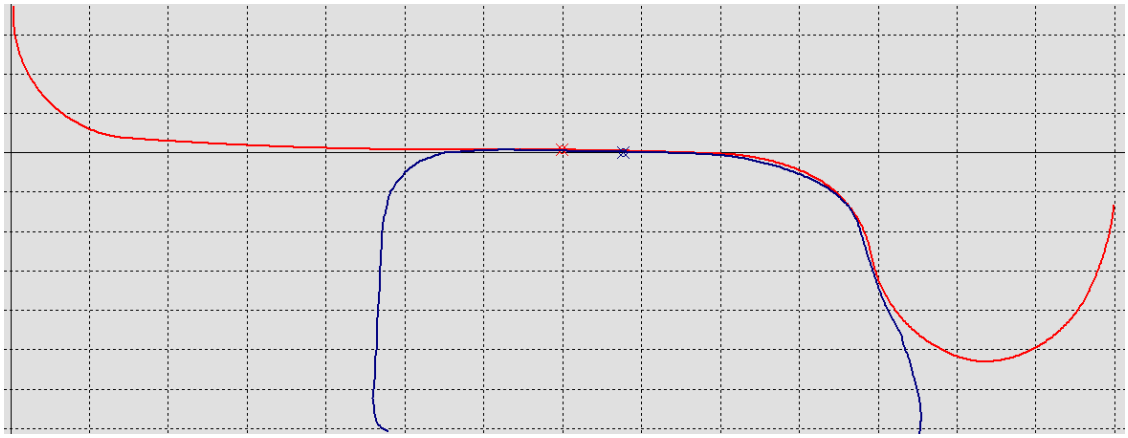

Figure 7. Contact between Worn Rail and Proposed Wheel Template Profiles

Simulations were performed to evaluate the proposed wheel profile and compare it with the existing AAR S-622-78 wheel template profile and the APTA 240 wheel profile and the results are given in the following section.

CHAPTER 5

Dynamic Performance Evaluation

5.1 Performance Criteria

Profile design is a matter of optimizing several criteria. Some criteria must be satisfied; others can be compromised to achieve an overall optimum solution. The following criteria have been used to evaluate the new wheel profiles (Wu et al. 2005):

- Wear Index – should be as low as possible to decrease wear on wheels and on the high rail in curves
- Rolling Resistance – should be as low as possible to reduce energy consumption and draft gear forces
- Contact Stress – should be as low as possible to decrease RCF and metal flow
- Lateral to Vertical (L/V) Ratio – should be less than the Nadal limit to avoid flange climbing derailments
- Lateral Stability – should be achieved for normal operating speeds for cars with deteriorated suspension system

5.2 Dynamic Modeling

Dynamic modeling was performed with a NUCARS® model of the PA5 car in the empty condition (Ketchum and Meddah 2014). Curving simulations were performed using curves with radii of 147 feet and 300 feet. Superelevations for these curves were 4 inches and 2.75 inches, respectively. The curving simulations did not include a restraining (guard) rail for the following reasons:

- Wheel flange back wear caused by contact on the restraining rail was less severe compared to tread wear. Most wheels wore on flange root and tread, as observed in the PATH railcar fleets.
- An optimized wheel profile can decrease wheel flange and high rail wear even with the existing configuration of the restraining rail (Ketchum and Meddah 2014).

To reduce wear on the restraining rail, the most effective way is by adjusting the restraining rail flange way clearance, not by changing wheel profile and back-to-back distance. Restraining rail installation guidelines have been published by TCRP (Shu and Wilson 2010).

The railcar running speed used in the simulations was 12 mph. The wheel/rail coefficient of friction was 0.5, representing a dry rail condition without lubrication. Table 1 summarizes the data used in the curving simulations.

Table 1. Curving Simulation Details

Radius (foot)	147	300
Superelevation (inch)	4	2.75
Speed (mph)	12	12

The following five different rail profiles were used in the curving simulations:

1. New 100RB rail
2. New AREMA 115RE rail

3. Slightly worn rail measured on tangent track located at milepost 1092+10 in Tunnel A-4
4. Moderately worn rail measured on the 300-foot radius curves located at milepost 1089+36 in Tunnel A-4
5. Heavily worn rail measured on the 147-foot radius curve located at milepost 1064+60 in Tunnel A-4

The same PA5 car model was used for the curving analysis and for the lateral stability simulations, except the suspension parameters (such as the lateral and longitudinal stiffness and damping on primary and secondary suspension system) were lower than normal values to simulate deteriorated suspension conditions.

A lateral track discontinuity was used to excite lateral motion. The discontinuity had a cosine shape with 50-foot wavelength and 1-inch amplitude. A 0.3 g truck frame acceleration root-mean-square value, defined in the Federal Railroad Administration 49 CFR Part 213 Track Safety Standard[8], was used to evaluate truck stability.

5.3 Curving Analysis

5.3.1 Wear Index

It is widely accepted that wheel/rail wear can be evaluated in terms of wear index. In NUCARS, the wear index is calculated as the sum of the tangential forces (T_x, T_y, and M_z) multiplied by the creepages (γ_x, γ_y, and ω_z) at the contact patch, as Equation 1 shows. A higher wear index can induce either RCF or higher rate of wear.

$$Wear\ Index = \sum_n T_x\gamma_x + T_y\gamma_y + M_z\omega_z \qquad (1)$$

Figure 8 shows the wear index results for the outside wheel of the leading axle on the 147-foot radius curve. Results are given for all combinations of wheel and rail profiles that have been modeled. Rail and wheel wear is proportional to the wear index when the wear index is greater than 50 lb-in/in. Below that value, the wear is mild and RCF may be expected. Figure 8 shows that in all cases, the wear index is greater than 50 lb-in/in.

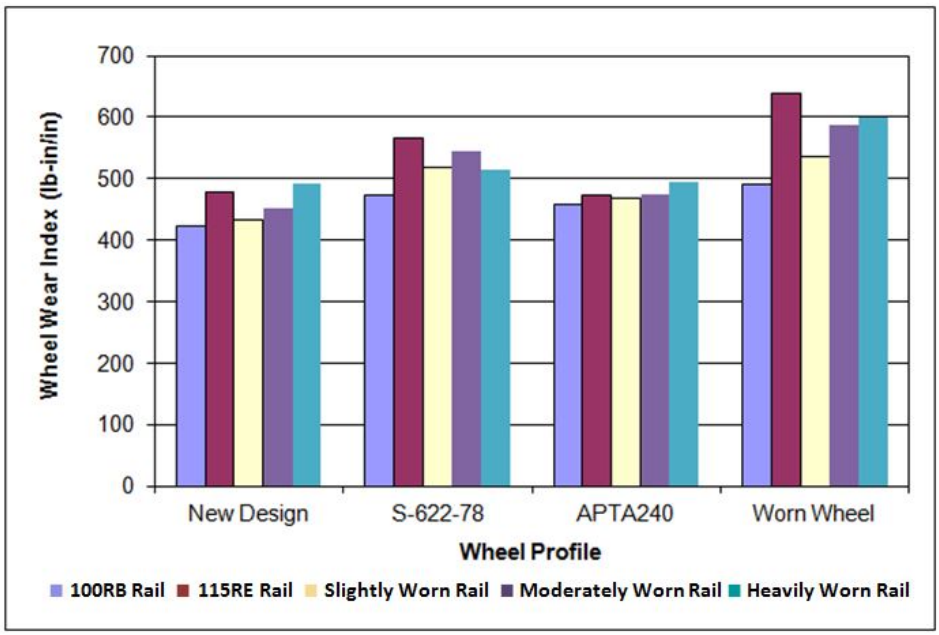

Figure 8. Wear Indices for Alternative Wheel and Rail Profiles – 147-foot Radius Curve

Figure 8 shows that the proposed wheel profile produces the lowest wear indices among all simulated rail profiles. The APTA 240 wheel provides the second lowest wear indices. A heavily worn wheel generates significantly higher wear indices on AREMA115RE rail and on worn rail, indicating the importance of proper wheel maintenance for control of wheel and rail wear.

Figure 9 shows the wear index for the outside wheel of the leading axle on a 300-foot radius curve. The proposed wheel profile produces the lowest wear indices on 300-foot radius curves among all simulated rail profiles.

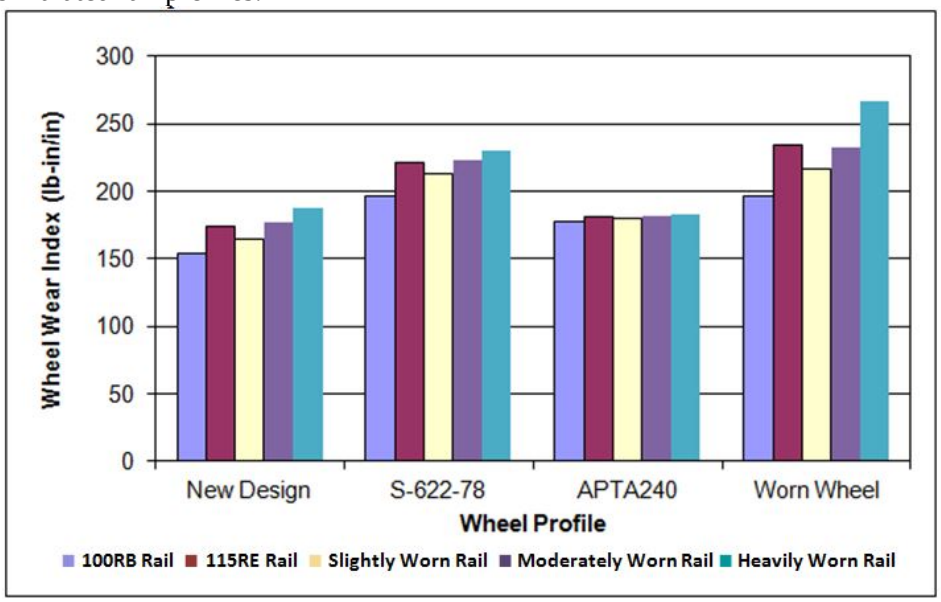

Figure 9. Wear Indices for Alternative Wheel and Rail Profiles – 300-foot Radius Curve

5.3.2 Rolling Resistance

Figure 10 shows the total rolling resistance from all eight wheels of the PA5 car on a 147-foot radius curve. Results are given for all combinations of wheel and rail profiles that have been modeled.

Figure 10 shows that the APTA 240 wheel produces the lowest rolling resistance on all simulated new rail profiles. The proposed wheel produces slightly higher rolling resistance on AREMA 115RE rail than the APTA 240 wheel does.

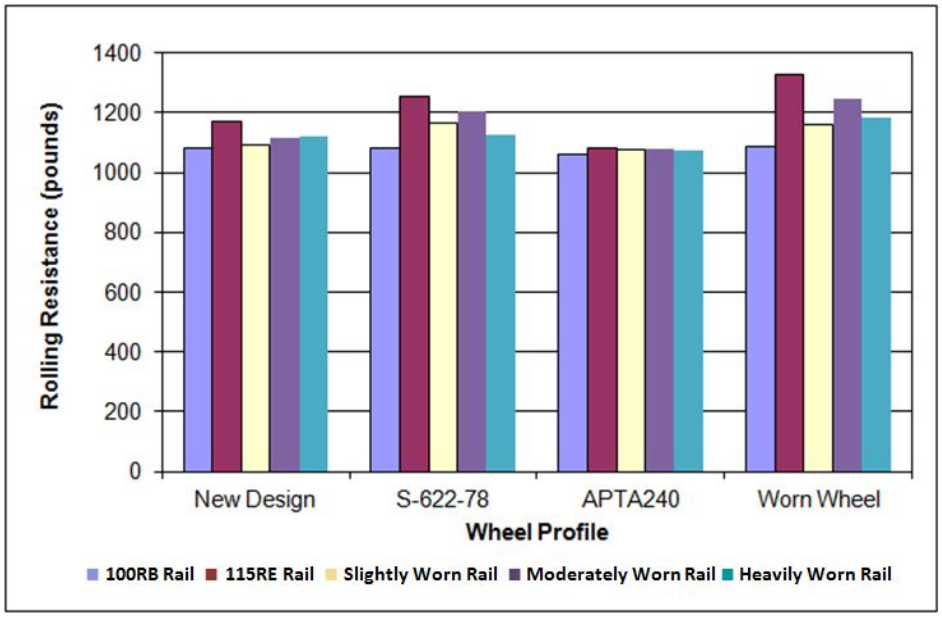

Figure 10. Rolling Resistances for Alternative Wheel and Rail Profiles – 147-foot Radius Curve

Figure 11 shows that the APTA 240 wheel produces the lowest rolling resistance on all simulated new rail profiles on a 300-foot radius curve, and the proposed wheel produces the second lowest rolling resistance. The large flange root arc radius of the APTA 240 wheels, which results in one-point contact on rails with a lower contact angle for most simulated cases, and its tapered tread contributes to the best curving performances compared to other alternative wheels.

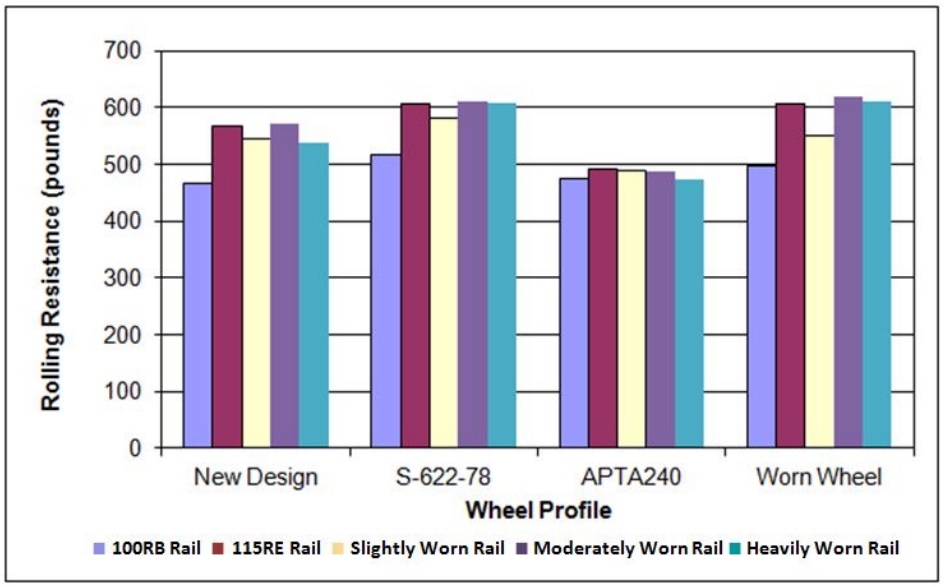

Figure 11. Rolling Resistances for Alternative Wheel and Rail Profiles – 300-foot Radius Curve

5.3.3 Contact Stress

Figure 12 compares the flange contact stress from the outside wheel of PA5 car on the high rail of a 147-foot radius curve for all combinations of wheel and rail profiles that have been modeled.

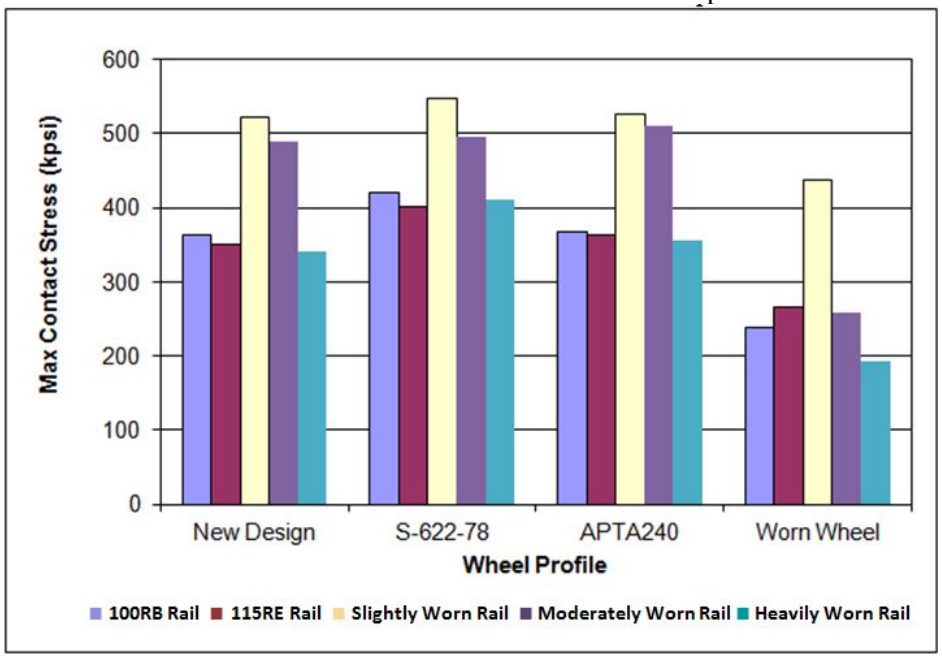

Figure 12. Contact Stresses for Alternative Wheel and Rail Profiles – 147-foot Radius Curve

Figure 12 shows that the worn wheel produces the lowest contact stresses on a 147-foot radius curve, especially on the worn rail due to a conforming shape between the worn wheel and rail. The proposed wheel produces the second lowest contact stress for most simulated cases.

The same conclusions can be drawn from the modeling results of the PA5 car traveling through a 300-foot radius curve, as Figure 13 shows.

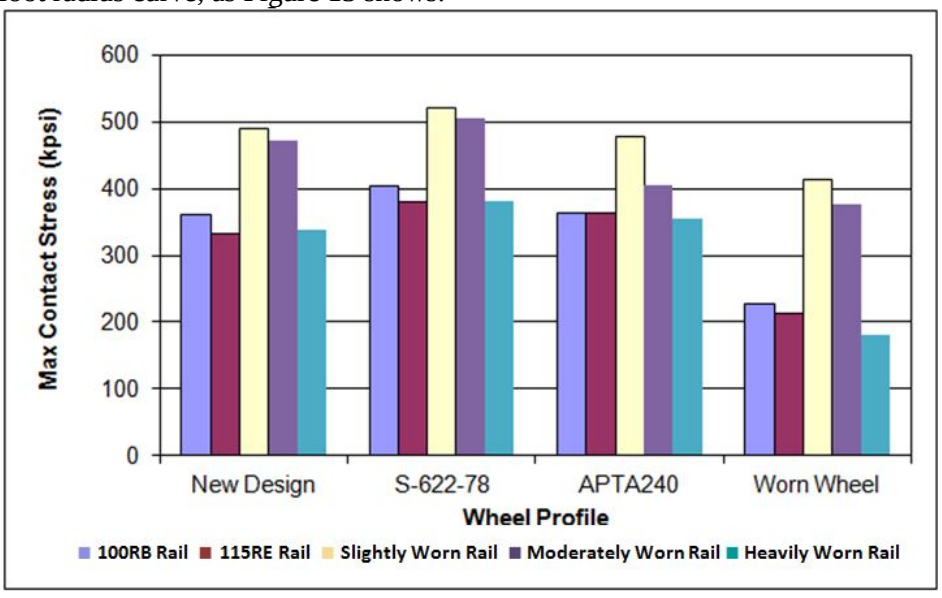

Figure 13. Contact Stresses for Alternative Wheel and Rail Profiles – 300-foot Radius Curve

5.3.4 Contact Angle

The maximum contact angle on the outside wheel of the lead axle during flange contact is 75 degrees for the proposed wheel profile. The maximum contact angle of existing S-622-78 wheel profile is 72 degrees. Higher flange angles provide a higher resistance to flange climb derailment.

5.3.5 L/V Ratio

Figure 14 shows the L/V ratio for the PA5 car on the outside wheel of the lead axle in the 147-foot radius curve. It is positive when the wheel is in flange contact with the high rail.

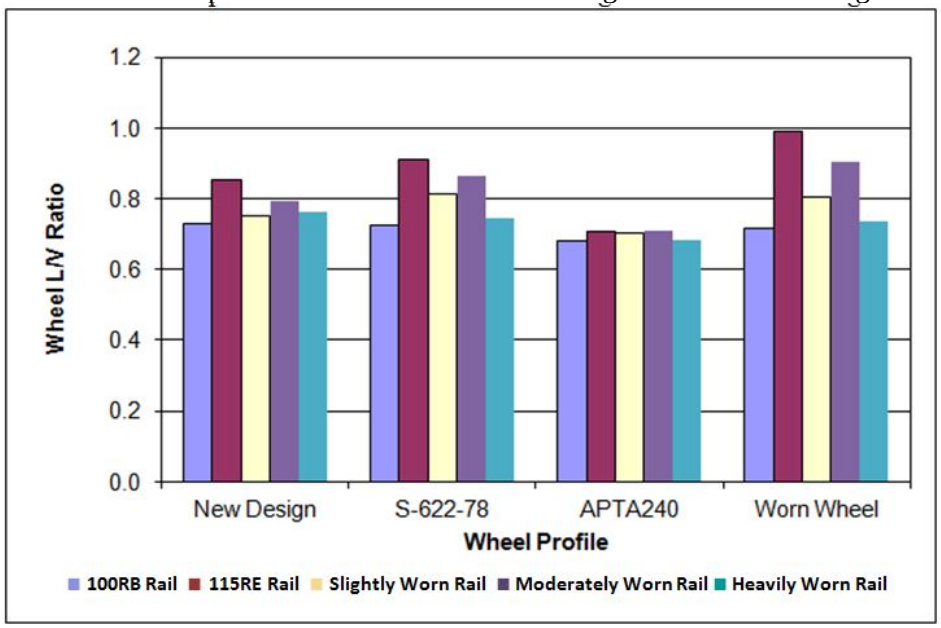

Figure 14. L/V Ratios for Alternative Wheel and Rail Profiles – 147-foot Radius Curve

Figure 14 shows that the APTA 240 wheel produces the lowest L/V ratio (lower than 0.8) among all simulated wheel profiles on a 147-foot radius curve. The worn wheel produces the highest L/V ratio on the AREMA 115RE rail. The large flange root arc radius and tapered tread on the APTA 240 wheel contribute to the lowest L/V ratio. The proposed wheel produces the second lowest L/V ratio for most simulated cases. Similar conclusions can be drawn from the simulation results on the 300-foot radius curve, as Figure 15 shows.

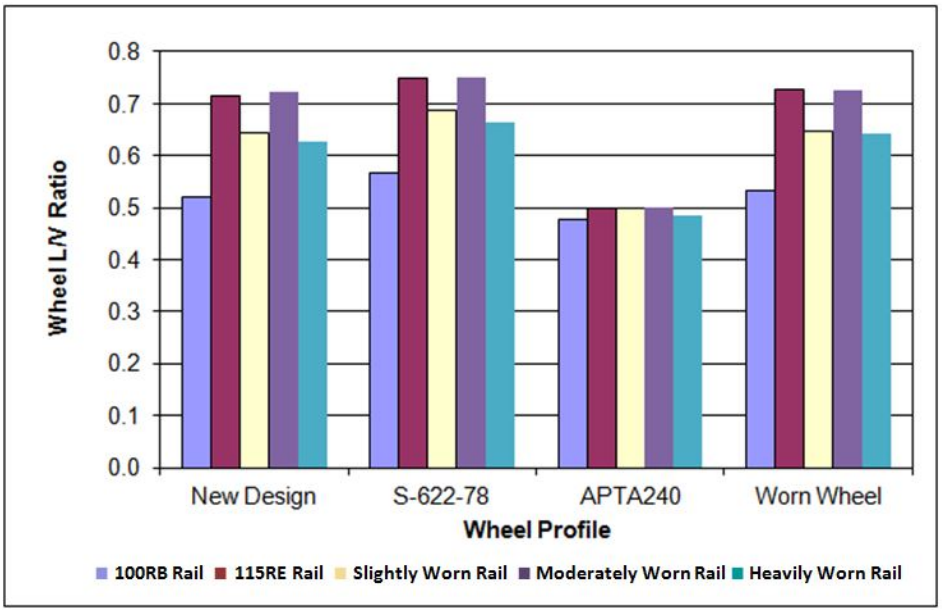

Figure 15. L/V Ratios for Alternative Wheel and Rail Profiles – 300-foot Radius Curve

A safe value of L/V ratio depends on the wheel/rail friction conditions and the distance over which the L/V ratio is high. Values below 0.8 are generally considered to be safe. PATH installs restraining rails on all curves with radii less than 800 feet, which increases resistance to flange climb derailment (Shu and Wilson 2010).

5.4 Stability Analysis

Hunting (lateral instability) is a common dynamic phenomenon for railroad and rail transit cars, and is primarily a function of the following:

- Wheel/rail conicity – higher conicity increases likelihood of hunting
- Vehicle speed – higher speeds increase likelihood of hunting
- Vehicle longitudinal, lateral, and yaw suspension stiffnesses – softer stiffness increases likelihood of hunting

Any disturbance on the track, such as track perturbations, can trigger hunting. Once hunting starts, the wheelset moves laterally and at the same time yaws around the vertical axis perpendicular to the track surface, with gradually increased amplitudes as it travels on the track. Hunting can sometimes be stopped, if the wheelset encounters another disturbance, or if the track curvature changes.

Tread conicity has a significant effect on wheelset hunting. The higher the conicity, the higher the risk of hunting. One way to avoid hunting is to use cylindrical wheels, which generate zero conicity when the two cylindrical treads contact on rails. However, due to wear, the wheel treads do not keep their cylindrical shape, and worn wheels promote hunting (Shu Part 1 2014).

Hunting mostly occurs on tangent track or shallow curves, and rarely occurs on tight curves (curve radius less than 750 feet). One obvious reason is that the speed on tangent track or shallow curves is normally higher than that on tight curves. Another reason could be that curvature variations disturb the hunting development before it reaches a stable limiting cycle.

Four types of rails, the new 100RB rail, new AREMA 115RE rail, slightly worn rail, and moderately worn rail, measured on tangent track were used to perform hunting simulation. The moderately worn rail shape was included, because most rails on tangent track wear into a worn shape after they were put in revenue service.

Figure 16 shows the lowest hunting speed (50 mph) occurs with the APTA 240 wheel running on 100RB rails indicating an unsafe operating condition. The reason is that its conicity on the tread is the highest among all simulated wheel profiles and increasing conicity lowers the hunting speed.

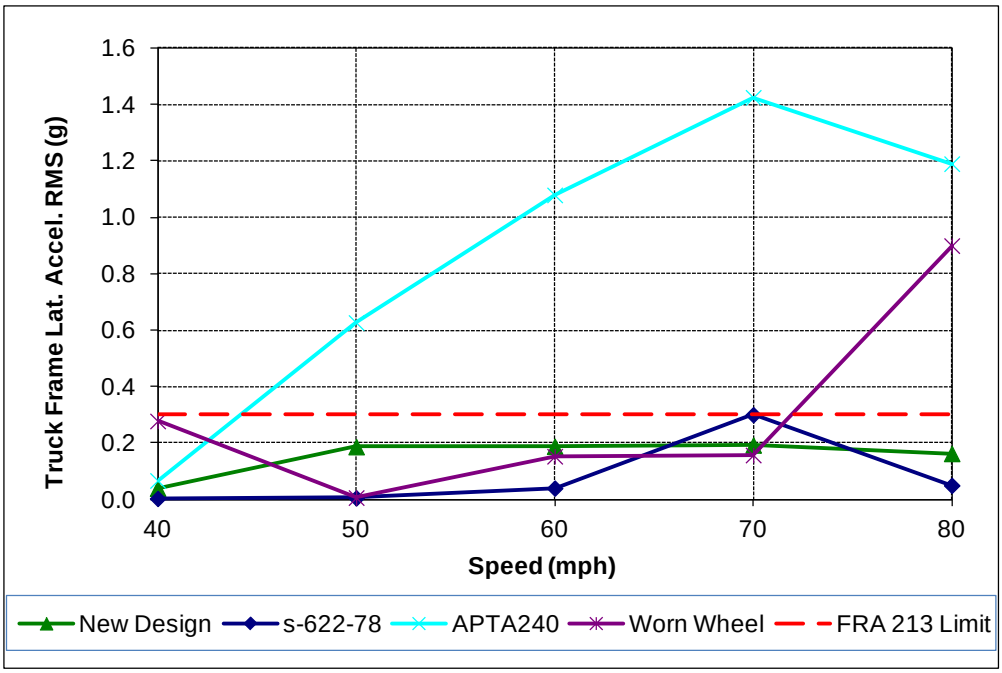

Figure 16. Truck Frame Lateral Acceleration for Alternative Wheel Profiles – New 100RB Rail

The conicity can be calculated from the wheel rolling radius difference (RRD) function. In general, the effective conicity is defined by Equation 2:

$$\lambda = \frac{RRD}{2y} \qquad (2)$$

where y is the wheelset lateral shift.

The equivalent conicity defined in Equation 2 is half of the slope of the linearized wheel RRD function in the range of wheel lateral shift before reaching flange contact.

Figure 17 shows how the RRD varies with lateral shift of the wheelset for the different wheel profiles. The new 100RB rail profile was used to calculate these results.

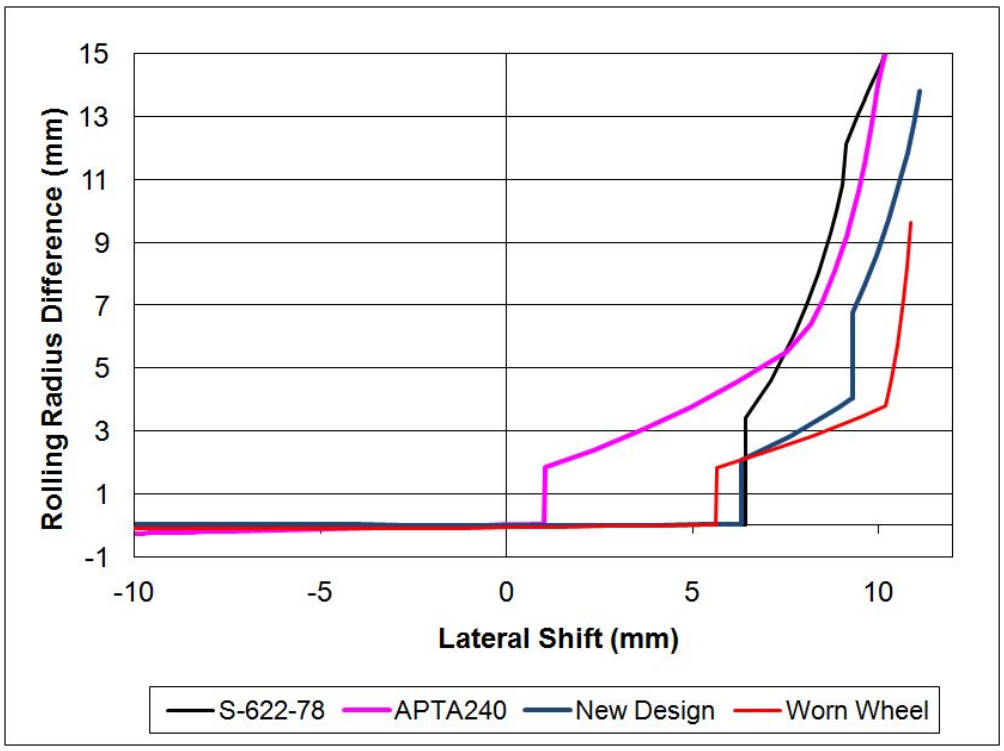

Figure 17. RRD for Alternative Wheel Profiles on New 100RB Rails

Figure 17 shows that the APTA 240 wheel profile produces a step increase in RRD with lateral shift before flange contact is made, which generates the highest conicity. The proposed wheel and S-622-78 wheel profiles produce zero conicity before flange contact. The worn wheel profile also introduces a step change in RRD before flange contact is made, which produces the second highest conicity. The proposed wheel conicity lies between that of the S-622-78 and worn wheels.

Figure 18 shows the comparisons of the axle lateral displacement and truck acceleration between APTA 240 and S-622-78 wheels at a speed of 50 mph. The cylindrical wheel deviates from the track center and stays on the right side of the track center once it passes the perturbation. This is to be expected, because the cylindrical profile does not steer well and results in some flange contact, which causes flange and gage face wear that can be seen in the tangent track worn profiles, whereas the APTA 240 wheel gradually increases lateral displacement amplitudes as it travels on the track with no signs of diminishing.

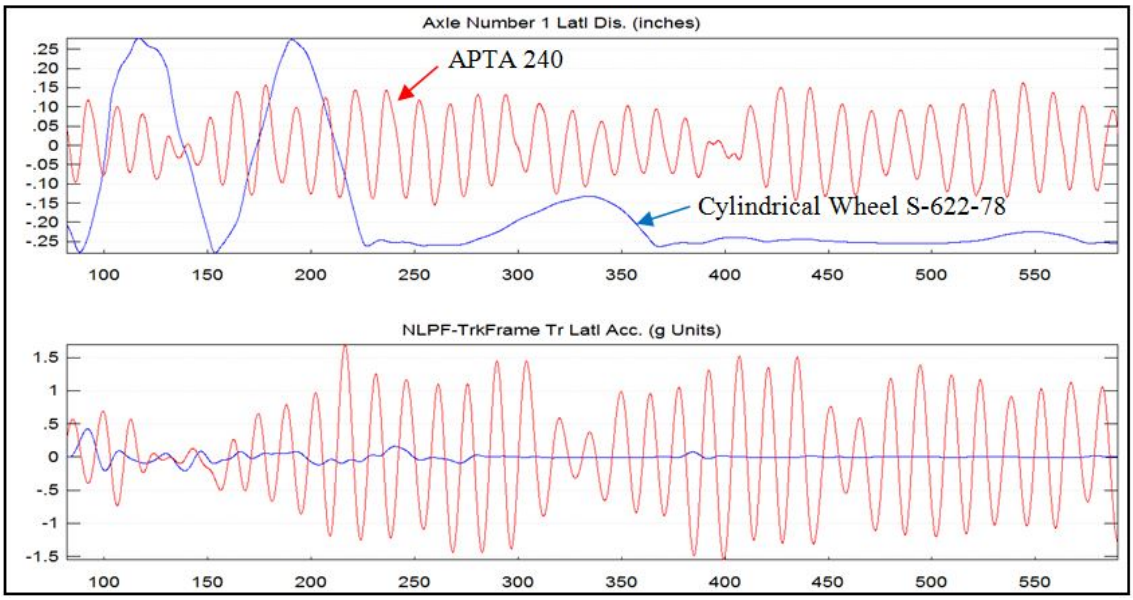

Figure 18. Comparisons of Axle and Truck Movement between APTA 240 and S-622-78 Wheels

Figure 19 shows the lowest hunting speed occurs with the APTA 240 wheel running on AREMA 115RE rails. Its truck frame acceleration root-mean-square (RMS) value exceeds the FRA CFR 213 Track Safety Standards limit at 70 mph. The other three wheel types did not show hunting for speeds up to 80 mph.

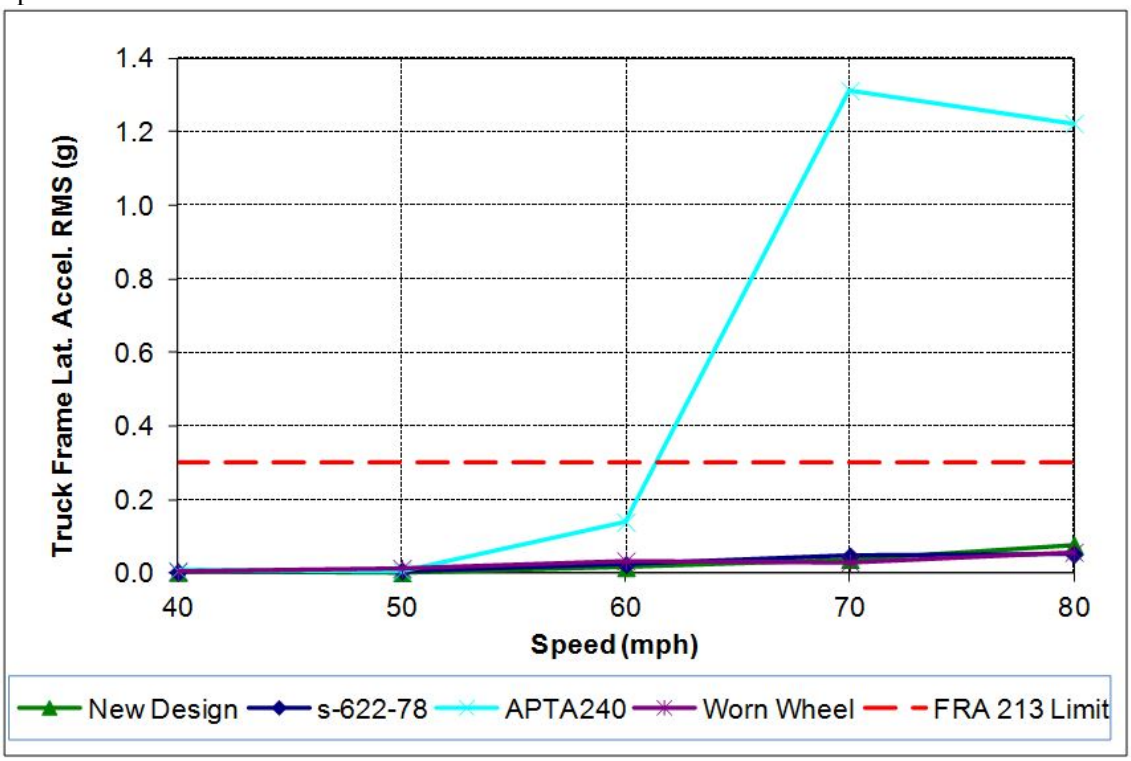

Figure 19. Truck Frame Lateral Acceleration for Alternative Wheel Profiles – AREMA 115RE Rail

Clearly, the increase of hunting speed was caused by the change of rail profiles, because other parameters used in the modeling did not change. Figure 20 overlays the two rail profiles. The 100RB rail has a protruding gage corner compared to the AREMA 115RE rail, which contacts on the wheel flange root. The APTA 240 wheel has the largest flange root arc radius among all simulated wheel profiles, which makes flange root contact on high rail on the rail gage corner when the axle moves only 1.0 millimeter laterally, as Figure 17 shows.

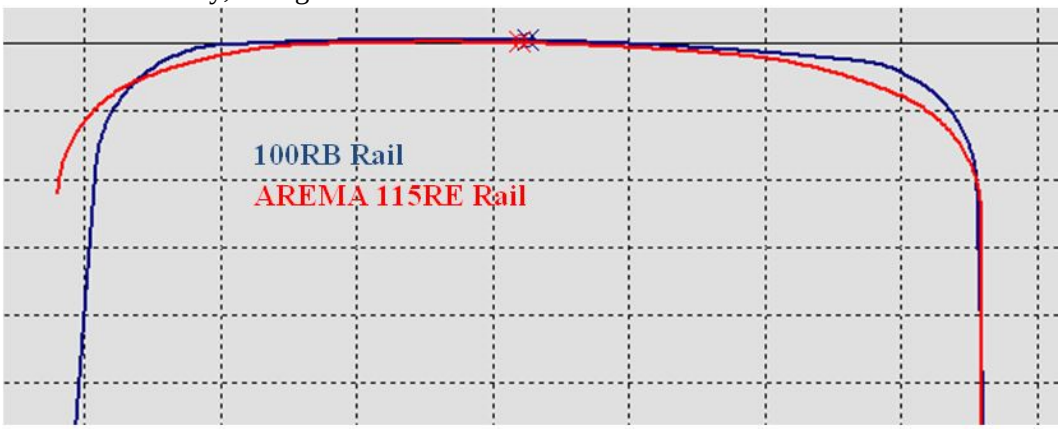

Figure 20. Comparison of Rail Profiles

Figure 21 shows the RRDs for alternative wheel profiles on new AREMA 115RE rails. The wheel/rail clearances increased for all wheels when the protruding gage corner on 100RB rail was replaced with a shape conformal to wheel flange root. However, when the APTA wheel contacts on the new AREMA 115RE rail it moves about 5.7 millimeters, and it still generates the highest conicity among all simulated wheels. Figures 22 and 23 also show the lowest hunting speed (70 mph) occurs with the APTA 240 wheel running on slightly worn rail and moderately worn rail measured on tangent track.

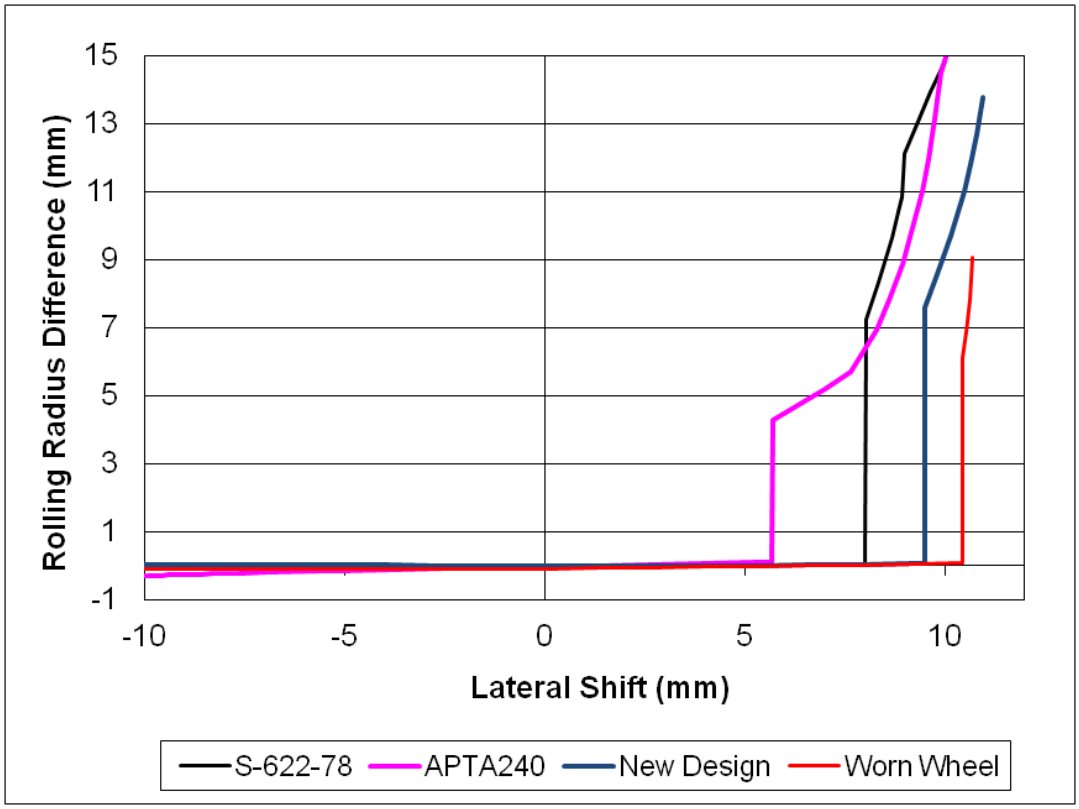

Figure 21. Rolling Radius Difference for Alternative Wheel Profiles on New 115RE Rails

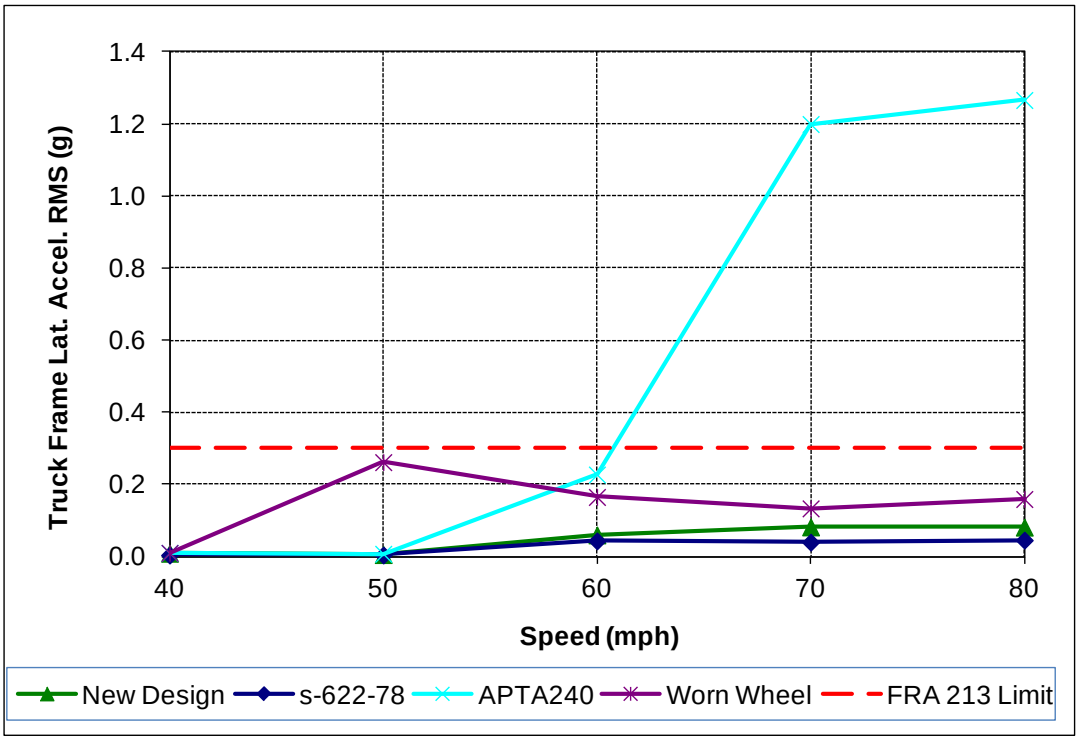

Figure 22. Truck Frame Lateral Acceleration for Alternative Wheel Profiles –Slightly worn Rail Measured on Tangent Track

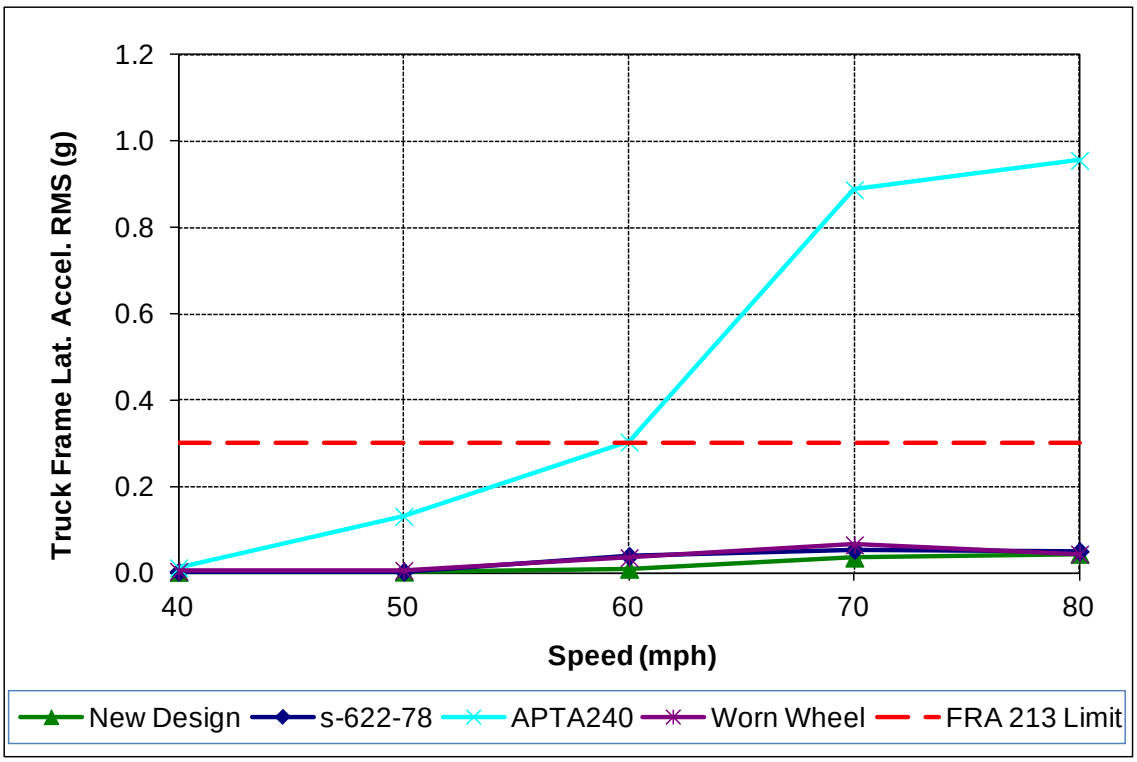

Figure 23. Truck Frame Lateral Acceleration for Alternative Wheel Profiles – Moderately Worn Rail Measured on Tangent Track

Figure 24 compares the slightly worn and moderately worn rail profiles measured on tangent track. The wheel/rail clearances increased for all wheels due to wear on the rail gage face. However, the APTA 240 wheel conicity is still the highest among all simulated wheels, which contributes to the lowest hunting speed.

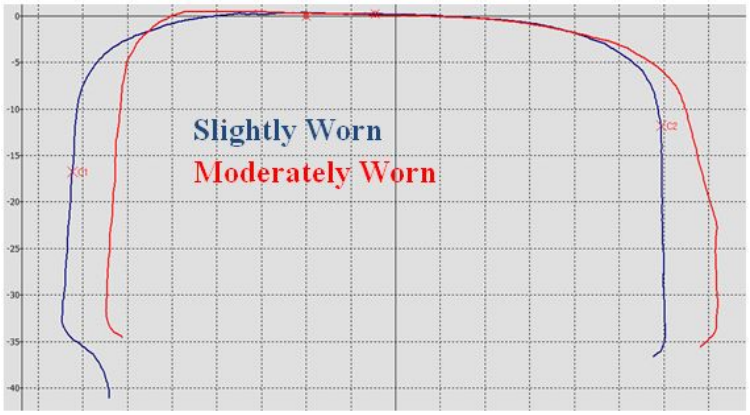

Figure 24. Slightly Worn and Moderately Worn Rail Profiles Measured on Tangent Track

Because the APTA 240 wheel is prone to hunt at speeds of 50 mph on 100RB rails, lower than the operation speed, it not recommended for use at PATH, even though it improves curving performance. The proposed wheel, which has the best wear performance and does not hunt at speeds up to 80 mph, is recommended to test on track and to conduct further evaluation.

CHAPTER 6

Validation

The curving and hunting performances of the proposed new wheel profile were further evaluated through simulation using measured track geometry and rail profiles from PATH. The track geometries, as Figure 25 shows, were measured from Journal Square Station to Exchange Place Station.

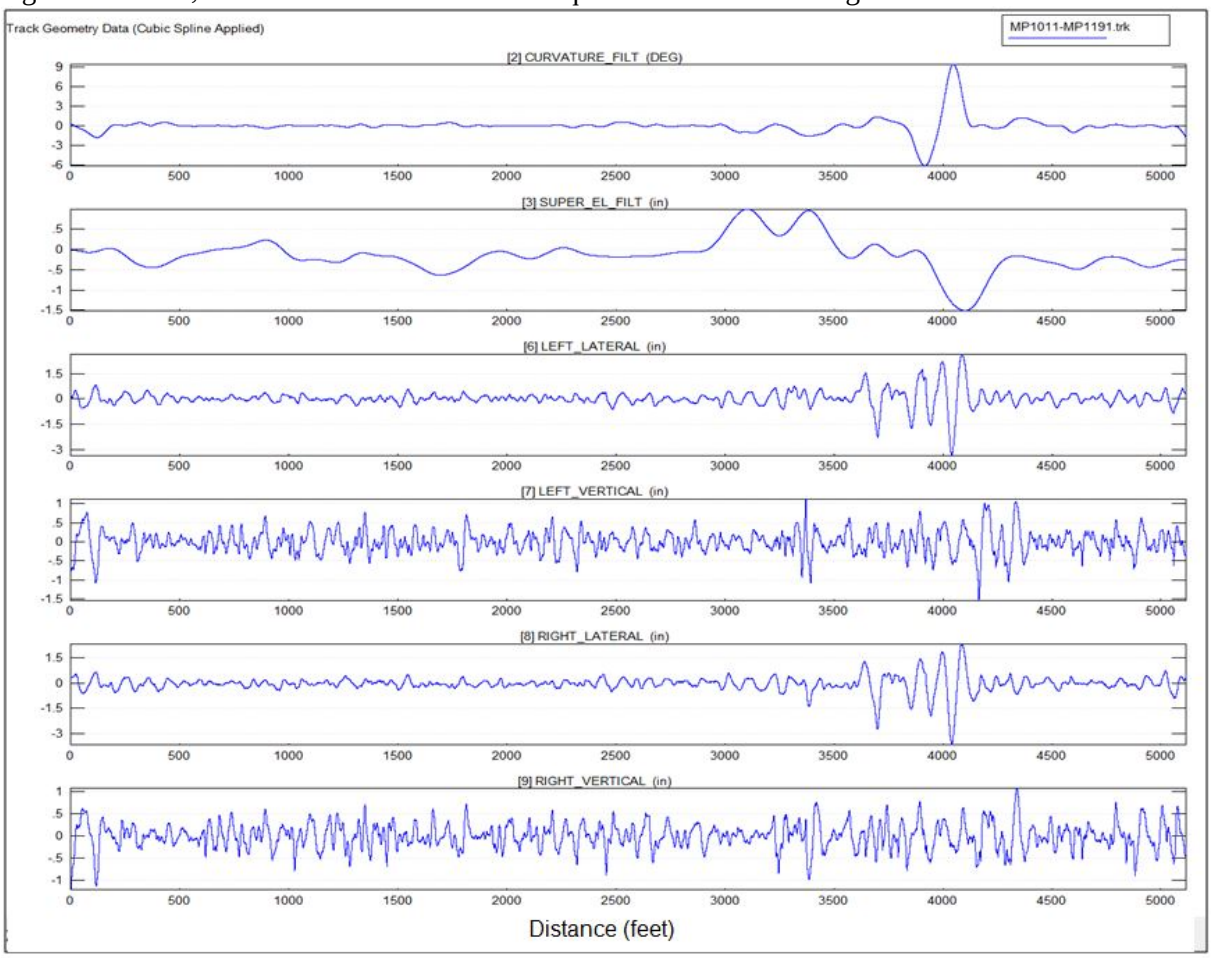

Figure 25. Measured Track Geometries

Figure 26 shows the time histories of the truck frame lateral acceleration, W/R forces, and wheel L/V ratios of the P5A car with three different alternative wheel profiles at a speed of 60 mph. On tangent track from 500 to 3,000 feet, the time history peak values were dominated by responses using APTA 240 wheels (red color); on curves from 3,300 to 4,400 feet, the time history peak values were dominated by responses using cylindrical wheels (green color).

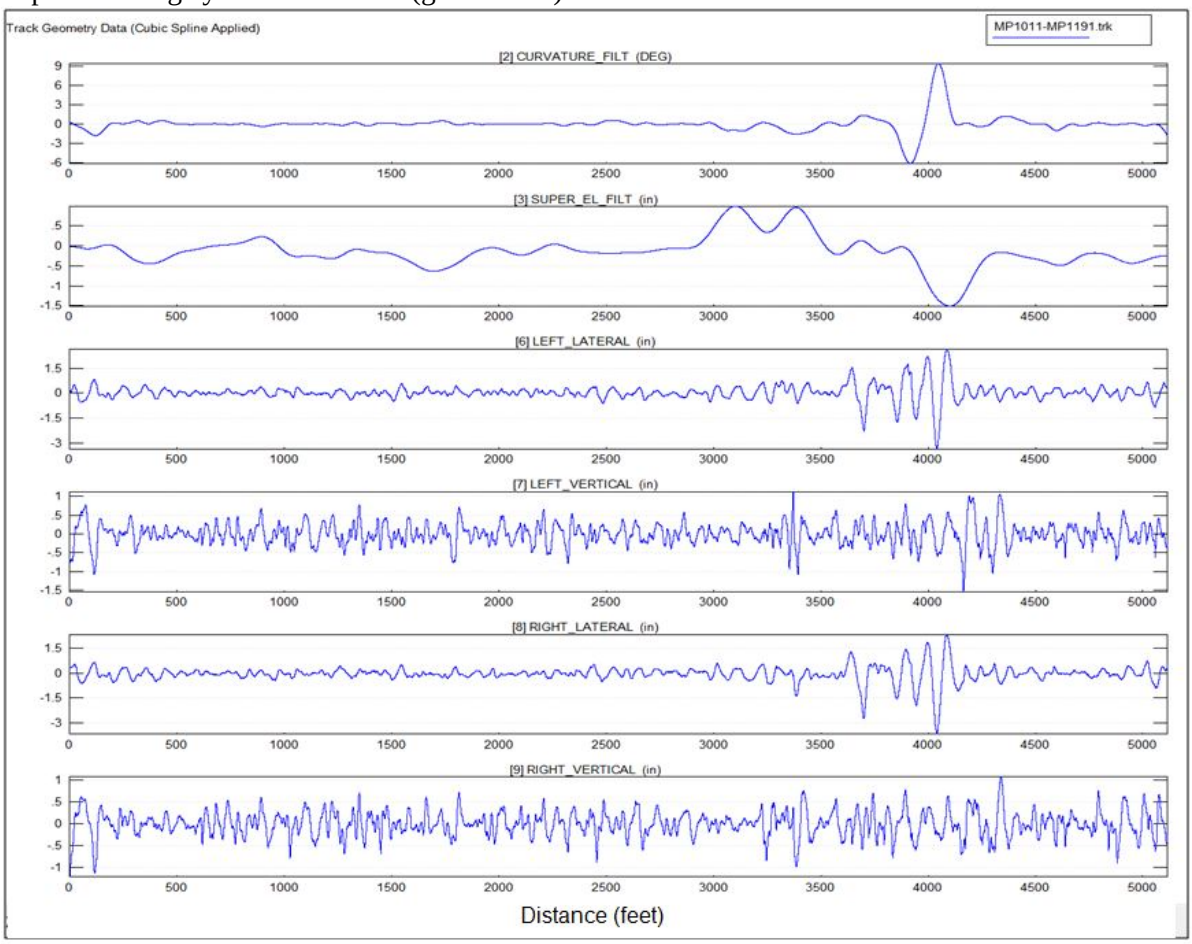

Figure 26. Car Response Time Histories of P5 Car running on Measured Track Geometry

The time histories were processed based on the FRA 213 Track Safety Standard (FRA CFR 213 2012). Figure 27 shows the truck frame acceleration RMS value of the P5A car equipped with cylindrical wheel (S-622-78) is the lowest among the three simulated wheels, indicating the best hunting performance. The new design wheel is stable at speeds up to 65 mph. The APTA 240 wheel starts hunting at speeds over 60 mph.

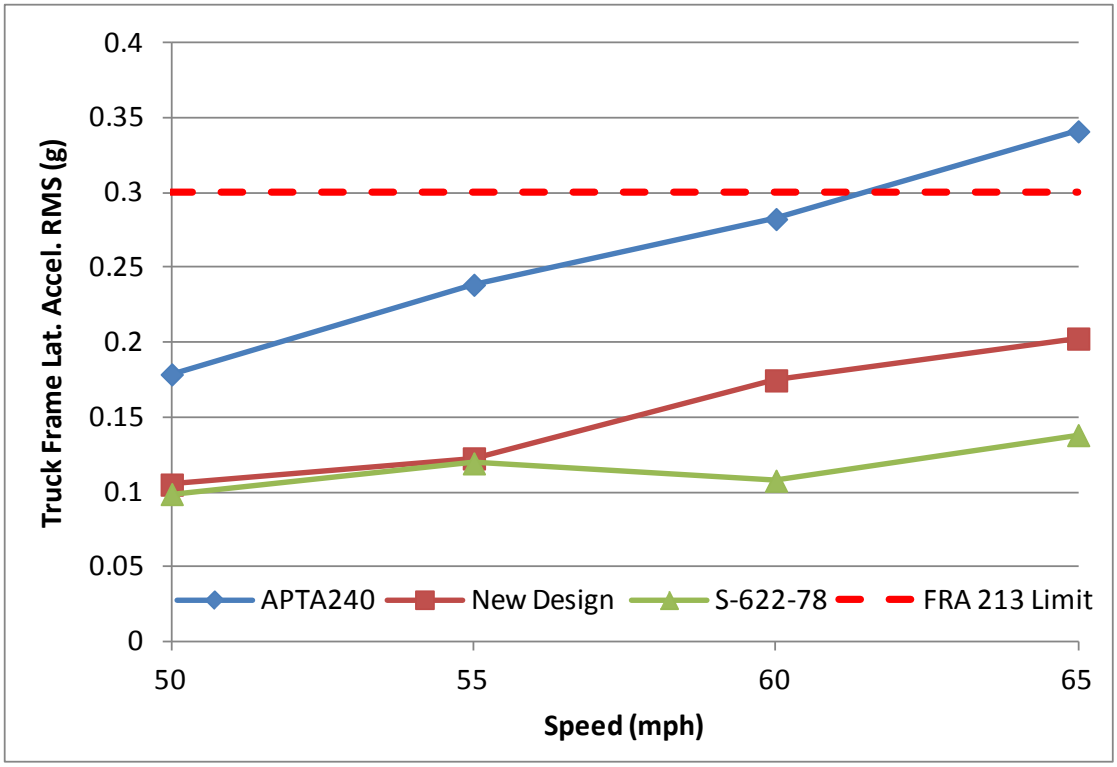

Figure 27. Comparisons of Truck Frame Lateral Acceleration RMS Values

Figure 28 shows the wheel L/V ratio of the P5A car equipped with APTA 240 wheel is the lowest among three simulated wheels, indicting the best curving performance. The cylindrical wheel (S-622-78) L/V ratio is higher that of other two wheels. The new design wheel ratio is lower than that of the existing cylindrical wheel.

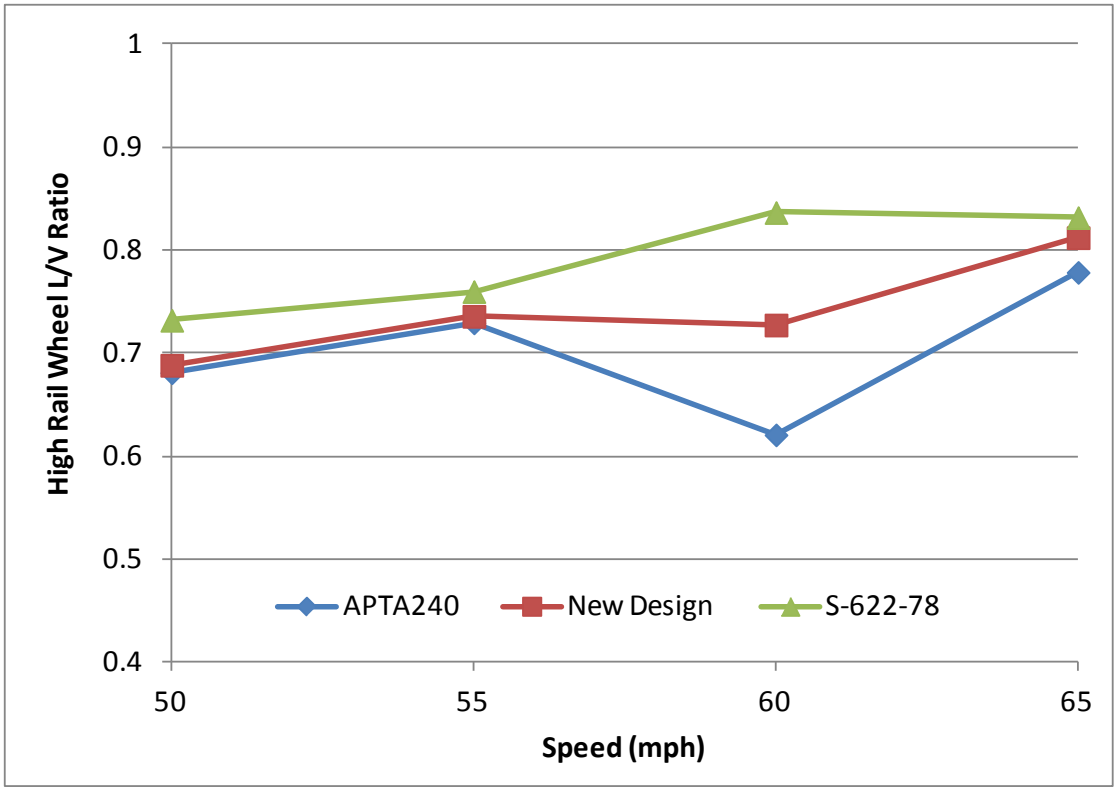

Figure 28. Comparisons of Wheel L/V Ratios

Clearly, the proposed new design wheel, which has similar hunting performance but better curving performance than the existing cylindrical wheel, demonstrates overall optimal dynamic performances under various track conditions.

CHAPTER 7

Conclusions and Recommendations

Preliminary analysis has shown that the proposed new wheel profile provides the overall best performance among all wheel profiles that were considered. The wheel wear index, contact stress, rolling resistance, and L/V ratio of the proposed new wheel profile are lower than those of the existing cylindrical AAR S-622-78 wheel template profile. For all simulated cases, trucks implemented with the proposed new wheel profiles did not hunt at speeds up to 80 mph.

The APTA 240 wheel profile offers good curving capability with the lowest L/V ratio and rolling resistance, but its hunting speed is the lowest among all wheel profiles considered. There is a higher risk of truck hunting when using the APTA 240 wheel profile in the PA5 car, especially on tangent track with newly installed 100RB rails.

It is recommended that the proposed new wheel profile be tested in revenue service over a one year period. The test should include the following steps:

1. Manufacture templates for the wheel lathe to produce the proposed new profile.
2. Lathe true four wheelsets using the new template and install them in a car.
3. True another set of four axle wheels using the existing wheel template and install them in another car.
4. Document two car numbers, wheel identification, and general conditions such as mileage and maintenance records.
5. Conduct revenue service tests to measure truck accelerations, carbody accelerations, and W/R forces by using instrumented wheelsets.
6. Analyze and compare the dynamic performance of the tested trucks.
7. Put the cars into service and periodically (every 3 months) locate the two test cars, measure wheel profiles, and record wheel surface conditions.
8. Record the reasons for reprofiling the two test car wheels when it becomes necessary. True the wheels to the same profiles (proposed or existing template) as trued in the beginning of the test.
9. Analyze all test results and report the results.

The wear monitoring test should be conducted over a period of one year.

Appendices A and B contain the geometric properties of the proposed new wheel profiles, in arc segment format and (X,Y) coordinates.

References

American Public Transit Association. APTA SS-M-015-06, Standard for Wheel Flange Angle for Passenger Equipment, 2007.

Federal Railroad Administration, Code of Federal Regulations 49 CFR 213, Track Safety Standards, Subpart G, Train Operations at Track Classes 6 and Higher, 2012.

Ketchum, C.D. and A. Meddah. "Performance Based Track Geometry Port Authority Trans Hudson (PATH) System." TCRP D-7 Task 19 Report, Transportation Research Board of the National Academies, Washington, D.C., 2014.

Madrill, B. and X. Shu. "PATH Wheel and Rail Profile Measurement and Summary." Letter Report, Transportation Technology Center, Inc., Pueblo, CO, 2012.

Shu, X. and N. Wilson. "Guidelines for Guard/Restraining Rail Installation." In *Transportation Research Record: Journal of the Transportation Research Board,* No. 71, Volume 7, Transportation Research Board of the National Academies, Washington, D.C., 2010.

Shu, X. "Survey of Current Wheel Profiles and Maintenance Practices." TCRP D-7 Task 20 Part 1 Report, Transportation Research Board of the National Academies, Washington, D.C., 2014.

Shu, X. "Wheel Profile Design and Maintenance Guidelines for Transit Rail Operation." TCRP D-7 Task 20 Part 2 Report, Transportation Research Board of the National Academies, Washington, D.C., 2014.

Wu, H., X. Shu, N. Wilson, and W. Shust. "Flange Climb Derailment Criteria and Wheel/Rail Profile Management and Maintenance Guidelines for Transit Operations." In *Transportation Research Record: Journal of the Transportation Research Board*, No. 71, Volume 5, Transportation Research Board of the National Academies, Washington, D.C., 2005.

APPENDIX A

Proposed New Wheel Profile Arc Radius, Arc Center, and Segment Point Coordinates

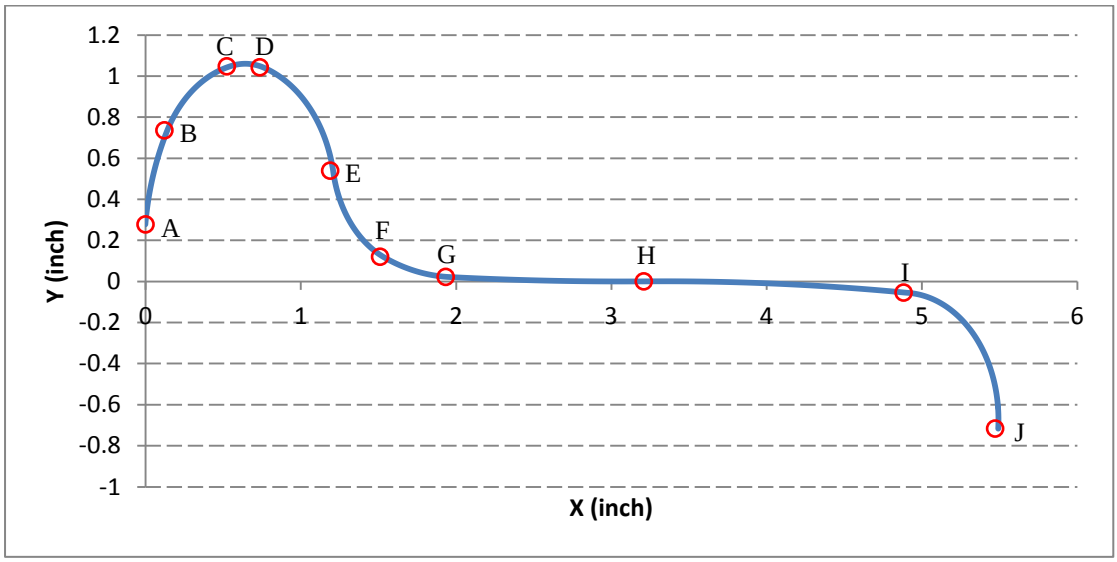

Figure A-1. Proposed New Wheel Profiles

Table A-1. Arc Segments (inch)

Segment Point	X	Y	Arc Radius	Arc Center X	Arc Center Y
A	0.000000	0.277953			
B	0.121260	0.736220	1.283465	1.251969	0.133071
C	0.523622	1.047244	0.622047	0.669291	0.444882
D	0.736220	1.043307	0.389370	0.618110	0.669291
E	1.188976	0.539370	0.669291	0.531496	0.401575
F	1.511811	0.120079	-0.562992	1.744094	0.633858
G	1.933071	0.021969	-1.161417	1.980315	1.181102
H	3.208661	0.000634	-28.425197	3.047244	28.425197
I	4.881890	-0.054724	21.614173	3.350394	-21.614173
J	5.472441	-0.716535	0.618110	4.881890	-0.673228

APPENDIX B

Proposed New Wheel Profile (X,Y) Coordinates

Table B-1. Proposed Wheel Profile (X,Y) Coordinates (millimeters)

X(mm)	Y(mm)
1.40E-02	7.562701829
4.75E-02	7.815829134
8.30E-02	8.06868635
0.120453897	8.321257966
0.159884653	8.573528488
0.201290048	8.82548244
0.244667541	9.077104367
0.290014471	9.328378832
0.337328055	9.579290421
0.386605392	9.829823742
0.437843459	10.07996343
0.491039113	10.32969413
0.546189089	10.57900053
0.603290006	10.82786733
0.66233836	11.07627927
0.723330528	11.32422111
0.78626277	11.57167764
0.851131224	11.81863368
0.917931912	12.06507408
0.986660735	12.31098371
1.057313477	12.55634751
1.129885804	12.8011504
1.204373265	13.04537739
1.280771288	13.28901347
1.359075189	13.53204372
1.439280163	13.77445321
1.52138129	14.01622709
1.605373534	14.25735051
1.691251742	14.49780868
1.779010646	14.73758686
1.868644862	14.97667034

X(mm)	Y(mm)
1.960148892	15.21504444
2.053517122	15.45269455
2.148743826	15.68960609
2.24582316	15.92576452
2.344749169	16.16115535
2.445515786	16.39576415
2.548116828	16.62957653
2.652546001	16.86257814
2.7587969	17.09475468
2.866863006	17.32609192
2.97673769	17.55657566
3.088414211	17.78619176
3.201885719	18.01492614
3.317145253	18.24276477
3.434185742	18.46969367
3.553000006	18.69569892
3.675625614	18.92031043
3.801872942	19.14290643
3.931708874	19.36342854
4.06509935	19.5818189
4.202009377	19.79802022
4.342403041	20.0119758
4.486243512	20.2236295
4.633493057	20.4329258
4.784113048	20.63980979
4.938063975	20.84422721
5.09530545	21.04612443
5.255796227	21.24544849
5.419494202	21.44214709
5.586356435	21.63616865
5.756339153	21.82746226
5.929397763	22.01597774
6.105486869	22.20166564
6.284560278	22.38447724
6.466571013	22.5643646
6.651471329	22.74128052
6.83921272	22.91517859
7.029745938	23.0860132
7.223021	23.25373952
7.418987205	23.41831356
7.617593145	23.57969215
7.818786721	23.73783296

X(mm)	Y(mm)
8.022515154	23.89269449
8.228725001	24.04423613
8.437362168	24.19241812
8.648371922	24.33720158
8.861698911	24.47854855
9.077287173	24.61642194
9.295080153	24.75078557
9.515020719	24.88160421
9.737051174	25.00884354
9.961113272	25.13247017
10.18714824	25.25245169
10.41509678	25.3687566
10.64489909	25.48135441
10.87649489	25.59021558
11.10982343	25.69531154
11.3448235	25.79661473
11.58143345	25.89409858
11.81959121	25.98773751
12.05923431	26.07750696
12.30029988	26.16338337
12.54272469	26.24534423
12.78644514	26.32336803
13.03139729	26.3974343
13.27751689	26.46752361
13.52473937	26.53361758
13.77299989	26.59569887
14.01419372	26.65612442
14.25683038	26.71046743
14.50075651	26.75869354
14.74581792	26.80077226
14.99185971	26.836677
15.23872636	26.86638506
15.48626183	26.88987766
15.73430966	26.90713997
15.98271306	26.91816105
16.23131502	26.92293396
16.47995839	26.92145567
16.72848602	26.91372711
16.97674081	26.89975317
17.22456585	26.87954269
17.47180448	26.85310843
17.71830044	26.82046711

X(mm)	Y(mm)
17.96389791	26.78163936
18.20844166	26.73664972
18.45177712	26.68552664
18.69375046	26.62830241
18.93420876	26.56501322
19.17300001	26.49569907
19.41799922	26.41565651
19.66175675	26.33190873
19.90421658	26.244475
20.14532296	26.1533754
20.38502048	26.05863088
20.62325404	25.96026322
20.85996887	25.85829502
21.09511057	25.75274973
21.32862507	25.64365161
21.56045871	25.53102573
21.7905582	25.41489799
22.01887063	25.29529507
22.24534354	25.17224448
22.46992485	25.04577449
22.69256295	24.91591418
22.91320667	24.7826934
23.13180527	24.64614277
23.34830852	24.50629368
23.56266665	24.36317827
23.77483038	24.21682945
23.98475094	24.06728086
24.19238008	23.91456686
24.39767008	23.75872257
24.60057373	23.59978381
24.80104441	23.43778711
24.99903604	23.2727697
25.19450309	23.10476953
25.38740064	22.93382521
25.57768434	22.75997604
25.76531047	22.58326197
25.95023588	22.40372363
26.13241808	22.22140228
26.31181517	22.03633984
26.48838594	21.84857885
26.66208978	21.65816246
26.83288677	21.46513445

X(mm)	Y(mm)
27.00073764	21.26953918
27.16560383	21.07142163
27.32744742	20.87082732
27.48623122	20.66780237
27.64191872	20.46239344
27.79447414	20.25464776
27.94386242	20.04461308
28.09004921	19.83233767
28.2330009	19.61787034
28.37268465	19.40126037
28.50906834	19.18255757
28.64212062	18.96181221
28.7718109	18.73907502
28.89810938	18.51439721
29.02098702	18.28783042
29.14041558	18.05942673
29.2563676	17.82923865
29.36881644	17.59731909
29.47773624	17.36372135
29.58310197	17.12849914
29.6848894	16.89170652
29.78307514	16.65339793
29.87763662	16.41362814
29.9685521	16.17245227
30.05580069	15.92992576
30.13936232	15.68610435
30.2192178	15.4410441
30.29534876	15.19480133
30.36773771	14.94743264
30.436368	14.69899491
30.50122385	14.44954523
30.56229037	14.19914095
30.61955352	13.94783962
30.67300012	13.69569901
30.71835876	13.44057994
30.7683326	13.18632464
30.82290521	12.93301658
30.88205869	12.68073893
30.94577361	12.42957453
31.01402905	12.17960586
31.08680261	11.93091498
31.16407037	11.68358354

X(mm)	Y(mm)
31.24580699	11.43769277
31.3319856	11.1933234
31.42257793	10.95055566
31.51755423	10.70946927
31.6168833	10.47014338
31.72053254	10.23265658
31.82846792	9.99708685
31.94065398	9.763511528
32.05705391	9.532007311
32.17762947	9.302650213
32.30234108	9.075515542
32.43114779	8.850677876
32.56400731	8.628211039
32.70087601	8.408188078
32.84170895	8.190681235
32.9864599	7.975761928
33.13508132	7.763500724
33.28752441	7.553967318
33.44373912	7.347230509
33.60367416	7.143358177
33.76727702	6.942417264
33.93449397	6.744473748
34.10527012	6.54959262
34.27954938	6.357837871
34.45727453	6.169272461
34.63838723	5.983958305
34.82282799	5.80195625
35.01053627	5.623326055
35.20145043	5.448126372
35.39550778	5.276414727
35.59264461	5.108247501
35.79279619	4.94367991
35.99589679	4.78276599
36.20187973	4.625558575
36.41067739	4.472109284
36.62222119	4.3224685
36.83644169	4.176685358
37.05326853	4.034807725
37.27263054	3.896882185
37.49445568	3.762954026
37.71867112	3.633067222
37.94520324	3.50726442

X(mm)	Y(mm)
38.17397765	3.385586927
38.40491925	3.268074696
38.63795219	3.154766311
38.87299998	3.045698976
39.10851511	2.942842131
39.34491735	2.842040913
39.58218876	2.743302973
39.82031135	2.646635804
40.05926702	2.552046741
40.29903766	2.459542965
40.53960505	2.369131495
40.78095095	2.280819194
41.02305704	2.194612763
41.26590493	2.110518746
41.50947622	2.028543524
41.75375239	1.948693319
41.99871492	1.870974191
42.24434522	1.795392039
42.49062465	1.721952598
42.7375345	1.650661442
42.98505605	1.581523983
43.23317051	1.514545467
43.48185904	1.449730977
43.73110278	1.387085432
43.98088281	1.326613588
44.23118017	1.268320032
44.48197586	1.212209191
44.73325085	1.158285321
44.98498607	1.106552515
45.23716242	1.0570147
45.48976076	1.009675636
45.74276191	0.964538914
45.99614667	0.921607961
46.24989582	0.880886036
46.5039901	0.842376227
46.75841021	0.806081459
47.01313686	0.772004485
47.26815071	0.740147892
47.5234324	0.710514098
47.77896257	0.683105351
48.03472182	0.657923733
48.29069073	0.634971153

X(mm)	Y(mm)
48.54684989	0.614249354
48.80317984	0.595759909
49.05966114	0.579504221
49.31627433	0.565483523
49.57299991	0.55369888
49.83206092	0.543593774
50.09112553	0.533581694
50.35019373	0.52366264
50.60926547	0.513836614
50.86834072	0.504103616
51.12741945	0.494463649
51.38650162	0.484916713
51.64558721	0.47546281
51.90467617	0.466101941
52.16376848	0.456834106
52.4228641	0.447659308
52.681963	0.438577548
52.94106514	0.429588826
53.2001705	0.420693144
53.45927903	0.411890503
53.7183907	0.403180904
53.97750549	0.394564348
54.23662335	0.386040836
54.49574426	0.37761037
54.75486817	0.36927295
55.01399507	0.361028578
55.27312491	0.352877255
55.53225765	0.344818981
55.79139328	0.336853758
56.05053175	0.328981586
56.30967303	0.321202468
56.56881708	0.313516403
56.82796388	0.305923392
57.08711339	0.298423438
57.34626558	0.29101654
57.6054204	0.2837027
57.86457784	0.276481919
58.12373786	0.269354197
58.38290041	0.262319535
58.64206548	0.255377935
58.90123302	0.248529397
59.160403	0.241773923

X(mm)	Y(mm)
59.4195754	0.235111512
59.67875017	0.228542166
59.93792728	0.222065886
60.1971067	0.215682672
60.45628839	0.209392526
60.71547233	0.203195448
60.97465847	0.197091438
61.2338468	0.191080499
61.49303726	0.18516263
61.75222983	0.179337833
62.01142448	0.173606107
62.27062116	0.167967454
62.52981986	0.162421875
62.78902053	0.15696937
63.04822314	0.15160994
63.30742766	0.146343586
63.56663405	0.141170308
63.82584229	0.136090107
64.08505233	0.131102983
64.34426414	0.126208938
64.6034777	0.121407972
64.86269296	0.116700085
65.1219099	0.112085278
65.38112848	0.107563552
65.64034866	0.103134908
65.89957042	9.88E-02
66.15879372	9.46E-02
66.41801853	9.04E-02
66.6772448	8.64E-02
66.93647252	8.24E-02
67.19570165	7.85E-02
67.45493214	7.47E-02
67.71416398	7.11E-02
67.97339713	6.75E-02
68.23263154	6.40E-02
68.4918672	6.06E-02
68.75110406	5.73E-02
69.01034209	5.40E-02
69.26958126	5.09E-02
69.52882154	4.79E-02
69.78806289	4.49E-02
70.04730528	4.21E-02

X(mm)	Y(mm)
70.30654868	3.93E-02
70.56579304	3.67E-02
70.82503835	3.41E-02
71.08428456	3.16E-02
71.34353164	2.93E-02
71.60277956	2.70E-02
71.86202828	2.48E-02
72.12127778	2.27E-02
72.38052801	2.07E-02
72.63977895	1.87E-02
72.89903056	1.69E-02
73.15828281	1.52E-02
73.41753566	1.36E-02
73.67678908	1.20E-02
73.93604304	1.06E-02
74.1952975	9.21E-03
74.45455243	7.95E-03
74.7138078	6.78E-03
74.97306358	5.70E-03
75.23231972	4.72E-03
75.4915762	3.82E-03
75.75083299	3.03E-03
76.01009004	2.32E-03
76.26934733	1.71E-03
76.52860482	1.19E-03
76.78786249	7.64E-04
77.04712029	4.32E-04
77.30637819	1.92E-04
77.56563616	4.57E-05
77.82489417	-7.70E-06
78.08415218	3.20E-05
78.34341016	1.65E-04
78.60266807	3.91E-04
78.86192589	7.10E-04
79.12118357	1.12E-03
79.38044109	1.63E-03
79.63969841	2.23E-03
79.8989555	2.92E-03
80.15821233	3.70E-03
80.41746886	4.58E-03
80.67672505	5.55E-03
80.93598088	6.61E-03

X(mm)	Y(mm)
81.19523632	7.77E-03
81.45449132	9.02E-03
81.71374585	1.04E-02
81.97299988	1.18E-02
82.23234905	1.32E-02
82.49169886	1.45E-02
82.75104924	1.57E-02
83.01040015	1.67E-02
83.26975151	1.76E-02
83.52910328	1.84E-02
83.7884554	1.91E-02
84.04780781	1.96E-02
84.30716045	2.01E-02
84.56651326	2.04E-02
84.82586618	2.05E-02
85.08521917	2.06E-02
85.34457215	2.05E-02
85.60392508	2.04E-02
85.86327788	2.01E-02
86.12263052	1.96E-02
86.38198292	1.91E-02
86.64133503	1.84E-02
86.9006868	1.76E-02
87.16003816	1.67E-02
87.41938905	1.56E-02
87.67873943	1.45E-02
87.93808922	1.32E-02
88.19743838	1.18E-02
88.45678684	1.02E-02
88.71613455	8.59E-03
88.97548145	6.81E-03
89.23482748	4.91E-03
89.49417259	2.89E-03
89.75351671	7.41E-04
90.01285978	-1.53E-03
90.27220176	-3.92E-03
90.53154258	-6.43E-03
90.79088218	-9.06E-03
91.05022051	-1.18E-02
91.30955751	-1.47E-02
91.56889312	-1.77E-02
91.82822728	-2.08E-02

X(mm)	Y(mm)
92.08755993	-2.41E-02
92.34689102	-2.74E-02
92.60622049	-3.09E-02
92.86554829	-3.46E-02
93.12487434	-3.83E-02
93.3841986	-4.22E-02
93.64352101	-4.61E-02
93.90284151	-5.02E-02
94.16216003	-5.45E-02
94.42147654	-5.88E-02
94.68079096	-6.33E-02
94.94010323	-6.79E-02
95.19941331	-7.26E-02
95.45872113	-7.74E-02
95.71802663	-8.24E-02
95.97732976	-8.75E-02
96.23663046	-9.27E-02
96.49592867	-9.80E-02
96.75522433	-0.103485714
97.01451739	-0.109061012
97.27380779	-0.114758801
97.53309546	-0.120579081
97.79238036	-0.126521851
98.05166242	-0.132587108
98.31094158	-0.138774853
98.5702178	-0.145085082
98.829491	-0.151517796
99.08876113	-0.158072992
99.34802814	-0.164750669
99.60729197	-0.171550826
99.86655256	-0.17847346
100.1258098	-0.185518571
100.3850638	-0.192686157
100.6443143	-0.199976216
100.9035613	-0.207388747
101.1628048	-0.214923748
101.4220448	-0.222581218
101.681281	-0.230361153
101.9405136	-0.238263554
102.1997424	-0.246288418
102.4589674	-0.254435743
102.7181885	-0.262705528

X(mm)	Y(mm)
102.9774057	-0.271097771
103.2366189	-0.279612469
103.495828	-0.288249621
103.755033	-0.297009225
104.0142339	-0.305891279
104.2734305	-0.314895782
104.5326229	-0.32402273
104.7918109	-0.333272122
105.0509945	-0.342643956
105.3101736	-0.35213823
105.5693483	-0.361754942
105.8285183	-0.371494089
106.0876838	-0.381355669
106.3468445	-0.391339681
106.6060005	-0.401446122
106.8651517	-0.41167499
107.124298	-0.422026281
107.3834395	-0.432499995
107.6425759	-0.443096129
107.9017073	-0.453814681
108.1608336	-0.464655647
108.4199548	-0.475619026
108.6790708	-0.486704815
108.9381814	-0.497913011
109.1972868	-0.509243613
109.4563868	-0.520696618
109.7154813	-0.532272022
109.9745704	-0.543969824
110.2336539	-0.555790021
110.4927318	-0.567732611
110.751804	-0.57979759
111.0108705	-0.591984955
111.2699312	-0.604294705
111.528986	-0.616726837
111.788035	-0.629281347
112.0470779	-0.641958233
112.3061149	-0.654757492
112.5651458	-0.667679121
112.8241706	-0.680723117
113.0831891	-0.693889478
113.3422015	-0.707178201
113.6012075	-0.720589281

X(mm)	Y(mm)
113.8602071	-0.734122718
114.1192004	-0.747778506
114.3781871	-0.761556644
114.6371673	-0.775457129
114.8961409	-0.789479957
115.1551079	-0.803625124
115.4140682	-0.817892629
115.6730216	-0.832282468
115.9319683	-0.846794637
116.1909081	-0.861429133
116.4498409	-0.876185954
116.7087667	-0.891065095
116.9676855	-0.906066554
117.2265972	-0.921190326
117.4855016	-0.93643641
117.7443989	-0.951804801
118.0032888	-0.967295495
118.2621715	-0.98290849
118.5210467	-0.998643783
118.7799144	-1.014501368
119.0387746	-1.030481243
119.2976273	-1.046583405
119.5564723	-1.06280785
119.8153096	-1.079154573
120.0741392	-1.095623572
120.332961	-1.112214843
120.5917749	-1.128928382
120.8505808	-1.145764185
121.1093788	-1.162722249
121.3681688	-1.17980257
121.6269506	-1.197005143
121.8857243	-1.214329966
122.1444898	-1.231777034
122.403247	-1.249346344
122.6619959	-1.267037891
122.9207364	-1.284851671
123.1794684	-1.302787681
123.438192	-1.320845917
123.6969069	-1.339026374
123.9556133	-1.357329049
124.214311	-1.375753937
124.473	-1.394301034

X(mm)	Y(mm)
124.7317048	-1.40732033
124.9901597	-1.424606046
125.2482942	-1.446153478
125.5060381	-1.47195676
125.7633211	-1.502008867
126.0200734	-1.53630162
126.2762249	-1.574825683
126.531706	-1.61757057
126.7864471	-1.664524645
127.0403789	-1.715675126
127.2934322	-1.77100809
127.5455381	-1.830508474
127.7966281	-1.894160082
128.0466338	-1.961945586
128.2954871	-2.033846536
128.5431203	-2.109843357
128.7894659	-2.189915364
129.034457	-2.274040759
129.2780268	-2.362196643
129.5201091	-2.454359017
129.7606378	-2.550502796
129.9995476	-2.650601806
130.2367735	-2.7546288
130.4722508	-2.86255546
130.7059154	-2.974352408
130.9377037	-3.08998921
131.1675527	-3.209434389
131.3953998	-3.33265543
131.6211829	-3.459618792
131.8448406	-3.590289912
132.066312	-3.724633221
132.2855369	-3.862612149
132.5024554	-4.004189136
132.7170087	-4.149325644
132.9291383	-4.297982163
133.1387864	-4.450118228
133.3458959	-4.605692425
133.5504106	-4.764662406
133.7522747	-4.926984896
133.9514333	-5.09261571
134.1478322	-5.26150976
134.3414179	-5.433621071

X(mm)	Y(mm)
134.5321376	-5.608902793
134.7199396	-5.787307211
134.9047726	-5.968785763
135.0865864	-6.153289046
135.2653314	-6.340766836
135.4409591	-6.531168101
135.6134215	-6.72444101
135.7826718	-6.920532952
135.9486639	-7.119390548
136.1113525	-7.320959667
136.2706935	-7.525185438
136.4266434	-7.73201227
136.5791598	-7.941383861
136.7282011	-8.153243217
136.8737269	-8.367532669
137.0156974	-8.584193882
137.1540741	-8.803167881
137.2888192	-9.024395056
137.4198961	-9.247815187
137.5472691	-9.473367457
137.6709036	-9.700990467
137.7907658	-9.930622256
137.9068232	-10.16220031
138.0190441	-10.3956616
138.127398	-10.63094257
138.2318555	-10.86797917
138.332388	-11.10670689
138.4289683	-11.34706072
138.5215699	-11.58897526
138.6101678	-11.83238463
138.6947378	-12.0772226
138.7752569	-12.3234225
138.8517031	-12.57091732
138.9240557	-12.81963969
138.9922949	-13.0695219
139.0564022	-13.32049593
139.1163601	-13.57249347
139.1721524	-13.82544591
139.2237637	-14.0792844
139.2711802	-14.33393984
139.3143887	-14.58934291
139.3533777	-14.84542409

X(mm)	Y(mm)
139.3881365	-15.10211367
139.4186556	-15.35934177
139.4449267	-15.61703837
139.4669427	-15.87513333
139.4846976	-16.13355638
139.4981865	-16.39223719
139.5074057	-16.65110534
139.5123529	-16.91009035
139.5130265	-17.16912173
139.5094265	-17.42812897
139.5015537	-17.68704157
139.4894105	-17.94578904
139.4729999	-18.20430094